NUREG/CR-6889
BNL-NUREG-74978-2005

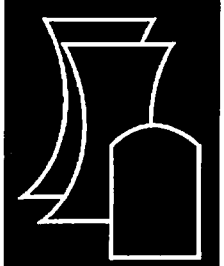

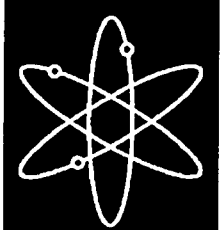

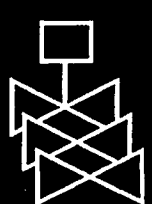

Seismic Analysis of Simplified Piping Systems for the NUPEC Ultimate Strength Piping Test Program

Brookhaven National Laboratory

U.S. Nuclear Regulatory Commission
Office of Nuclear Regulatory Research
Washington, DC 20555-0001

AVAILABILITY OF REFERENCE MATERIALS IN NRC PUBLICATIONS

NRC Reference Material

As of November 1999, you may electronically access NUREG-series publications and other NRC records at NRC's Public Electronic Reading Room at http://www.nrc.gov/reading-rm.html. Publicly released records include, to name a few, NUREG-series publications; *Federal Register* notices; applicant, licensee, and vendor documents and correspondence; NRC correspondence and internal memoranda; bulletins and information notices; inspection and investigative reports; licensee event reports; and Commission papers and their attachments.

NRC publications in the NUREG series, NRC regulations, and *Title 10, Energy*, in the Code of *Federal Regulations* may also be purchased from one of these two sources.

1. The Superintendent of Documents
   U.S. Government Printing Office
   Mail Stop SSOP
   Washington, DC 20402–0001
   Internet: bookstore.gpo.gov
   Telephone: 202-512-1800
   Fax: 202-512-2250
2. The National Technical Information Service
   Springfield, VA 22161–0002
   www.ntis.gov
   1–800–553–6847 or, locally, 703–605–6000

A single copy of each NRC draft report for comment is available free, to the extent of supply, upon written request as follows:

Address: Office of the Chief Information Officer,
Reproduction and Distribution
Services Section
U.S. Nuclear Regulatory Commission
Washington, DC 20555-0001
E-mail: DISTRIBUTION@nrc.gov
Facsimile: 301–415–2289

Some publications in the NUREG series that are posted at NRC's Web site address http://www.nrc.gov/reading-rm/doc-collections/nuregs are updated periodically and may differ from the last printed version. Although references to material found on a Web site bear the date the material was accessed, the material available on the date cited may subsequently be removed from the site.

Non-NRC Reference Material

Documents available from public and special technical libraries include all open literature items, such as books, journal articles, and transactions, *Federal Register* notices, Federal and State legislation, and congressional reports. Such documents as theses, dissertations, foreign reports and translations, and non-NRC conference proceedings may be purchased from their sponsoring organization.

Copies of industry codes and standards used in a substantive manner in the NRC regulatory process are maintained at—

The NRC Technical Library
Two White Flint North
11545 Rockville Pike
Rockville, MD 20852–2738

These standards are available in the library for reference use by the public. Codes and standards are usually copyrighted and may be purchased from the originating organization or, if they are American National Standards, from—

American National Standards Institute
11 West 42nd Street
New York, NY 10036–8002
www.ansi.org
212–642–4900

Legally binding regulatory requirements are stated only in laws; NRC regulations; licenses, including technical specifications; or orders, not in NUREG-series publications. The views expressed in contractor-prepared publications in this series are not necessarily those of the NRC.

The NUREG series comprises (1) technical and administrative reports and books prepared by the staff (NUREG–XXXX) or agency contractors (NUREG/CR–XXXX), (2) proceedings of conferences (NUREG/CP–XXXX), (3) reports resulting from international agreements (NUREG/IA–XXXX), (4) brochures (NUREG/BR–XXXX), and (5) compilations of legal decisions and orders of the Commission and Atomic and Safety Licensing Boards and of Directors' decisions under Section 2.206 of NRC's regulations (NUREG–0750).

NUREG/CR-6889
BNL-NUREG-74978-2005

Seismic Analysis of Simplified Piping Systems for the NUPEC Ultimate Strength Piping Test Program

Manuscript Completed: September 2005
Date Published: December 2005

Prepared by
G. DeGrassi and C. Hofmayer

Brookhaven National Laboratory
Upton, NY 11973-5000

S. Ali, NRC Project Manager

Prepared for
Division of Engineering Technology
Office of Nuclear Regulatory Research
U.S. Nuclear Regulatory Commission
Washington, DC 20555-0001
NRC Job Code N6076

ABSTRACT

The Nuclear Power Engineering Corporation (NUPEC) of Japan has conducted a multi-year test program for the Ministry of Economy, Trade and Industry (METI) of Japan to investigate the behavior of typical Nuclear Power Plant (NPP) piping systems under large seismic loads. The objectives of this program are to develop a better understanding of the elasto-plastic response and ultimate strength of nuclear piping systems, to ascertain the seismic safety margins in current piping design codes, and to assess new code allowable stress rules. The test program consisted of a series of static and dynamic material tests, piping component tests, simplified piping system tests, and large scale piping tests. As part of collaborative efforts between the United States and Japan on seismic issues, the U.S. Nuclear Regulatory Commission (NRC) and the Brookhaven National Laboratory (BNL) participated in this program by performing both pre-test and post-test analysis for selected tests, and by evaluation of program results. This report presents a summary of the NUPEC tests, describes the BNL post-test analyses of selected simplified piping system tests, and discusses the insights gained from this program.

FOREWORD

This report documents the collaborative efforts between the U.S. Nuclear Regulatory Commission (NRC) and the Nuclear Power Engineering Corporation of Japan (NUPEC) under the NRC-NUPEC agreement in the area of seismic engineering research. Under contract to the NRC, Brookhaven National Laboratory (BNL) participated in this program and performed this study. This piping test program is one of a series of large-scale seismic testing programs of nuclear power plant (NPP) structures, systems and components conducted by NUPEC. The research conducted and information exchanged under this collaborative agreement have allowed the NRC to obtain valuable seismic data from large-scale test programs that are not available anywhere else in the world. In addition, this program has enhanced interactions with various Japanese organizations to promote the exchange of information and awareness of ongoing seismic research in Japan.

The NUPEC Ultimate Strength Piping Test Program was a multi-year program to investigate the behavior of NPP piping systems under large seismic loads. The objectives were to develop a better understanding of the elasto-plastic response and ultimate strength of nuclear piping systems, ascertain the seismic safety margins in current piping design codes, and assess new code-allowable stress rules. The program included static and dynamic loading tests of piping material specimens and piping components, and seismic shaking table tests of piping systems. The seismic shaking tests involved small "simplified" piping system test specimen configurations, as well as large-scale representative piping system configurations. In both series of seismic tests, the specimens were shaken to levels well above typical design earthquake excitation levels. A summary description of these tests and their results is included in this report.

The NRC's primary contribution to this collaborative effort was the analysis of selected simplified piping system test runs. Specifically, the analyses included (1) linear analyses and stress evaluations in accordance with the piping design rules of the American Society of Mechanical Engineers (ASME) Boiler and Pressure Vessel Code, and (2) nonlinear analyses to predict the response of simplified piping systems under beyond-design-basis levels of earthquake motion. The results of the linear analyses provided comparative information on the minimum safety margins in various types of piping components provided by different versions of the ASME Code including the latest NRC-endorsed version (1993) and the most recent version (2004) which is still undergoing NRC review. The nonlinear analyses focused on the capability of current theoretical methods and computer programs for predicting the response of piping systems under large earthquake loads. Investigations using different material plasticity models demonstrated the difficulty of accurately predicting the piping response when it is subjected to large earthquake loads, and the importance of validating the analytical model against test data.

From a regulatory standpoint, it is essential to understand the limitations and sensitivities of these nonlinear analysis methods and the importance of validating these methods against test data. The NUPEC tests have provided valuable test data, which can be used to benchmark these analytical models and methods to provide a better understanding of their limitations. The NRC is continuing the collaborative efforts on the Ultimate Strength Piping Test Program and will analyze the large-scale piping system test runs and compare the results with test data. Further insights from these efforts will be provided in a followup report.

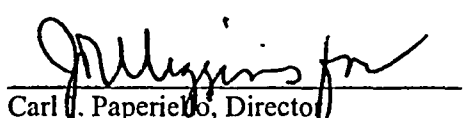

Carl J. Paperiello, Director
Office of Nuclear Regulatory Research
U.S. Nuclear Regulatory Commission

CONTENTS

Figures

Tables

EXECUTIVE SUMMARY

This report presents the results of BNL collaboration efforts on the NUPEC Ultimate Strength Piping Test Program. NUPEC conducted a multi-year test program to investigate the behavior of typical NPP piping systems under large seismic loads. NUPEC's objectives were to develop a better understanding of the elasto-plastic response and ultimate strength of nuclear piping systems, to ascertain the seismic safety margins in current piping design codes, and to assess new code allowable stress rules. This test program included monotonic and cyclic loading tests of piping material specimens, static and dynamic tests of piping components such as elbows and tees, seismic shaking table tests of two simple piping systems and of a representative large-scale piping system.

NRC and BNL participated in this NUPEC program under a collaboration agreement between the United States and Japan on seismic issues. As part of the collaboration, BNL performed pre-test and post-test analyses for selected tests. NUPEC presented their test results to NRC and BNL and provided selected test data in electronic format. Periodic technical meetings were held in Japan and the U.S. during the course of the program to discuss and exchange ideas on the test program plans, to review and evaluate the test results, and to review and evaluate both pre-test and post-test analyses. This report provides a summary of the NUPEC tests, describes the BNL post-test analyses, and discusses the insights gained from this program.

A major goal of the NUPEC test program was to perform a seismic proving test of a representative NPP large-scale piping system. In order to gain a better understanding of the behavior of piping under severe seismic loads, NUPEC first carried out a series of material and piping component tests and shaking table tests of small (simplified) piping systems. The material specimen tensile tests provided stress-strain curves and basic material strength properties including yield and ultimate stresses, percent elongation and ultimate strain. Strain-controlled cycling tests were also performed which provided cyclic stress-strain curves and stress-strain hysteresis curves for incremental cycling amplitudes. The piping component tests included static and dynamic cycling tests of pressurized elbows, tees, nozzles and reducers. The tests were carried out at high strain levels and illustrated the accumulation of ratcheting strain. The specimens were cycled until a through-wall crack occurred.

The simplified piping system tests were designed to excite the systems to seismic levels well above the typical design earthquake levels in order to induce elasto-plastic response in the system's components. The test systems were simple two-dimensional (Model A) and three-dimensional (Model B) geometric configurations of 65 mm (2 ½ inch) nominal diameter pipe. The Model A pipe routing configuration was in the horizontal plane and was excited on a shaking table in the horizontal direction. The Model B routing was in the horizontal and vertical planes and was subjected to horizontal, vertical, or simultaneous horizontal and vertical seismic motions. The piping systems were pressurized and instrumented with accelerometers, displacement sensors and strain gages at critical locations which were monitored during each test. A number of tests to high strain levels were carried out to investigate different loadings and design variations. There were no failures reported during the application of any single time history. However, NUPEC repeated selected high input level tests for both a Model A and a Model B specimen to induce failure. In these tests, cracking at an elbow was observed in the Model A configuration after five tests at a high seismic level. For the Model B, 18 applications of a high level seismic input resulted in a crack at a nozzle weld. In both cases, the failures were attributed to fatigue ratcheting.

In the final phase of the test program, NUPEC carried out a series of shaking table tests on a representative large-scale piping system. The test specimen was a 200 mm (8 inch) nominal diameter Schedule 40 carbon steel pipe. It included straight pipe, nine elbows, a tee, and a 1000 kg (2200 lb) added mass representing a valve. The system was pressurized and supported by nozzles, an anchor, five two-directional restraints, and a spring hanger. The three-dimensional routing of the piping was

representative of nuclear power plant piping systems. The system was instrumented with accelerometers, displacement sensors, and strain gages at critical locations.

Two series of tests were performed: a design confirmation test and an ultimate strength test. For the design confirmation test, the first input motion was selected to induce a maximum stress equal to the Japanese Code primary stress limit of $3S_m$. Additional design confirmation tests were then performed using the same test specimen with the seismic input incrementally increased up to a maximum elastically-calculated stress of 13.5 S_m in the system. The tests were conducted at room temperature and simultaneous horizontal and vertical seismic input motions were applied in all test runs. No evidence of pipe failure was observed.

The ultimate strength test used a similar but modified piping test specimen. An additional mass was added and a support was removed. The intent of these modifications was to induce failure in the system. The pipe was internally pressurized and the tests were performed at room temperature. Horizontal seismic input motion corresponding to a maximum elastically-calculated stress level of $24S_m$ was applied. The test was repeated until failure occurred. During the fifth test run, a through-wall crack developed in an elbow. An examination confirmed that the failure was the result of fatigue ratcheting.

In accordance with the collaboration agreement, BNL performed finite element analyses for selected simplified piping test runs. The BNL analyses had two major objectives. First, linear analyses were performed in accordance with ASME Code requirements. Since the ASME seismic evaluation requirements have been undergoing significant changes in recent years, a comparative study was carried out in which the piping systems were analyzed and evaluated according to three different Code versions. They include the latest NRC-endorsed version (1993 Addenda), the 1994 Addenda which incorporated an alternative higher seismic stress allowable which was not endorsed by NRC, and the most recent 2004 Edition which reinstated the original (1993) stress allowable but introduced an alternative method for calculating seismic stresses in certain piping components. Since the NUPEC simplified piping tests loaded the piping systems to stress levels above ASME Code allowables, the analyses were used to identify the degree to which the calculated stresses exceeded the Code allowable stresses. The ratios of calculated to allowable stress define the minimum margins of safety provided by different versions of the ASME Code rules. The BNL study includes a comparison of the ratios calculated in accordance with the different rules which provides a measure of the relative safety margins between different code versions. Additional analyses and Code evaluations are recommended for other tests in the NUPEC program, including those in which the simplified and the large-scale piping systems were tested to failure, to provide further substantiation of Code margins.

The second major objective of the BNL analysis was to perform nonlinear analyses to investigate and evaluate the adequacy of the latest commercially available methods and computer programs for predicting the elasto-plastic response of piping systems subjected to large earthquake loads. BNL used the ANSYS computer program for performing these analyses. ANSYS is a computer program commonly used by the nuclear industry which has been enhanced in recent years to include a number of improvements in its nonlinear analysis capability. Among these improvements was the inclusion of the Chaboche nonlinear kinematic hardening model. This plasticity model was expected to provide better simulation of the strain ratcheting behavior that a pressurized pipe is expected to exhibit under seismic loading than is possible with classical linear hardening models. BNL utilized results of the NUPEC material tests to develop input parameters for the piping models. As part of the development process, BNL first created a finite element model of a piping elbow that was subjected to static cycling tests in the NUPEC component test program. Three sets of simulation analyses were carried out using three different plastic hardening models: bilinear kinematic hardening, multilinear kinematic hardening, and Chaboche nonlinear hardening. The results of the analyses confirmed that the first two linear hardening models did not

adequately predict the strain ratcheting behavior observed in the test. The Chaboche nonlinear model provided the most accurate simulation of strain ratcheting behavior.

ANSYS models were developed for the two-dimensional (Model A) and the three-dimensional (Model B) simplified piping systems. Preliminary seismic time history analyses were first performed for the Model A high seismic level (A-2) test run. A number of studies were performed to investigate the sensitivity of modeling and analysis parameters on the results. The studies demonstrated the importance of accurately modeling the piping system to predict the correct system dynamic characteristics in an elasto-plastic analysis. Small changes in system frequencies resulted in significant differences in response. Analyses were also conducted using the two linear kinematic hardening models and the Chaboche nonlinear hardening model. Comparisons of time history results to test data clearly showed that the Chaboche model predicted displacement and strain ratcheting with the greatest accuracy.

The Chaboche model was used in all subsequent nonlinear analyses of the simplified piping tests. A total of five analyses were performed: two levels of horizontal seismic time history input motion for the two-dimensional system (test runs A-1 and A-2), and a horizontal, a vertical, and a combined horizontal and vertical seismic input motion for the three-dimensional system (test runs B-1, B-2 and B-3). Displacements and strains at critical locations were compared to test measurements. The application of the Chaboche nonlinear kinematic hardening model to the simulation analyses of the other four simplified piping system tests demonstrated that the displacement time history responses were predicted with reasonably good accuracy. Accurate simulation of strain and strain ratcheting was achieved in some but not all cases which indicates that even the Chaboche nonlinear model has limitations which need to be better understood. From a regulatory standpoint, these analyses demonstrated the importance of understanding the limitations and sensitivities of nonlinear analysis methods and of commonly applied plasticity models. Further studies to investigate the limitations of plasticity models on representative large-scale piping systems may provide additional insights.

The NRC and BNL are continuing the collaboration efforts with Japan and plan to analyze the large-scale piping system test models and compare the results with the test data. Further insights from this collaboration effort will be provided in a follow-up report.

ACKNOWLEDGMENTS

The research program described in this report was sponsored by the Office of Nuclear Regulatory Research of the U.S. Nuclear Regulatory Commission. The authors would like to express their gratitude to Dr. Syed Ali and Dr. Andrew Murphy, NRC Project Managers, for the technical and administrative support they have provided in performing this study.

This research program was performed as part of the Implementing Agreement between the U.S. Nuclear Regulatory Commission and the Nuclear Power Engineering Corporation of Japan in the Area of Seismic Engineering Research. This agreement is an item of the Implementing Arrangement between the United States Nuclear Regulatory Commission and the Nuclear and Industrial Safety Administration of Japan for Cooperation in the Field of Nuclear Regulatory Matters and Nuclear Safety Research and Development.

All of the test results and information about the test models included in this report were provided by NUPEC and are greatly appreciated. The authors especially thank Dr. Kenichi Suzuki, Program Manager, Seismic Engineering Center of NUPEC, for his support and technical guidance throughout the collaborative study. The authors also wish to acknowledge the helpfulness and cooperation provided by Mr. Hiroshi Abe and Dr. Yoshio Namita of NUPEC, Mr. Koichi Tai of Mitsubishi Heavy Industries, and Mr. Tatsuya Fujiwaka of IHI Heavy Industries.

The authors also express special thanks to Ms. Susan Signorelli for her secretarial help throughout this program and in the preparation of this report.

1.0 INTRODUCTION

The Nuclear Power Engineering Corporation (NUPEC) of Japan conducted a multi-year test program for the Ministry of Economy, Trade and Industry (METI) of Japan to investigate the behavior of typical Nuclear Power Plant (NPP) piping systems under large seismic loads. The objectives of this program were to develop a better understanding of the elasto-plastic response and ultimate strength of nuclear piping systems, to ascertain the seismic safety margins in current piping design codes, and to assess new code allowable stress rules. The test program consisted of a series of static and dynamic material tests, piping component tests, simplified piping system tests, and large scale piping tests.

As part of collaborative efforts between the United States and Japan on seismic issues, the U.S. Nuclear Regulatory Commission (NRC) and the Brookhaven National Laboratory (BNL) participated in this program. The collaboration program included a series of periodic technical meetings held in Japan and the U.S. to discuss and exchange ideas on the test program plans, to review and evaluate the test results, and to review and evaluate both pre-test and post-test analyses. In accordance with the collaboration agreement, NUPEC provided their test results to NRC and BNL in the form of presentations and also provided selected test data for test runs analyzed by BNL in electronic format. NRC agreed to have BNL perform pre-test and post-test analyses for selected tests and provide the results in a series of presentations and reports.

The purpose of this report is to present a summary of the NUPEC test program, to describe the BNL post-test analyses performed to date, and to discuss the insights gained from the program. Section 2.0 of this report provides a description and summary results of the NUPEC test program which consisted of four phases of testing: material tests, piping component tests, simplified piping system tests, and large-scale piping system tests. Section 3.0 presents the BNL linear seismic piping analysis and ASME Code evaluations for selected simplified piping system tests. These analyses identify the highest stressed components and the degree to which the maximum stresses exceed Code allowables. By performing the evaluations in accordance with different versions of the Code, the minimum margins to failure associated with the NRC endorsed Code version (1993 Addenda) are calculated and compared with the margins based on the 1994 Addenda and the latest 2004 Edition.

The results of the BNL nonlinear analyses are presented in Sections 4.0 and 5.0. Section 4.0 focuses on the development of an accurate nonlinear plasticity model. Analyses of an elbow component test were performed using two linear hardening models and a nonlinear hardening model. Comparison of the analysis results to test data demonstrated the nonlinear model's superior capability in predicting strain ratcheting compared to the linear models. Section 5.0 presents the results of the post-test analyses for the two-dimensional (Model A) and the three-dimensional (Model B) simplified piping system tests and compares key displacements and strains to test measurements. A summary of conclusions including regulatory insights and lessons learned from the program, and recommendations for further research are presented in Section 6.0.

2.0 DESCRIPTION OF NUPEC TEST PROGRAM

2.1 Introduction

A major goal of the NUPEC test program was the performance of a seismic proving test of a representative large-scale piping system. In order to gain a better understanding of the piping behavior prior to performing the proving test, NUPEC conducted a series of material and piping component static and dynamic tests, and simplified piping system seismic tests. This chapter provides a summary description of each of these series of tests.

2.2 Material Tests

NUPEC carried out a series of static monotonic loading and cyclic loading tests to develop stress-strain curves and properties for typical piping materials. The materials included carbon steel (grades STS410 and SCV410), stainless steel (grade SUS304TP), and low-alloy steel (STPA24). Typical test specimens are shown in Figures 2-1(a) and 2-1(b). The tests were performed at room temperature and at 300°C (572°F). In the monotonic loading tests, the specimens were tensile tested to failure. The results of the tests provided the stress-strain curves and basic material properties including yield strength, ultimate strength, percent elongation, percent area reduction, and ultimate strain. A typical stress-strain curve for STS410 carbon steel is shown in Figure 2-2. In the cyclic loading tests, the specimens were subjected to strain-controlled incremental cycling in consecutive blocks of twenty increasing amplitude cycles followed by twenty decreasing amplitude cycles. Within each block of cycles, the strain amplitude was incrementally increased linearly from 0% to a maximum of 2.5% strain (5% strain range) at 20 cycles, and then incrementally decreased back to 0% strain. These tests provided stress-strain hysteresis curves for the four piping materials at room temperature and at 300°C (572°F). They also provided cyclic stress-strain curves for the materials for strains up to 2.5%. A typical series of hysteresis curves for STS410 carbon steel are shown in Figure 2-3. A typical cyclic stress-strain curve is shown in Figure 2-4.

NUPEC also carried out a series of low-cycle strain-controlled ratcheting fatigue tests for typical piping materials at room temperature and at 300°C (572°F). Both uniaxial and biaxial loading tests were performed. The uniaxial tests also used the test specimen shown in Figure 2-1(b), as well as the same four materials identified above. A unique aspect of the uniaxial fatigue tests is that in some of the test runs, an accumulated mean strain was artificially induced at a given rate per cycle to simulate the ratcheting strain that may develop in components. Test run variations included different cyclic strain ranges, mean strain accumulation rates, and temperatures. Test results provided data on strain versus number of cycles for different strain ranges and mean strain accumulation rates. They demonstrated that higher mean strain accumulation rates result in shorter fatigue lives for all materials and temperatures. The biaxial tests used a miniature pipe specimen shown in Figure 2-1(c) to simulate the stress field of piping components subjected to internal pressure and seismic loading. These tests were performed for STS410 carbon steel and SUS304TP stainless steel specimens. Test run variations included internal pressure, displacement amplitude, and temperature. The test results demonstrated that the test specimens experienced circumferential swelling due to ratcheting and developed through-wall circumferential cracks in all but two cases in which longitudinal through-wall cracks developed. The test results were plotted on S-N diagrams (strain range versus number of cycles to failure), and on Dd-Df diagrams (where Df = (failure cycles)/(failure cycles without ratcheting) and Dd = (accumulated strain)/(fracture strain)) [1, 2].

2.3 Piping Component Tests

In the second phase of the program, NUPEC conducted static and dynamic tests on typical piping components which included elbows, tees, nozzles and reducers. A total of sixteen static tests were performed. A typical test setup for a static elbow test is shown in Figure 2-5. A summary of the test

conditions for each load case is presented in Table 2-1. Test specimen variations included component type, material, diameter, and pipe schedule. All tests were conducted at room temperature except for one elbow test which was conducted at 300°C (572°F). The test specimens were subjected to either cyclic or monotonic loads. Nearly all of the tests were deflection controlled with the exception of one elbow test which was load controlled. In the monotonic loading tests, the specimens were unpressurized and loaded to failure to determine the lower bound collapse moment. In the cyclic loading tests, the test specimens were pressurized to induce an internal pressure stress equal to S_m, and then subjected to quasi-static sinusoidal displacements until a fatigue crack developed. The applied displacement amplitudes were selected to induce a maximum strain range of 3% in all cases but one, in which a larger displacement amplitude corresponding to a 6% strain range was applied. The specimens were cycled until through-wall cracks were detected. The test specimens were instrumented with strain gages at critical locations as illustrated in Figure 2-6. Load cells and displacement transducers were used to monitor force-deflection data as shown in Figure 2-5. NUPEC reported the monotonic test results as plots of load versus deflection and strain versus deflection up to the collapse load. The cyclic test results were reported as plots of load-deflection hysteresis curves, strain distributions at critical component sections, and maximum strain versus number of cycles. The strain versus cycle plots illustrated the accumulation of ratcheting strain during the tests. A typical plot of strain versus number of cycles up to failure for the SE-4 test is shown in Figure 2-7.

The component dynamic tests were performed on a seismic shaking table. The test specimens were subjected to either sinusoidal or seismic wave acceleration input motions. A large mass on rollers was attached to one end of the test specimen. A typical test setup for a dynamic elbow test is shown in Figure 2-8. A total of twelve dynamic load tests were carried out. A summary of the test conditions is presented in Table 2-2. Test specimen variations included pipe component type, material (STS410 carbon steel or SUS304TP stainless steel), and diameter. All tests were conducted at room temperature. All specimens were pressurized to induce a stress level of either S_m or 0.5 S_m. The acceleration input levels were selected to induce a maximum strain range of 3% in ten load cases and 1.5% in two load cases. The specimens were tested until though-wall cracking was observed. The test specimens were instrumented with strain gages at critical locations are shown in Figure 2-6. Accelerometers and displacement transducers were used to monitor acceleration input and response and displacement response as shown in Figure 2-8. The test results were reported as plots of load-deflection hysteresis curves, displacement time histories, and strain time histories. The strain versus time plots illustrated the accumulation of ratcheting strain during the tests.

2.4 Simplified Piping System Tests

In the third phase of the program, NUPEC conducted a series of simplified piping system shaking table tests to investigate the elasto-plastic response of small systems with typical piping components under large seismic excitations. These tests included two-dimensional test model configurations (Model A) and three-dimensional configurations (Model B). In the two-dimensional configuration, the pipe routing was in the horizontal plane and was subjected to single-direction horizontal seismic input motion. A typical Model A simplified piping system test setup is shown in Figure 2-9. The system consists of three straight pipe runs connected by two long radius elbows. The pipe was 65 mm (2-½ inch) Schedule 40 carbon steel grade JIS STS410. The system was supported at both ends by specially designed ball bearing pinned supports. The system was pressurized to 19.8 MPa (2870 psi) to induce a pressure stress equal to S_m. Two 200 kg (440 lb) concentrated masses and two 30 kg (66 lb) masses were clamped to the pipe to provide the desired dynamic characteristics for the system. The larger weights were on rollers which provided vertical gravity support. The system was instrumented with accelerometers, displacement sensors, and strain gages at critical locations as shown in Figures 2-10 and 2-11.

Pipe routing for the three-dimensional configuration (Model B) was identical to the Model A routing in the horizontal plane with the addition of a branch line in the vertical plane as shown in Figure 2-12. The branch line was connected to the horizontal run pipe with a tee, and consisted of a riser pipe, a long radius elbow, and a horizontal straight pipe which terminated at a nozzle. An additional 30 kg (66 lb) concentrated mass was attached to the horizontal portion of the branch line. The system was supported by ball bearing pinned supports at the ends of the lower horizontal run and by the fixed nozzle at the end of the upper branch pipe. Instead of using roller supports at the large masses, variable spring hangers were used to provide gravity support to the system without constraining vertical motion. The system was pressurized to 19.8 MPa (2870 psi). In this three-dimensional configuration, the Model B piping could be subjected to horizontal, vertical, or simultaneous horizontal and vertical seismic input motion. The system was instrumented with accelerometers, displacement sensors, and strain gages at critical locations as shown in Figures 2-13 and 2-14.

The basic seismic input excitations for the tests were selected to represent typical horizontal and vertical building floor response spectra for Japanese PWR and BWR plants. However, the time scales were adjusted to provide near resonant responses and the amplitudes of the seismic waves were modified to obtain the desired large elasto-plastic responses. The tests were performed at two excitation levels. The basic level identified as "medium" was intended to produce a maximum strain range of 1.5% with equivalent pipe stress of 6 S_m to 9 S_m and an anticipated fatigue life of 1000 cycles. The higher input level identified as "large" was selected to produce a maximum strain range of 3% corresponding to equivalent pipe design stress of 10 S_m to 12 S_m and a fatigue life of 60 to 300 cycles.

NUPEC conducted a number of tests of both Model A and Model B specimens to investigate different loading and design variations. Table 2-3 provides a summary of the load cases. In all cases, the test specimen was a 65 mm (2-½ inch) Schedule 40 pipe pressurized to 19.8 MPa (2870 psi). The basic two-dimensional test (A-1) subjected the pipe to a single horizontal direction medium level seismic load. In test A-2, a large level seismic load was applied. In test A-3, one of the pinned supports was changed to a fixed support. In test A-4, the frequency of excitation was reduced to about one-half of the resonant frequency. Test A-5 used a stainless steel instead of carbon steel test specimen. In test A-6 an actuator was used at one of the pinned supports to provide independent support motion. Seismic acceleration time history input motions for the A-1 and A-2 load cases are shown in Figures 2-15 and 2-16.

The three-dimensional test (Model B) load cases subjected the test specimens to horizontal, vertical and simultaneous horizontal and vertical motions as summarized in Table 2-3. Test B-1 subjected the pipe to a single horizontal direction medium level seismic load. Test B-2 subjected the pipe to a vertical direction medium level seismic load. In test B-3, simultaneous horizontal and vertical medium level seismic motions were applied. In test B-4, a large level seismic motion was applied. Finally in test B-5, lower frequency horizontal and vertical seismic input motions were applied simultaneously. Seismic acceleration time history input motions for the B-1, B-2 and B-3 load cases are shown in Figures 2-17, 2-18, and 2-19.

The piping systems were monitored during each test to measure accelerations, displacements, and strains at selected locations. Representative time history response plots for the A-2 test including displacements at the pipe center, elbow A opening and closing displacements, and hoop and axial strains at the elbow A flank are shown in Figures 2-20 though 2-23. Representative B-3 test time history responses including horizontal and vertical displacements at the pipe center, and hoop and axial strains at the nozzle are shown in Figures 2-24 through 2-27. The plots illustrate the accumulation of permanent deformations and strains that occurred during the tests. There were no failures reported during the application of a single seismic time history. However, NUPEC repeated selected high input level tests to induce failure. NUPEC reported that cracking at the elbow A location was observed after five tests of the A-2 high level seismic time history. Cracking at the nozzle occurred after 18 applications of the B-4 high level seismic

time history. For both the two-dimensional and three-dimensional tests, the failures were attributed to fatigue ratcheting.

2.5 Large-Scale Piping System Tests

In the final phase of the test program, NUPEC performed a series of seismic shaking table tests on a representative large-scale piping system. The tests were performed using the large high performance shaking table at the Tadotsu Engineering Laboratory. The test specimen was a 200 mm (8 inch) nominal diameter) Schedule 40 carbon steel (STS410) pipe. It included straight pipe, nine elbows, a tee, and a 1000 kg (2200 lb) added mass representing a valve. The system was supported by nozzles, an anchor, five two-directional restraints, and a spring hanger. The three-dimensional routing of the piping system represented typical configuration characteristics of safety-related Japanese nuclear power plant piping systems as illustrated in Figure 2-28. The system was instrumented with accelerometers, displacement sensors, and strain gages at critical locations.

Two series of tests were performed using two different test specimens. The first was a design confirmation test and the second was an ultimate strength test. The seismic input motion was selected based on the Japanese "S_2" seismic wave for a PWR with modified time pitch and excitation level to achieve the desired test responses. For the design confirmation test, the first input motion was selected to induce a maximum stress equal to the Japanese Code primary stress limit of $3S_m$. Additional design confirmation tests were then performed using the same test specimen in which the seismic input was incrementally increased until a maximum elastically-calculated stress of 13.5 S_m was reached. In all tests, the piping was internally pressurized to induce a hoop stress equal to the design stress intensity S_m. The tests were conducted at room temperature and simultaneous horizontal and vertical seismic input motions were applied in all test runs. No evidence of pipe failure was observed. A summary of the test cases is presented in Table 2-4.

The ultimate strength test used a similar but slightly modified test specimen. An additional 1000 kg (2200 lb) mass was added and a two-directional support was removed. These modifications were needed in order to induce failure at the highest stressed elbow within the shaking capability of the Tadotsu shaking table. The pipe was internally pressurized and the tests were performed at room temperature. As indicated in Table 2-4, horizontal seismic input motion corresponding to a maximum elastically-calculated stress level of $24S_m$ was applied. The test was repeated until failure occurred. During the fifth test run, a through-wall crack developed in the elbow. An examination confirmed that the failure was the result of fatigue ratcheting.

Table 2-1 NUPEC Static Piping Component Test Load Cases

Test No.	Component Type	Material	O.D.	Thickness	Internal Pressure Stress	Temp.	Load Wave	Load Level	Load Direction	Control Type	Viewpoint
SE-1	Elbow	STS410 (A)	200A	Sch40	Sm	Room Temp.	Sine	Large	In-plane	Cyclic Deflection	Elbow Basic Case (Carbon Steel)
SE-2										Cyclic Load	Load Control
SE-3					None	300C (572F)				Cyclic Deflection	Temperature
SE-4			65A		Sm	Room Temp.					Pipe Diameter
SE-5			200A	Sch20							Diameter/Thickness Ratio
SE-6		SGV410	400A	STD							
SE-7		SUS304 TP	200A	Sch40							Elbow Basic Case (Stainless Steel)
SE-8								Extra Large			Load Level
SE-9				STD	None			–		Monotonic Deflection	Lower Collapse Load
ST-1	Tee	STS410 (A)	200A/ 200A	Sch40	Sm			Large		Cyclic Deflection	Tee Basic Case
ST-2		SGV410	400A/ 400A	STD							Diameter/ Thickness Ratio
ST-3					None			–		Monotonic	Lower Collapse Load
SN-1	Nozzle	STS410 (A)	200A/ 250A	Sch40	Sm			Large	Bend	Cyclic Deflection	Nozzle Basic Case
SN-2									Torsion		Load Direction
SN-3				Sch20	None			–	Bend	Monotonic Deflection	Lower Collapse Load
SR-1	Reducer		200A/ 150A	Sch40	Sm			Large		Cyclic Deflection	Reducer Basic Case

Note) Load Level---- Extra Large (around 6% in Max. Strain Range), Large (around 3% in Max. Strain Range), Small (Current Design Allowable Level)
O.D.---------- Outside Diameter (65A=2.5B, 150A=6B, 200A=8B, 250A=10B, 400A=16B)

Table 2-2 NUPEC Dynamic Piping Component Test Load Cases

Test No.	Component Type	Material	O.D.	Thickness	Internal Pressure Stress	Temp.	Load Wave	Load Level	Load Direction	Control Type	Viewpoint
DE-1	Elbow	STS410 (A)	200A	Sch40	Sm	Room Temp.	Sine	Large	In-plane	Acceleration	Elbow Basic Case (Carbon Steel)
DE-2			"				Seismic				Load Wave
DE-3			"				Sine	Middle			Load Level
DE-4			"		0.5Sm			Large			Internal Pressure Level
DE-5			65A		Sm		Seismic				Diameter
DE-6		SUS304 TP	200A				Sine				Elbow Basic Case (Stainless Steel)
DE-7			"				Seismic				Load Wave
DE-8			"				Sine	Middle			load Level
DE-9			"		0.5Sm			Large			Internal Pressure Level
DT-1	Tee	STS410 (A)	200A/ 200A		Sm		Seismic				Tee Basic Case
DN-1	Nozzle		200A/ 250A						Bend		Nozzle Basic Case
DR-1	Reducer		200A/ 150A								Reducer Basic case

Note) Load Level---- Large (around 3% in Max. Strain Range), Middle (around 1.5% in Max. Strain Range), Small (Current Design Allowable Level)

Table 2-3 NUPEC Simplified Piping System Test Load Cases

	Test No	A－1	A－2	A－3	A－4	A－5	A－6
2D-Piping system Investigation on elasto-plastic behavior of piping components	Conceptual drawing of piping system	o Pipe size:2-1/2"×sch40 (φ76.3mm×5.2mm) o Stress due to internal pressure ≒ Sm o Stress due to dead weight ≦ 0.5Sm	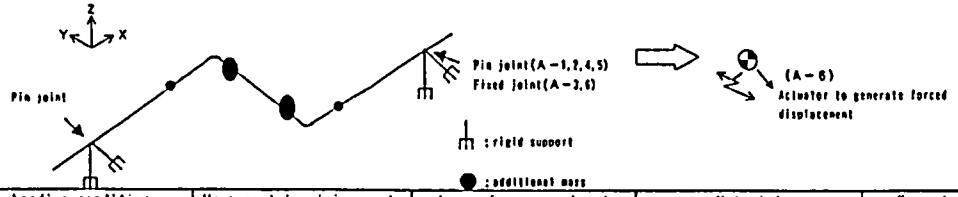				
	Purpose of the test (Test parameter)	Base data (symmetric piping route)	Loading condition [refer A-1]	Un-symmetric piping route [refer A-1, A-6]	Lower frequency input [refer A-1]	Material [refer A-1]	Forced displacement [refer A-3]
	loading condition: wave type	artificial seismic wave	artificial seismic wave	artificial seismic wave	artificial seismic wave	artificial seismic wave	artificial seismic wave
	loading condition: frequency	including resonance frequency	including resonance frequency	including resonance frequency	including Low frequency	including resonance frequency	including resonance frequency
	loading condition: direction	Y	Y	Y	Y	Y	Y (forced displacement = Y)
	Loading level	Medium	Large	Medium	Medium	Medium	Medium
	Pipe material	JIS:STS410 (Carbon steel)	JIS:STS410 (Carbon steel)	JIS:STS410 (Carbon steel)	JIS:STS410 (Carbon steel)	JIS:SUS304TP (equivalent SA312 TP304)	JIS:STS410 (Carbon steel)
	Test No	B－1	B－2	B－3	B－4	B－5	
3D-Piping system Investigation on dynamic behavior of piping syetem	Conceptual drawing of piping system	o Pipe size:2-1/2"×sch40 (φ76.3mm×5.2mm) o Stress due to internal pressure ≒ Sm o Stress due to dead weight ≦ 0.5Sm	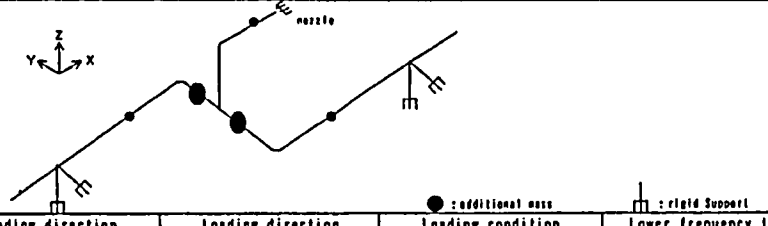				
	Purpose of the test (Test parameter)	Base data (horizontal) [refer A-1]	Loading direction (vertical) [refer B-1]	Loading direction (vertical + horizontal) [refer B-1, B-2]	Loading condition (vertical + horizontal) [refer A-2, B-3]	Lower frequency input (vertical + horizontal) [refer A-4, B-3]	
	loading condition: wave type	artificial seismic wave	artificial seismic wave	artificial seismic wave	artificial seismic wave	artificial seismic wave	
	loading condition: frequency	inducing resonance frequency	inducing resonance frequency	inducing resonance frequency	inducing resonance frequency	inducing resonance frequency	
	loading condition: direction	Y	Z	Y, Z	Y, Z	Y, Z	
	Loading level	Medium	Medium	Medium	Large	Medium	
	Pipe material	JIS:STS410 (Carbon steel)	JIS:STS410 (Carbon steel)	JIS:STS410 (Carbon steel)	JIS:STS410 (Carbon steel)	JIS:STS410 (Carbon steel)	

Table 2-4 NUPEC Large-Scale Piping System Test Load Cases

Test Case			Excitation Wave	Excitation Direction	Design Stress Level	Dominant Frequency
Design Method Confirmation Test	Preliminary Test	DM1-1	Sweep	Horizontal	(Elastic)	–
			Sweep	Vertical	(Elastic)	–
		DM1-2	Seismic	Horizontal	(≒DM2-1,2)	Off-resonance
			Seismic	Vertical	(≒DM2-1,2)	
	Allowable Stress Test	DM2-1	Seismic	H + V	3Sm(≒S_2 limit)	Off-resonance
		DM2-2	Seismic	H + V	4.5Sm	
	Elasto-Plastic Response Test	DM4-1	Seismic	H + V	6Sm	On-resonance
		DM4-2(1)	Seismic	H + V	1.5Sm	
		DM 4-2(2)	Seismic	H + V	13.5Sm	
Ultimate Strength Test	Preliminary Test	US1	Sweep	Horizontal	(Elastic)	–
			Sweep	Vertical	(Elastic)	–
	Ultimate Strength Test	US2	Seismic	Horizontal	24Sm	On-resonance

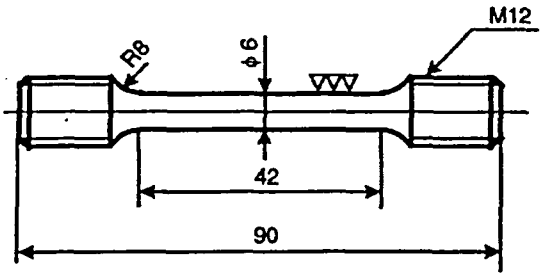

(a) Uniaxial Static Monotonic Loading Test Specimen

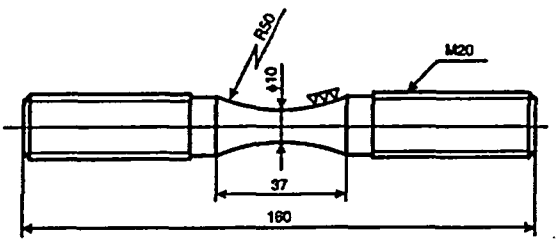

(b) Uniaxial Cyclic Loading Test Specimen

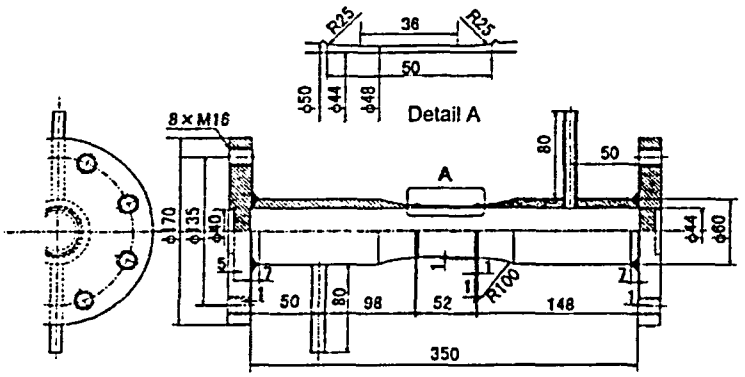

(c) Biaxial Ratcheting Fatigue Test Specimen

Dimensions shown in mm; 1 mm = 0.03937 in

Figure 2-1 Test Specimens from the NUPEC Material Tests

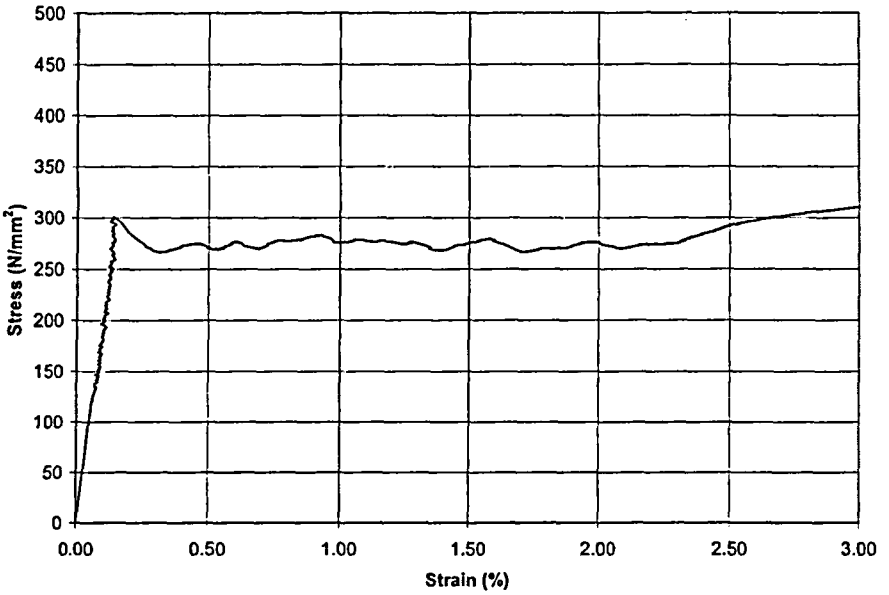

Figure 2-2 Monotonic Loading Stress-Strain Curve for STS410 Carbon Steel
(1 N/mm^2 = 145 psi)

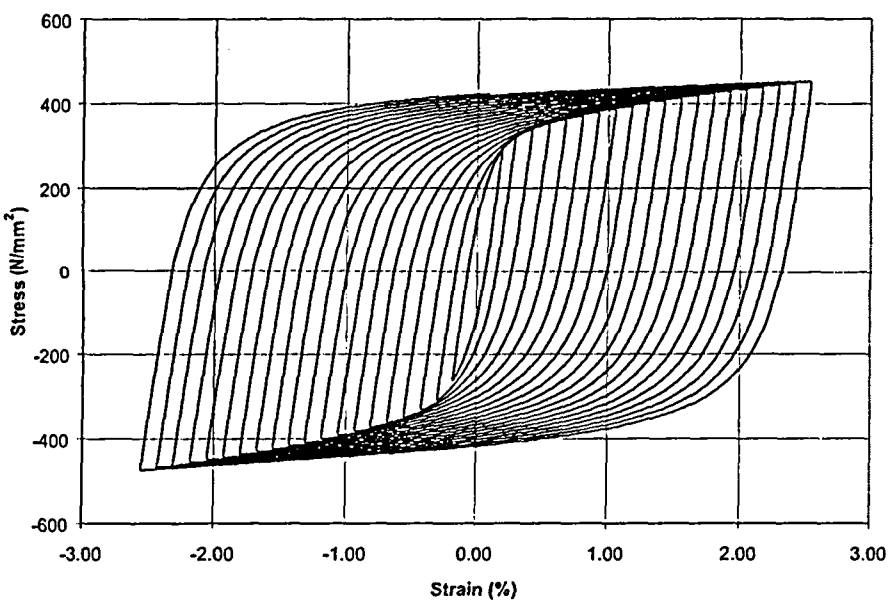

Figure 2-3 Uniaxial Cycling Test Hysteresis Curves for STS410 Carbon Steel
(1 N/mm^2 = 145 psi)

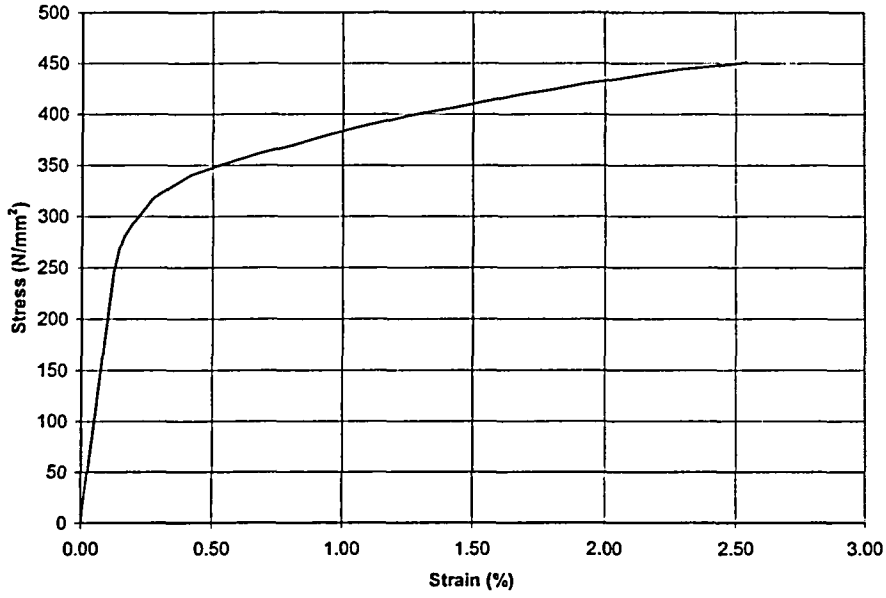

Figure 2-4 Cyclic Stress-Strain Curve for STS410 Carbon Steel
(1 N/mm^2 = 145 psi)

Dimension shown in mm;
1 mm = 0.03937 in

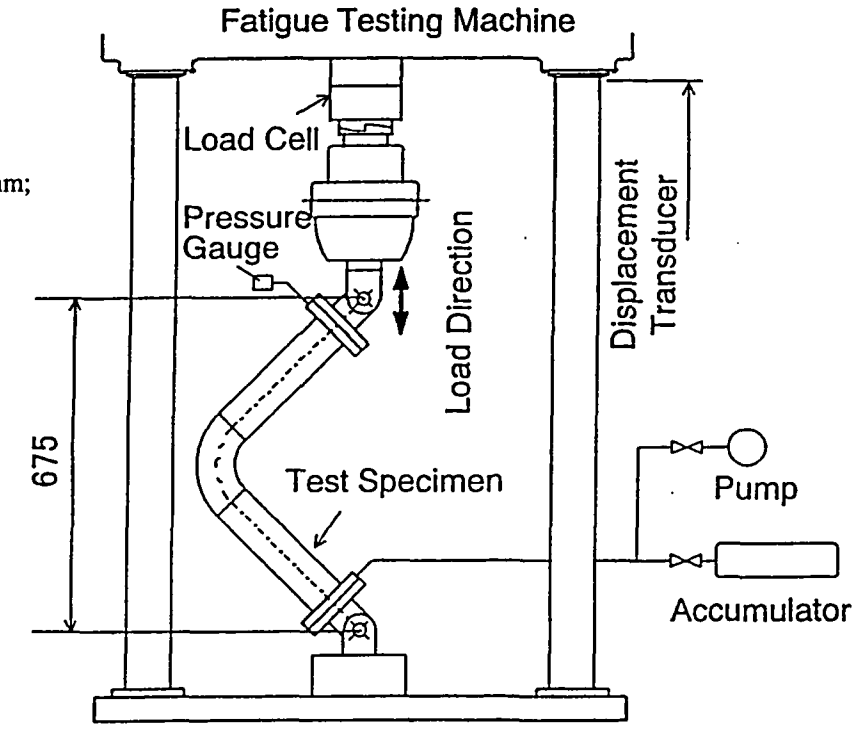

Figure 2-5 Static Elbow Cycling Test Setup

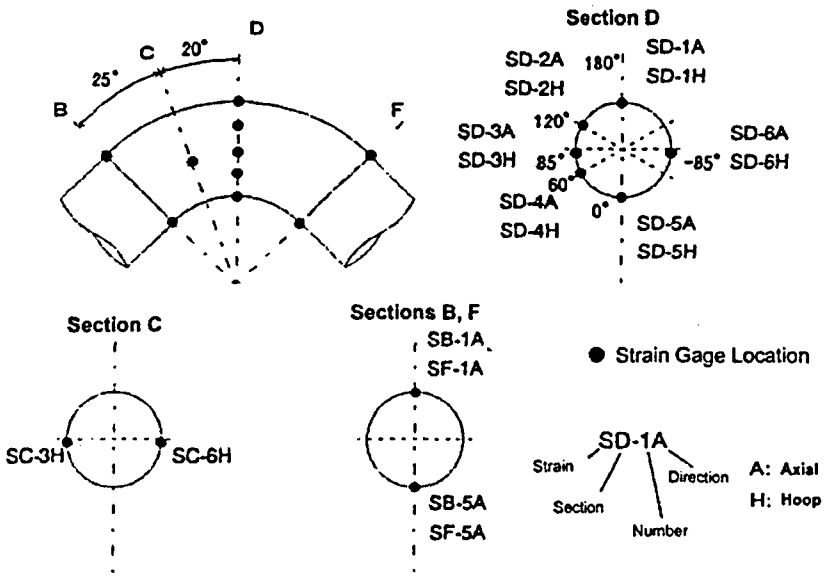

Figure 2-6 Static Elbow Cycling Test Strain Gage Locations

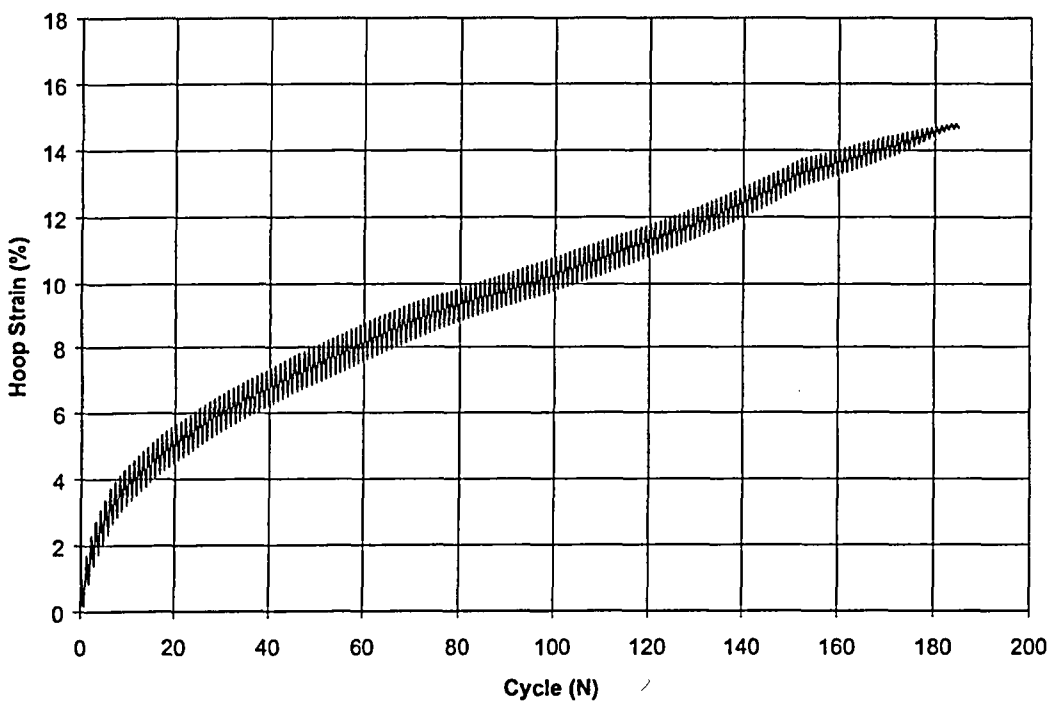

Figure 2-7 Elbow Static Cycling Test SE-4 Hoop Strain vs. Cycle at Elbow Flank

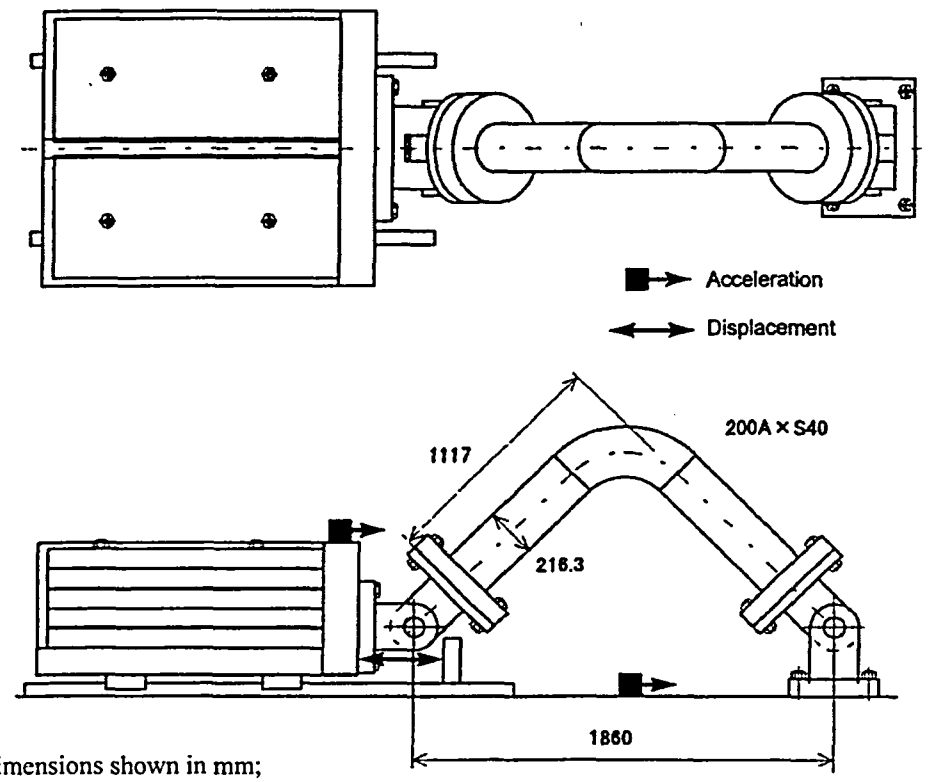

Length dimensions shown in mm;
1 mm = 0.03937 in

Figure 2-8 Dynamic Elbow Test Setup

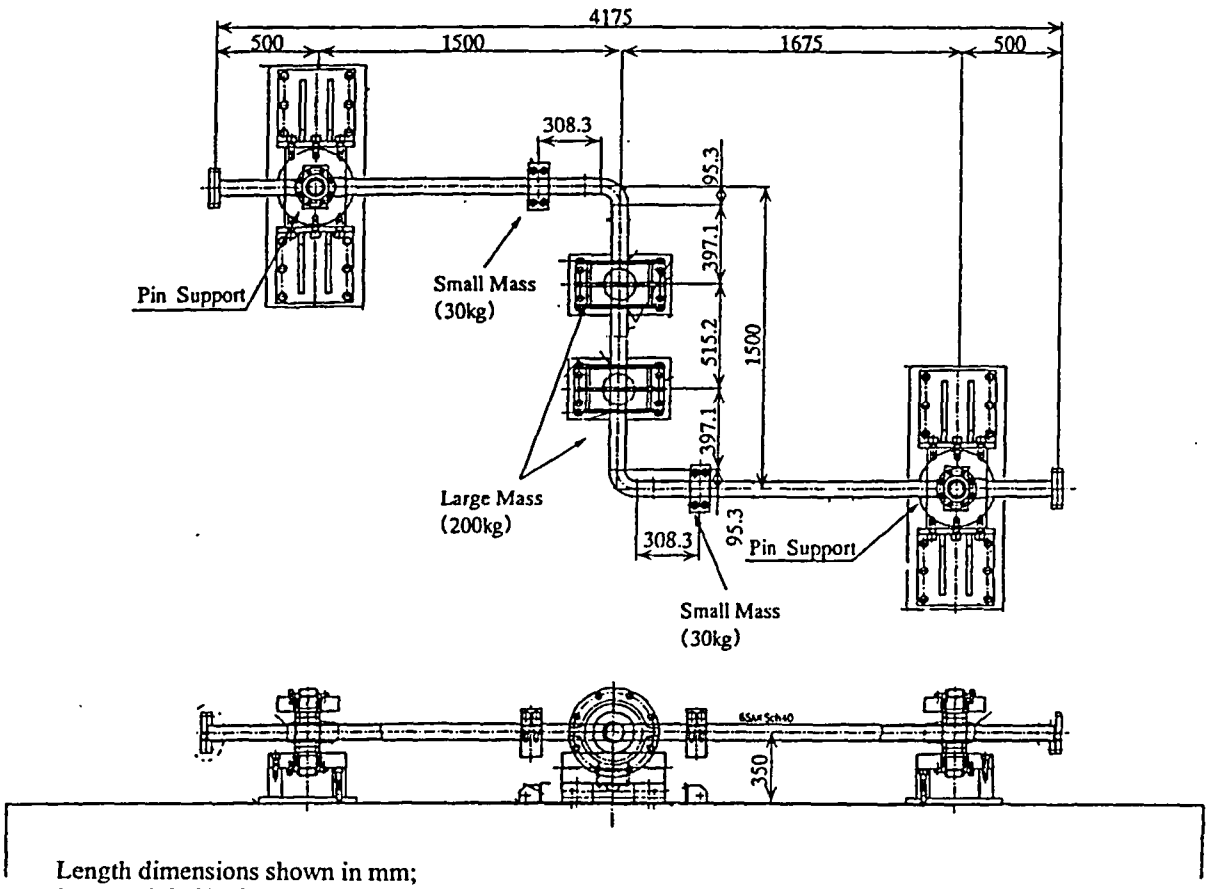

Length dimensions shown in mm;
1 mm = 0.03937 in; 1 kg = 2.2 lbm

Figure 2-9 Model A Simplified Piping System Test Setup

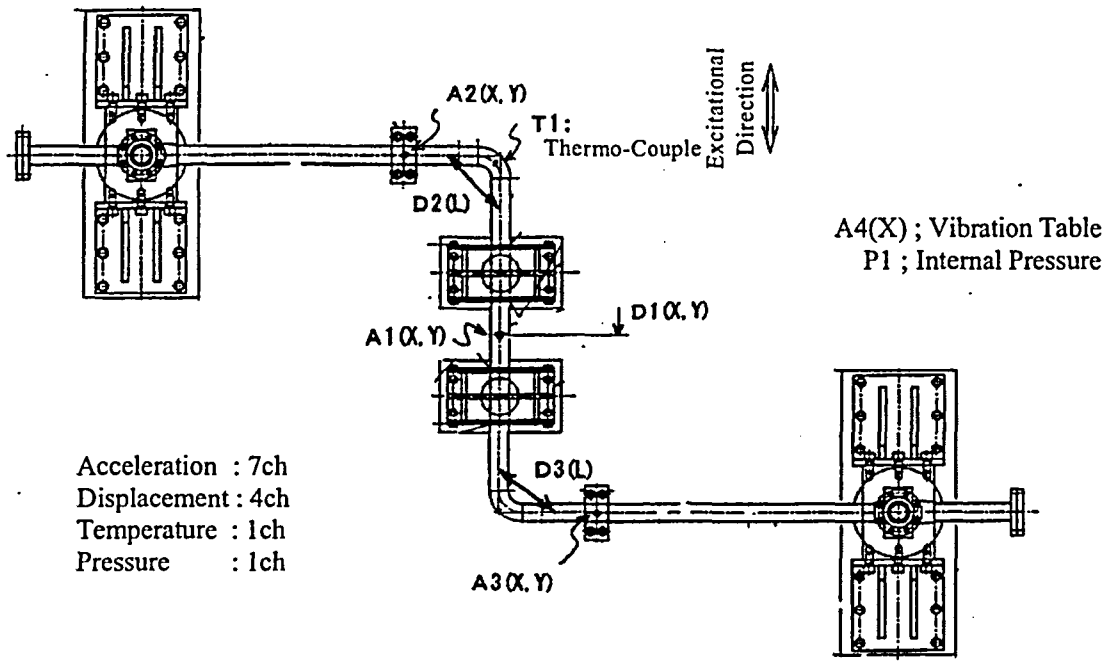

Figure 2-10 Model A Test Instrumentation

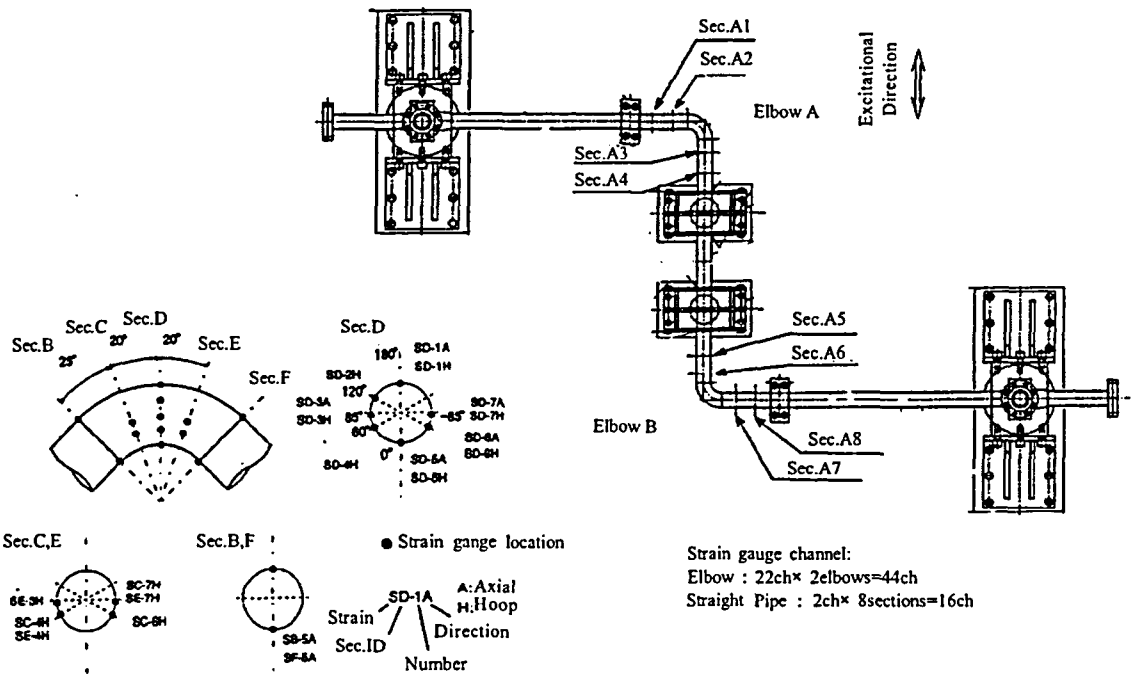

Figure 2-11 Model A Test Strain Gage Locations

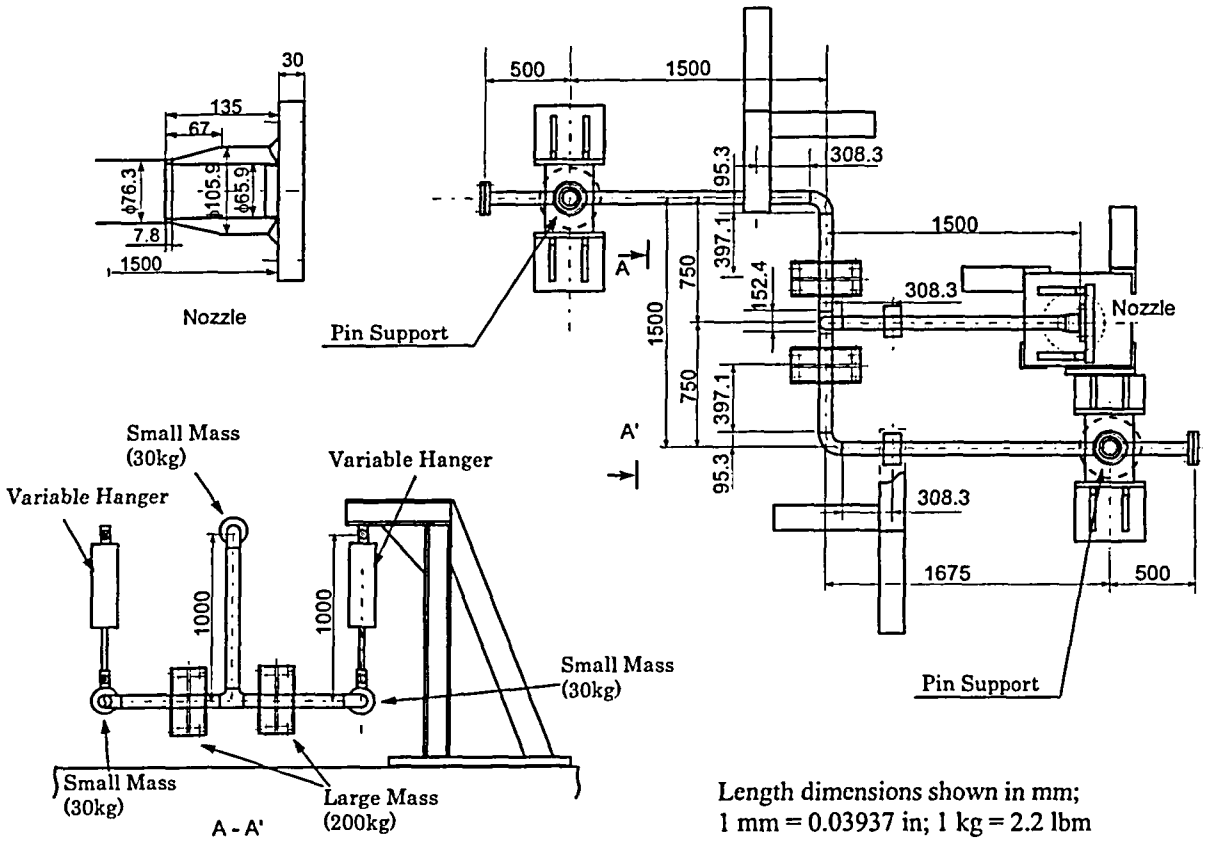

Figure 2-12 Model B Simplified Piping System Test Setup

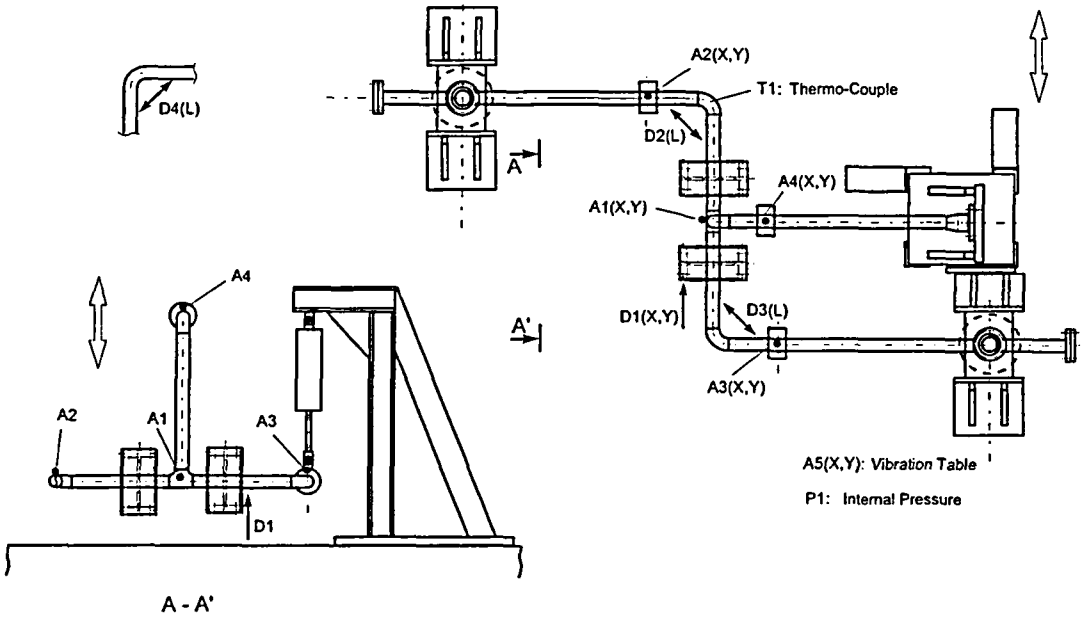

Figure 2-13 Model B Test Instrumentation

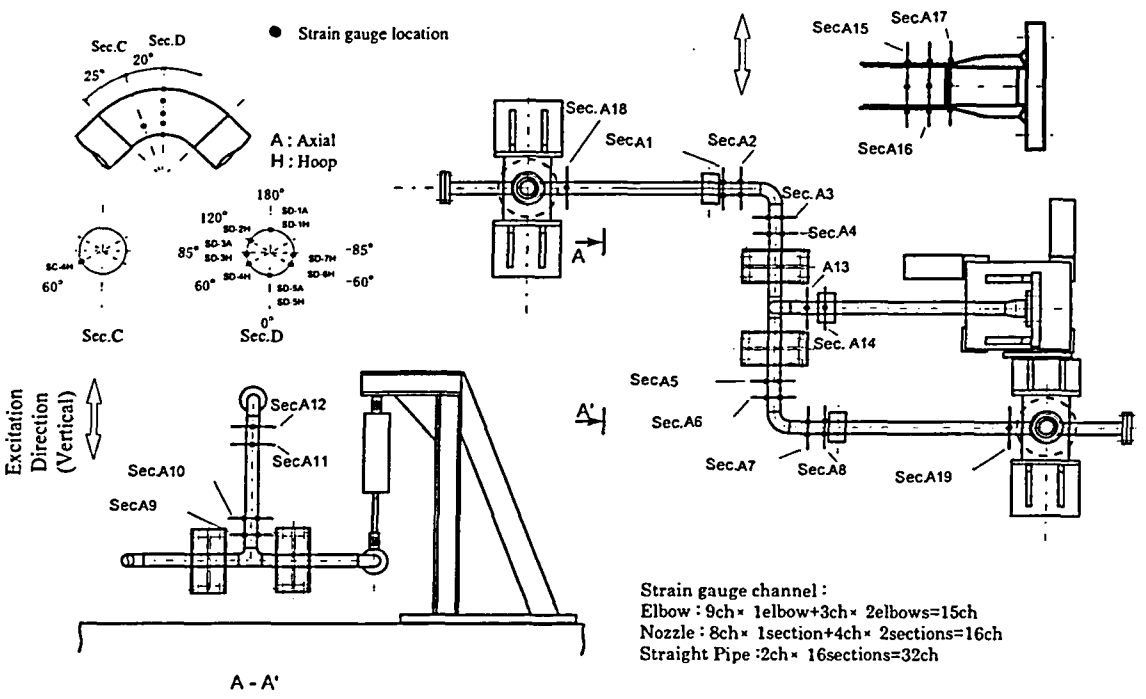

Figure 2-14 Model B Test Strain Gage Locations

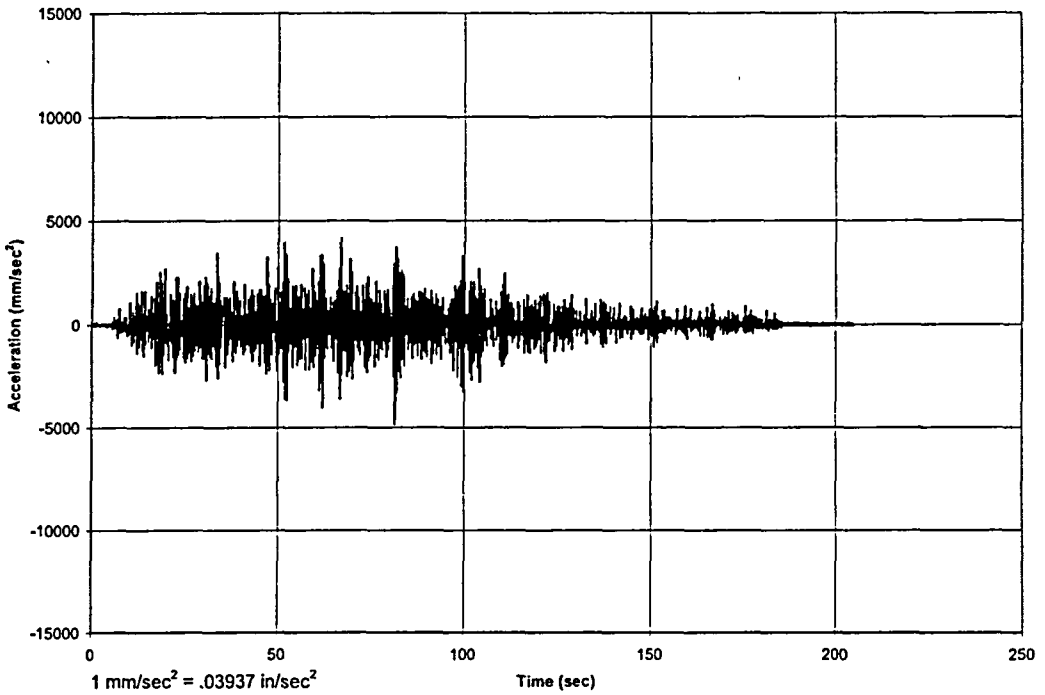

Figure 2-15 A-1 Test Acceleration Time History Input Motion

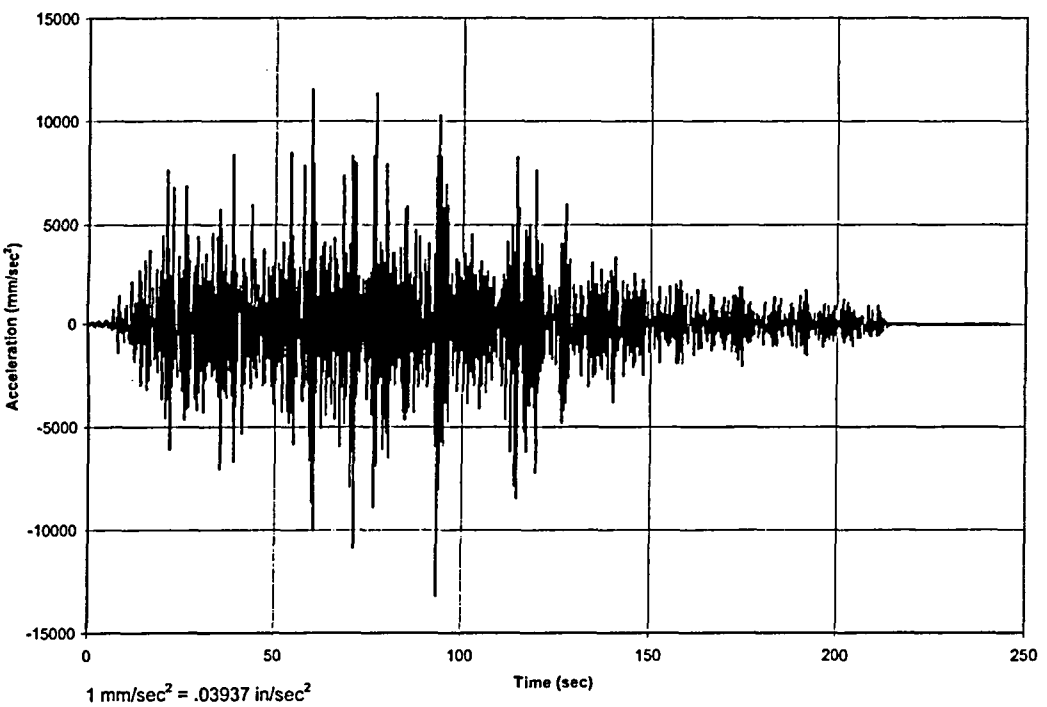

Figure 2-16 A-2 Test Acceleration Time History Input Motion

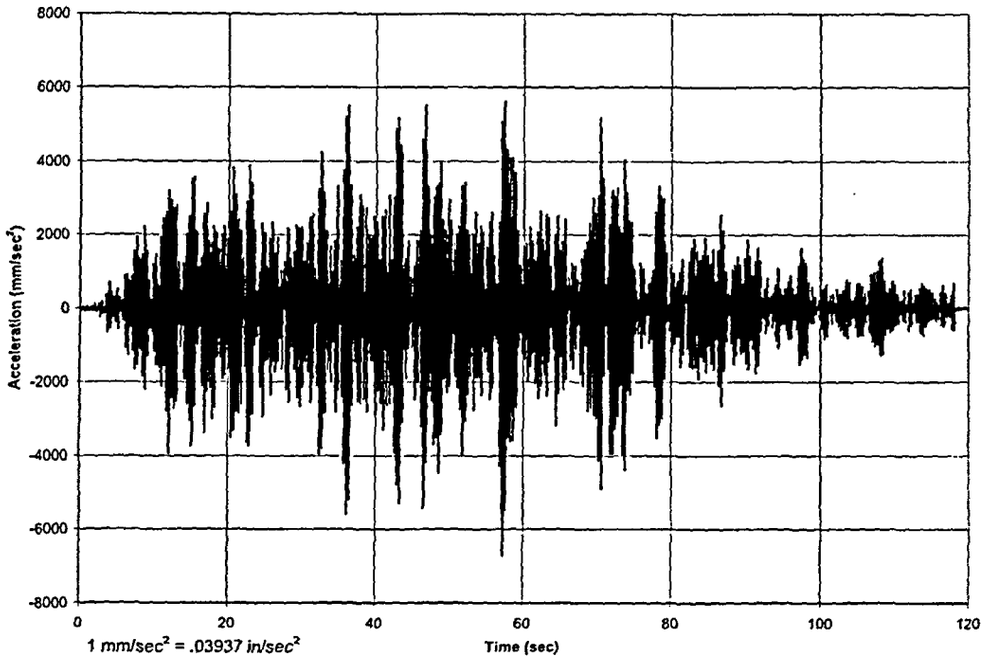

Figure 2-17 B-1 Test Acceleration Time History Input Motion (Horizontal)

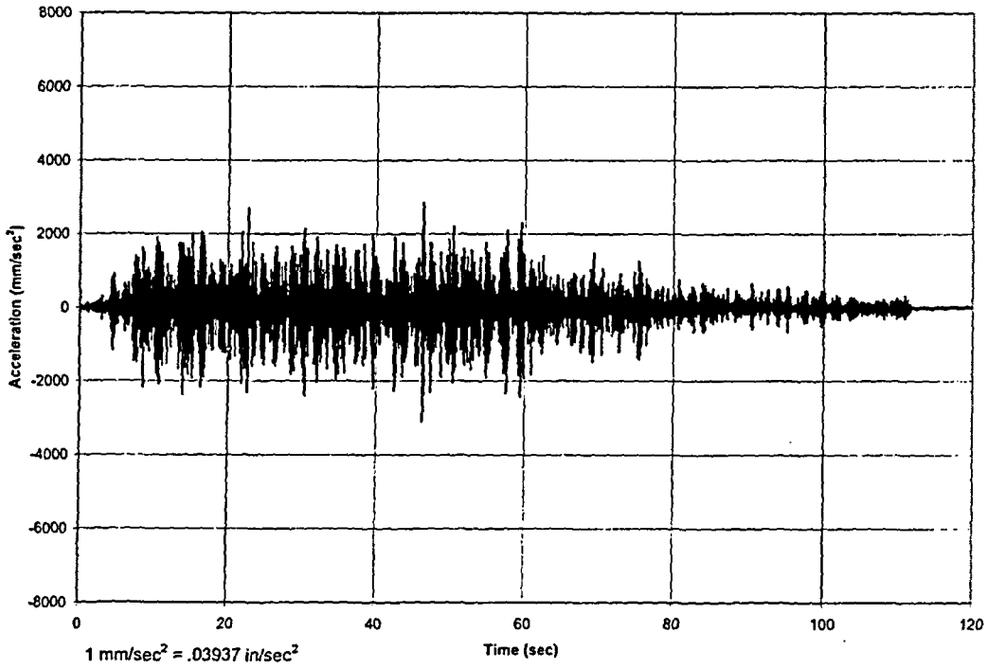

Figure 2-18 B-2 Test Acceleration Time History Input Motion (Vertical)

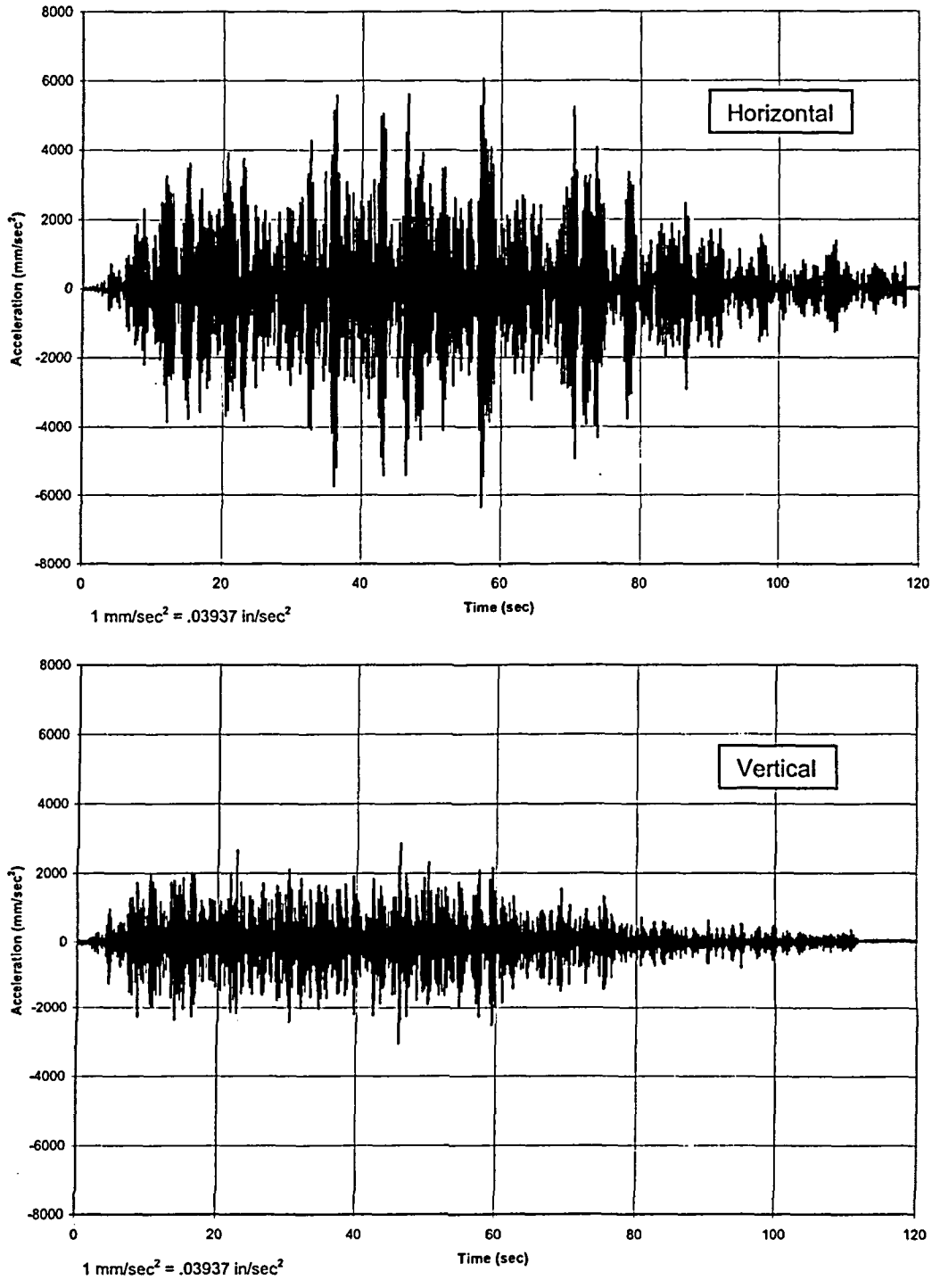

Figure 2-19 B-3 Test Acceleration Time History Input Motion (Horizontal and Vertical)

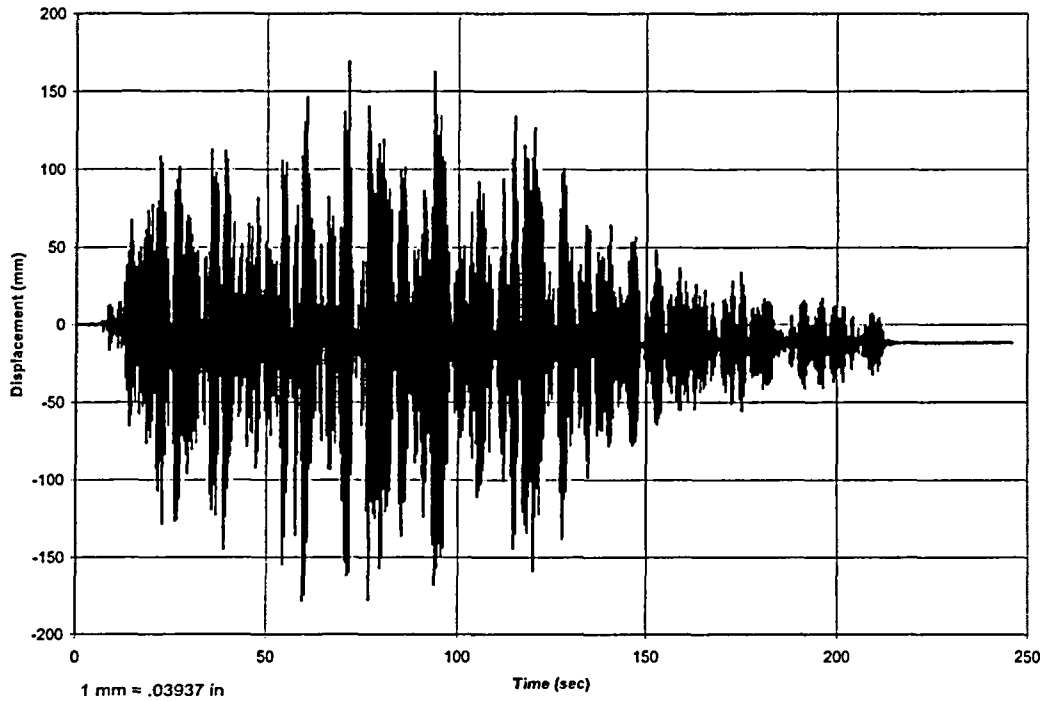

Figure 2-20 A-2 Test - Pipe Center Displacement - D1(X)

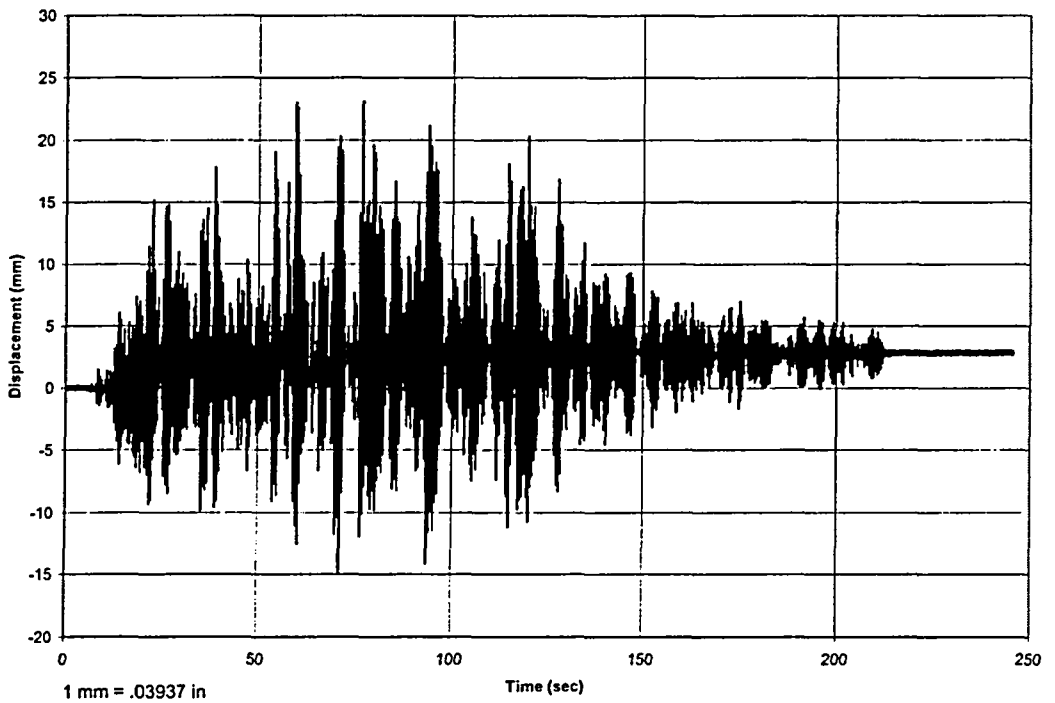

Figure 2-21 A-2 Test - Elbow A Opening Displacement – D2(L)

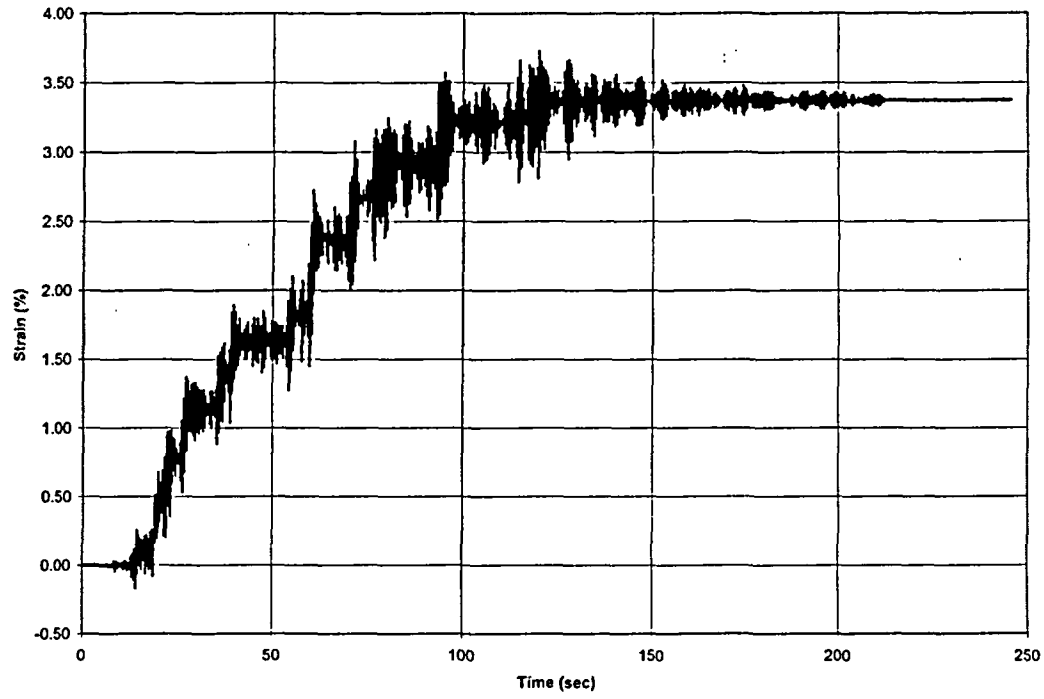

Figure 2-22 A-2 Test – Hoop Strain at Elbow A Flank – SAD-3H

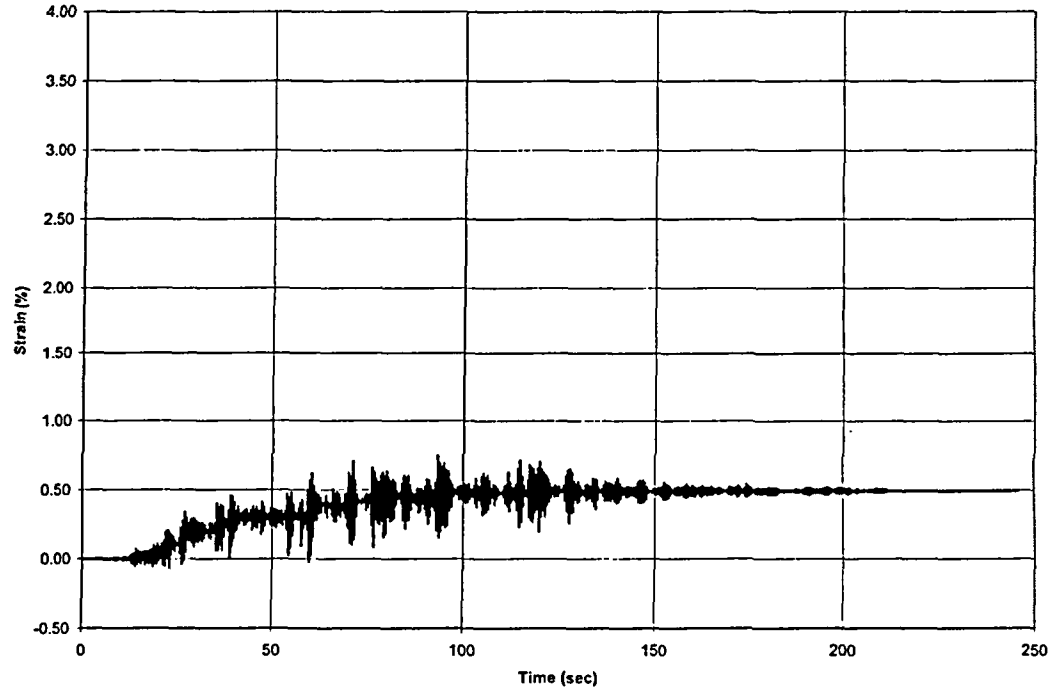

Figure 2-23 A-2 Test – Axial Strain at Elbow A Flank – SAD-3A

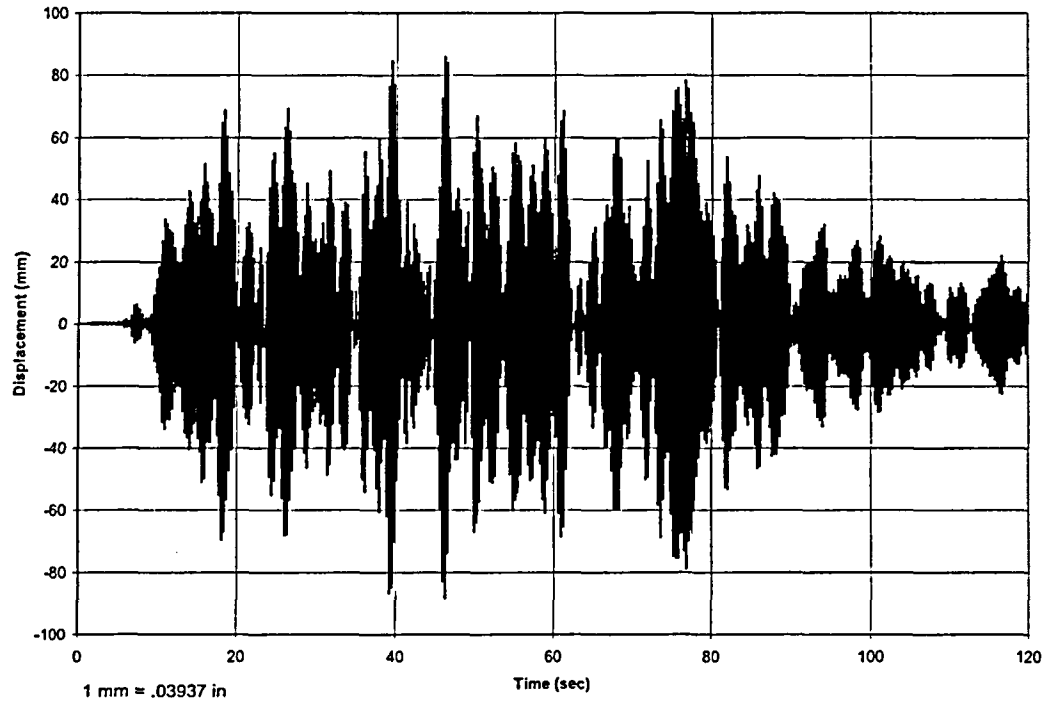

Figure 2-24 B-3 Test - Pipe Center Horizontal Displacement - D1(X)

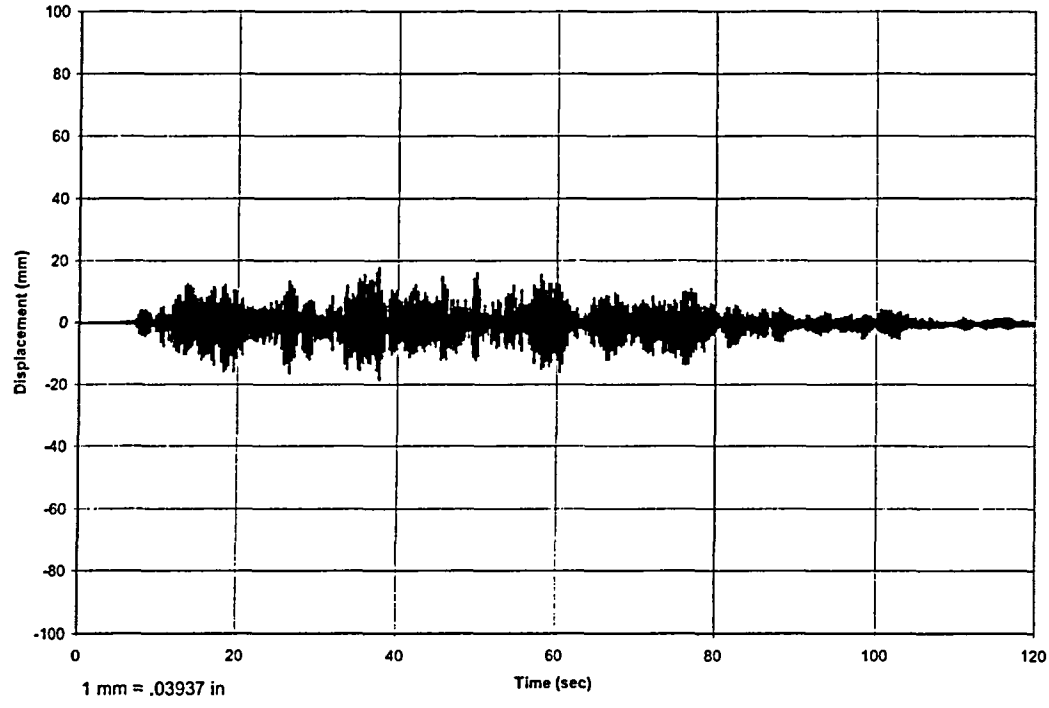

Figure 2-25 B-3 Test - Pipe Center Vertical Displacement - D1(Z)

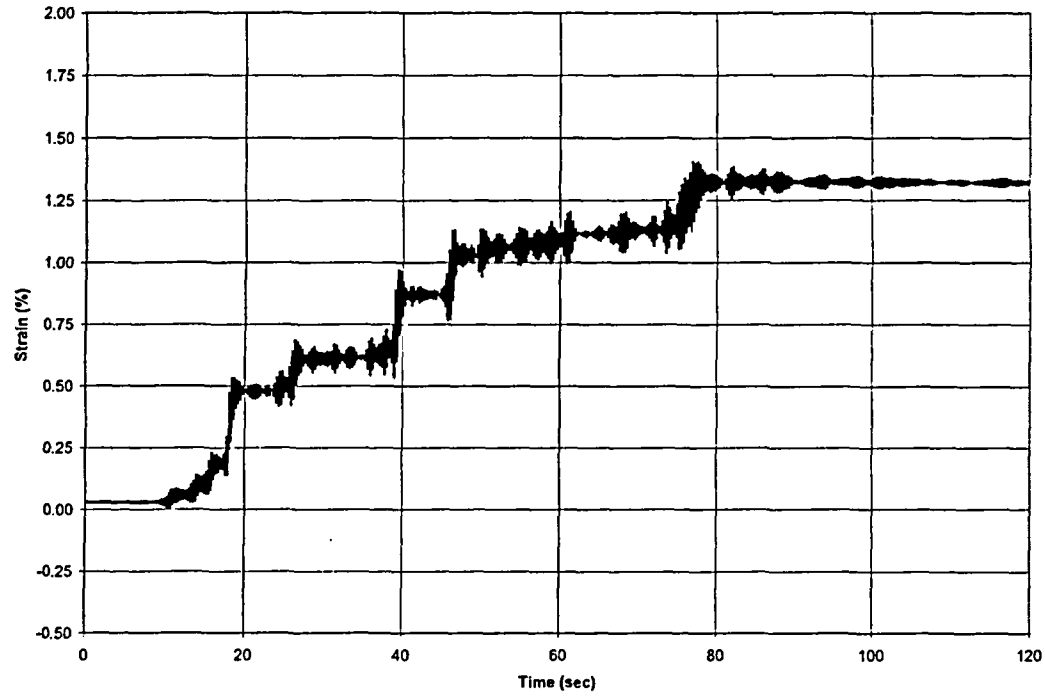

Figure 2-26 B-3 Test – Hoop Strain at Nozzle – SA16-2H

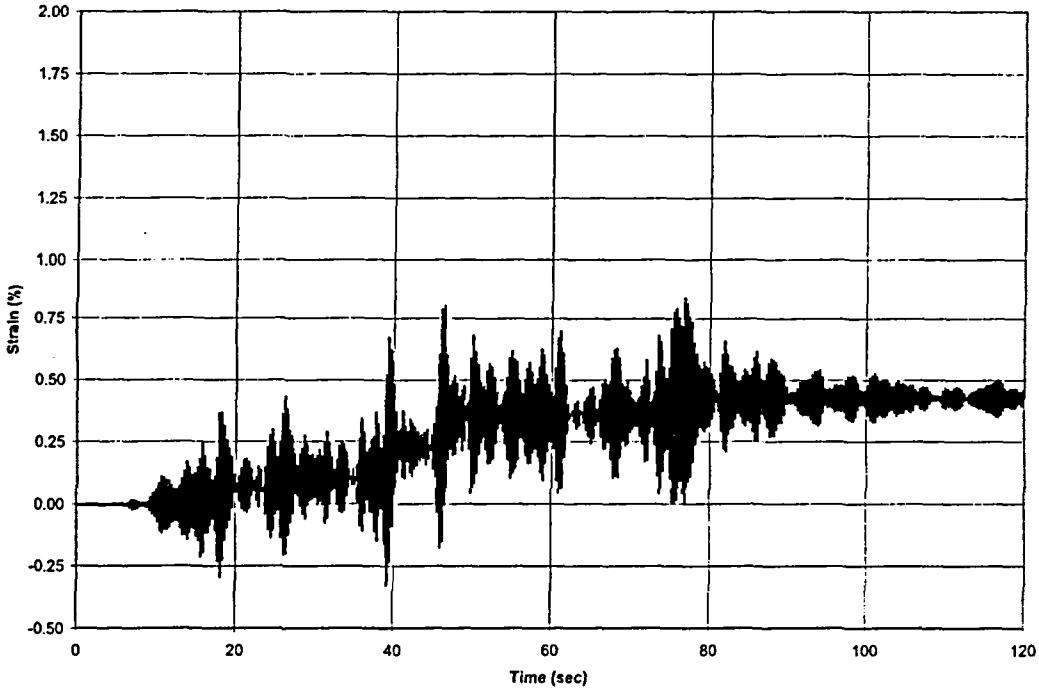

Figure 2-27 B-3 Test – Axial Strain at Nozzle – SA17-2A

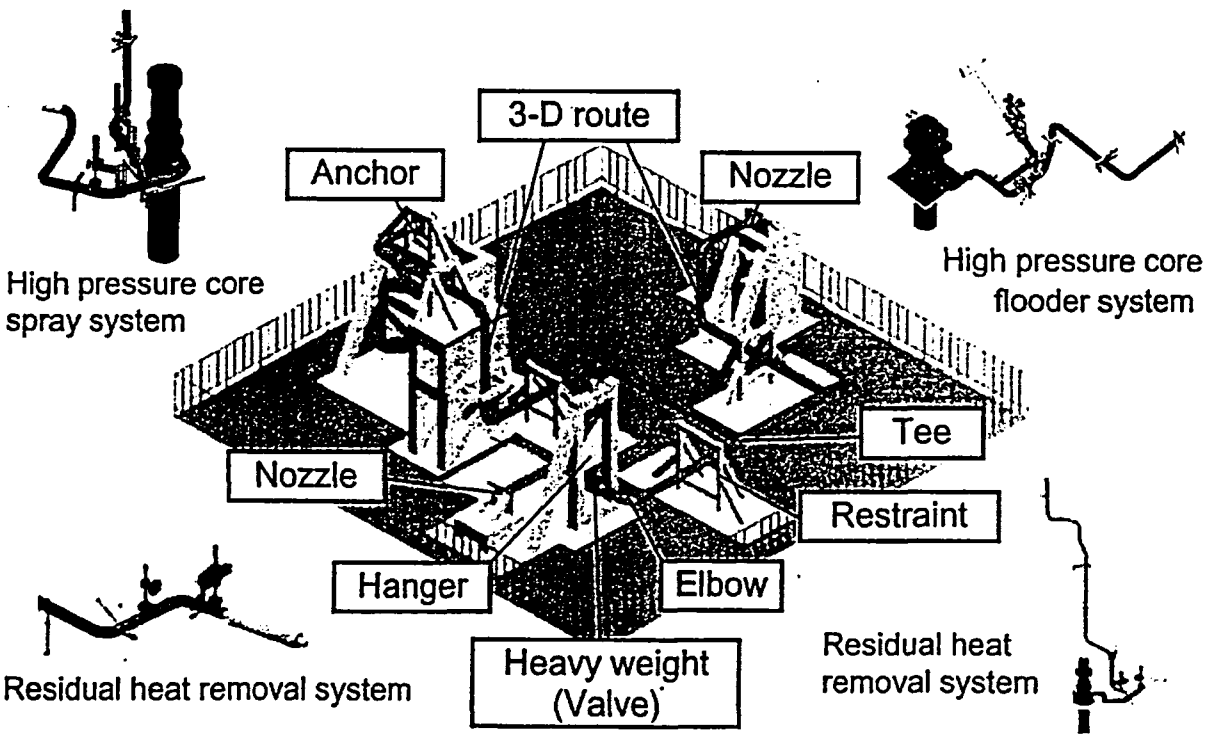

Figure 2-28 Large Scale Piping System Test Setup

3.0 BNL LINEAR ANALYSES AND CODE EVALUATIONS

3.1 Introduction

BNL conducted a series of linear elastic seismic analyses and ASME Code evaluations for the NUPEC simplified piping system tests. The primary objective of these studies was to calculate and compare the minimum factors of safety to failure in piping systems designed in accordance with different versions of the Code. In 1994, the ASME Code rules for seismic design of piping underwent a major revision based on a number of studies. Due to NRC staff concerns regarding the technical basis for the revisions, this Code version was not endorsed by the NRC. As a result of efforts to resolve the staff's concerns, the Code Committee proposed new rules in 2001. The new rules were approved with some additional changes and were incorporated into the 2004 Edition of the ASME Code.

Since the simplified piping system tests were expected to load the piping systems to stress levels beyond Code allowables, the test results would provide data on minimum safety margins in critical piping components designed in accordance with different Code rules. During the pre-test analysis phase of this program, BNL performed linear response spectrum analyses using the defined seismic wave input motions and carried out the Code evaluations in accordance with the NRC-endorsed (1993) Code rules, the 1994 revised rules and the 2001 proposed rules. During the test program, NUPEC determined that the damping values for the simplified piping systems were lower than anticipated and subsequently revised the table input motions in order to achieve the desired output. Therefore, during the post-test analysis phase of the program, BNL repeated these calculations using the revised seismic table motions and the different versions of the ASME Code rules. However, for these evaluations, the final 2004 rules were used in place of the proposed 2001 rules. The post-test analysis results are presented below.

3.2 ASME Code Criteria

The latest version of the ASME Code Piping Design Criteria endorsed by NRC is the 1992 Edition including the 1993 Addenda. The piping design rules are defined in Section III, Division 1, Subsections NB, NC, and ND for Class 1, 2 and 3 components, respectively. Stress limits for piping subjected to seismic and other Level D loads are given in paragraphs NB/NC/ND-3656. For Class 1 piping, the Code stress equation for Level D primary stresses is as follows:

$$B_1 \frac{PD_o}{2t} + B_2 \frac{D_o}{2I} M_i \leq 3.0 S_m \qquad (3\text{-}1)$$

where:

P = pressure
D_0 = outside diameter
t = wall thickness
B_1, B_2 = primary stress indices
I = moment of inertia
M_i = resultant moment
S_m = allowable stress intensity

The resultant moment term in the above equation includes deadweight, seismic and other Level D moments. The revised 1994 Addenda to the Code provided an alternate stress limit which was 50% higher than the old limit which could be applied when certain additional conditions were met. The new equation was:

$$B_1 \frac{PD_0}{2t} + B_2 \frac{D_0}{2I} M_E \leq 4.5 S_m \qquad (3\text{-}2)$$

The resultant moment term, M_E, in the above equation includes deadweight, seismic inertia and other "reversing" Level D moments. Additional conditions for application of this equation included the following:

(1) The analysis must be based on the linear elastic response spectrum method with 5% damping and 15% peak broadening.
(2) The ratio of outside pipe diameter to wall thickness shall not exceed 50.
(3) Stress due to weight moments is limited to 0.5 S_m.
(4) Stress due to seismic anchor motion moments is limited to 6 S_m.
(5) Stress due to seismic anchor motion longitudinal forces is limited to S_m.
(6) Maximum pressure during the SSE must not exceed the design pressure.

In 2001, the following changes were proposed to the alternate Level D primary stress limit equation:

$$B_1 \frac{PD_0}{2t} + B_2' \frac{D_0}{2I} M_E \leq 3.0 S_m \qquad (3\text{-}3)$$

where:

$B_2' = B_2$ for all piping components except:

$B_2' = ¾\ B_2$ for elbows, bends, and tees
$B_2' = 1.33$ for girth butt welds between items which do not have nominally identical thicknesses.

When this equation is used, the same additional conditions must be met, except that the ratio of outside pipe diameter to wall thickness shall not exceed 40. This equation reinstated the original 3.0 S_m stress limit but modified the stress indices for critical components. Compared to the 1993 Code, for straight pipes, the equation is identical to equation (3-1). For elbows, bends and tees, the change is approximately equivalent to using a stress limit of 4.0 S_m in equation (3-1). For girth butt welds at equipment nozzles, the change is approximately equal to a stress limit of 2.25 S_m in equation (3-1).

Equation (3-3) and the new B_2' stress indices for seismic loads listed above were acceptable to the NRC staff and would have been formally endorsed. However, ASME comments submitted March 22, 2004, on the proposed 10 CFR 50.55a rulemaking (Federal Register Volume 69, Number 4, January 7, 2004) indicated that these B_2' stress indices were a typographical error that will be corrected by an errata. According to the ASME position, the criteria should be $B_2' = 2/3\ B_2$ for elbows, bends, and tees. Subsequently, the following alternate Code stress equation for seismic and other "reversing" stresses was published in the 2004 Edition of the ASME Code as follows:

$$B_1 \frac{PD_0}{2t} + B_2' \frac{D_0}{2I} M_E \leq 3.0 S_m \qquad (3\text{-}4)$$

where:

$B_2' = B_2$ for all piping components except:

$B_2' = 2/3\ B_2$ for elbows, bends, and tees
$B_2' = 1.33$ for girth butt welds between items which do not have nominally identical thicknesses.

As in Equations (3-2) and (3-3) above, the resultant moment term, M_E, includes deadweight, seismic inertia and other "reversing" Level D moments. Additional conditions for application of this equation are the same as those for Equation (3-3):

(1) The analysis must be based on the linear elastic response spectrum method with 5% damping and 15% peak broadening.
(2) The ratio of outside pipe diameter to wall thickness shall not exceed 40.
(3) Stress due to weight moments is limited to 0.5 S_m.
(4) Stress due to seismic anchor motion moments is limited to 6 S_m.
(5) Stress due to seismic anchor motion longitudinal forces is limited to S_m.
(6) Maximum pressure during the SSE must not exceed the design pressure.

Compared to the 1993 Code, for straight pipes, this equation is identical to equation (3-1). For elbows, bends and tees, the change is approximately equivalent to using a stress limit of 4.5 S_m in equation (3-1). For girth butt welds at equipment nozzles, the change is approximately equivalent to a stress limit of 2.25 S_m in equation (3-1). Although this alternate stress criterion has been published in the 2004 Edition of the ASME Code, to date, it has not been endorsed by the NRC.

3.3 Linear Analysis and Evaluation of Simplified Piping Systems

The two-dimensional (Model A) and three-dimensional (Model B) simplified piping systems were analyzed and evaluated using ASME Code seismic criteria by applying linear analysis methods and assumptions in accordance with nuclear industry practice. For consistency with the nonlinear simulation analyses performed under this program, the ANSYS general purpose finite element analysis code [3] was used. Both the Model A and Model B piping specimens were modeled using ANSYS three-dimensional linear elastic straight pipe (PIPE16) and curved pipe (PIPE18) elements as shown in Figures 3-1(a) and 3-1(b). MASS21 elements were used to represent the added masses attached to the pipes. For the pre-test analyses, it was assumed that the added masses would also provide additional stiffness to the pipes. Therefore, over the length of the added masses, the pipe's cross-sectional properties were modified to reflect the rigid stiffness of the added masses. However, frequency test results for the actual piping specimens demonstrated that this assumption resulted in excessively stiff piping models with higher frequencies than were observed in the tests. Therefore, for the post-test analyses, the stiffnesses at the locations of the added masses were not included. This modeling assumption is consistent with the final nonlinear models as discussed in Section 5.3 of this report. In Model B, the nozzle was represented by a series of straight pipe elements with cross-sectional properties of the nozzle. The spring hangers in Model B were represented by linear spring elements (COMBIN14). Model A boundary conditions included vertical translational restraint at the large mass rollers and restraint of all translations and horizontal axis rotations at the pinned supports. In Model B, the nozzle end nodes and spring hanger ground attachment point nodes were fully restrained, and pinned support point nodes were restrained from all translations and from rotations about the horizontal axes.

Linear response spectrum analyses were performed in accordance with industry practice and regulatory guidelines [4] for piping design with only two exceptions: (1) since actual piping dimensions had been provided by NUPEC, as-built rather than design dimensions were used in the models; and (2) since the input motion was defined and the objective was to identify minimum margins to failure, unbroadened

instead of broadened response spectra were applied in the analyses. The response spectra for two-dimensional simplified piping tests A-1 and A-2 are shown in Figures 3-2 and 3-3. The response spectra for the three-dimensional piping tests B-1, B-2 and B-3 are shown in Figures 3-4 through 3-7. The modal damping values used in the analyses were consistent with the practices and requirements of the respective Code version. The 1993 Code version did not specify a damping value for analysis. For this case, two different analyses were performed with damping values based on industry practice. In the first analysis, two percent damping was used based on NRC Regulatory Guide 1.61 for pipe diameters less than 12 inches (300 mm). In the second analysis, frequency dependent damping values based on ASME Code Case N-411 damping were used. These values are 5 percent for modes with frequencies less than 10 Hz and 2 percent for modes with frequencies greater than 20 Hz. For frequencies between 10 Hz and 20 Hz, the damping values are linearly interpolated between 2 and 5 percent. For the 1994 and 2004 Code versions, both analyses used the Code-specified value of five percent damping.

Linear analyses were carried out for pressure, deadweight and seismic loading. For each test case, the results were post-processed to calculate stresses in accordance with the three different code versions. The highest stresses in the critical components (elbows for Model A; elbows, tee, and nozzle for Model B) were determined in accordance with the different equations, stress indices and stress allowables of each code version. The component with the largest ratio of stress to allowable stress was identified as the critical component. The results for each load case are summarized in Tables 3-1 though 3-5.

In order to properly interpret the results of these analyses, it should be noted that the "margins" presented in Tables 3-1 through 3-5 represent the ratios of the highest stress in a piping system (calculated in accordance with the specific code version rules which include the stress equation, stress indices, and damping) divided by the allowable stress (defined by the specific code version). Since none of the simplified piping systems failed during a single seismic load application, they should not be interpreted as margins to failure. Instead they should be considered minimum margins to failure or minimum Code stress margins. For example, Table 3-1 shows that the piping system in test A-1 was able to sustain a maximum stress equal to 2.99 times the Code allowable without failure according to the rules of 1993 ASME Code and R.G .1.61 damping. The same test shows that the piping system was able to sustain a maximum stress of 1.20 times the Code allowable according to the 2004 ASME Code rules. Had the test been conducted to higher stress levels resulting in failure the calculated margins to failure would have been proportionally higher.

In addition to providing information on minimum margins to failure, the results provide a measure of the relative safety margins between the different code versions. The margins in Table 3-1 indicate that the 1994 and 2004 Code rules would provide essentially equal margins to failure while the 1993 rules with N-411 damping would provide 50% greater margin. The 1993 rules with R.G. 1.61 damping would provide about 150% greater margin. The margin comparisons can be used to evaluate the relative conservatisms between the different Code versions.

For both the A-1 and A-2 tests, the highest stresses were at Elbow A. Since the level of input excitation was greater in the A-2 test, the margins were also greater for all code versions. The 1994 and 2004 Code calculations provided nearly identical margins of 1.83 and 1.84, respectively. The 1993 Code calculations provided margins of 2.74 with N-411 damping and 3.56 with R.G. 1.61 damping.

For the Model B tests, the stresses and margins were generally lower. In the B-1 and B-3 tests, the highest stresses were either at the tee or at the nozzle weld. Stresses at these locations were very close in value in nearly all cases except for the 2004 code stress calculation which has lower stress indices for tees and higher indices for nozzle welds. In the B-2 vertical motion test, the stresses were always highest at the nozzle weld but the magnitudes were lower and the margins were less than one in all cases. The highest margins were in the B-3 (horizontal + vertical) tests. The 2004 Code calculations provided a

margin of 1.76 at the nozzle weld. The other code versions also provided highest stresses at the nozzle welds. The margin based on the 1994 Code was less than one (0.91). The margins based on the 1993 version were 1.37 with N-411 damping and 1.85 with R.G. 1.61 damping.

In summary, the linear analyses described above demonstrated that the NUPEC simplified piping system high level seismic tests subjected the piping components to stresses well above Code allowables. By performing analyses and evaluations in accordance with different versions of the Code rules, minimum margins to failure were determined, and the relative differences in safety margins between the different versions were compared for the tested components. Based on the 2004 Code rules, these evaluations demonstrated minimum margins to failure of 1.84 for elbows and 1.76 for nozzle welds. The most conservative margins were provided by the 1993 Code version with R.G. 1.61 damping. Those evaluations demonstrated minimum margins to failure of 3.56 for elbows and 1.85 for nozzle welds. It should be clearly noted, however, that these margins are simply minimum safety margins based on the limited simplified piping system test data. Since no pipe failures were observed during a single test, the actual margins to failure are higher. As discussed in Section 2.4 of this report, NUPEC conducted tests to failure for a Model A and a Model B piping system. For the Model A test, a crack at the Elbow A location occurred after five high level seismic tests. For Model B, a nozzle crack was observed after 18 applications of a high level seismic time history. The failures in both cases were attributed to fatigue cracking.

Table 3-1 A-1 Test Maximum Code Stresses and Margins

Code Edition	Damping	Maximum Stress (MPa)	Critical Location	Stress/Allowable (Margin)
1993	R.G. 1.61	1228	Elbow A	2.99
1993	N-411	731	Elbow A	1.78
1994	5%	731	Elbow A	1.19
2004	5%	492	Elbow A	1.20

1 MPa = 145 psi

Table 3-2 A-2 Test Maximum Code Stresses and Margins

Code Edition	Damping	Maximum Stress (MPa)	Critical Location	Stress/Allowable (Margin)
1993	R.G. 1.61	1461	Elbow A	3.56
1993	N-411	1126	Elbow A	2.74
1994	5%	1126	Elbow A	1.83
2004	5%	755	Elbow A	1.84

1 MPa = 145 psi

Table 3-3 B-1 Test Maximum Code Stresses and Margins

Code Edition	Damping	Maximum Stress (MPa)			Critical Location	Stress/Allowable (Margin)
		Elbow	Tee	Nozzle		
1993	R.G. 1.61	564	733	728	Tee	1.78
1993	N-411	405	536	539	Nozzle Weld	1.31
1994	5%	405	536	539	Nozzle Weld	0.87
2004	5%	274	424	692	Nozzle Weld	1.68

1 MPa = 145 psi

Table 3-4 B-2 Test Maximum Code Stresses and Margins

Code Edition	Damping	Maximum Stress (MPa)			Critical Location	Stress/Allowable (Margin)
		Elbow	Tee	Nozzle		
1993	R.G. 1.61	117	124	262	Nozzle Weld	0.64
1993	N-411	98	109	226	Nozzle Weld	0.55
1994	5%	98	109	226	Nozzle Weld	0.37
2004	5%	70	93	276	Nozzle Weld	0.67

1 MPa = 145 psi

Table 3-5 B-3 Test Maximum Code Stresses and Margins

Code Edition	Damping	Maximum Stress (MPa)			Critical Location	Stress/Allowable (Margin)
		Elbow	Tee	Nozzle		
1993	R.G. 1.61	577	747	759	Nozzle Weld	1.85
1993	N-411	413	544	564	Nozzle Weld	1.37
1994	5%	413	544	564	Nozzle Weld	0.91
2004	5%	280	430	725	Nozzle Weld	1.76

1 MPa = 145 psi

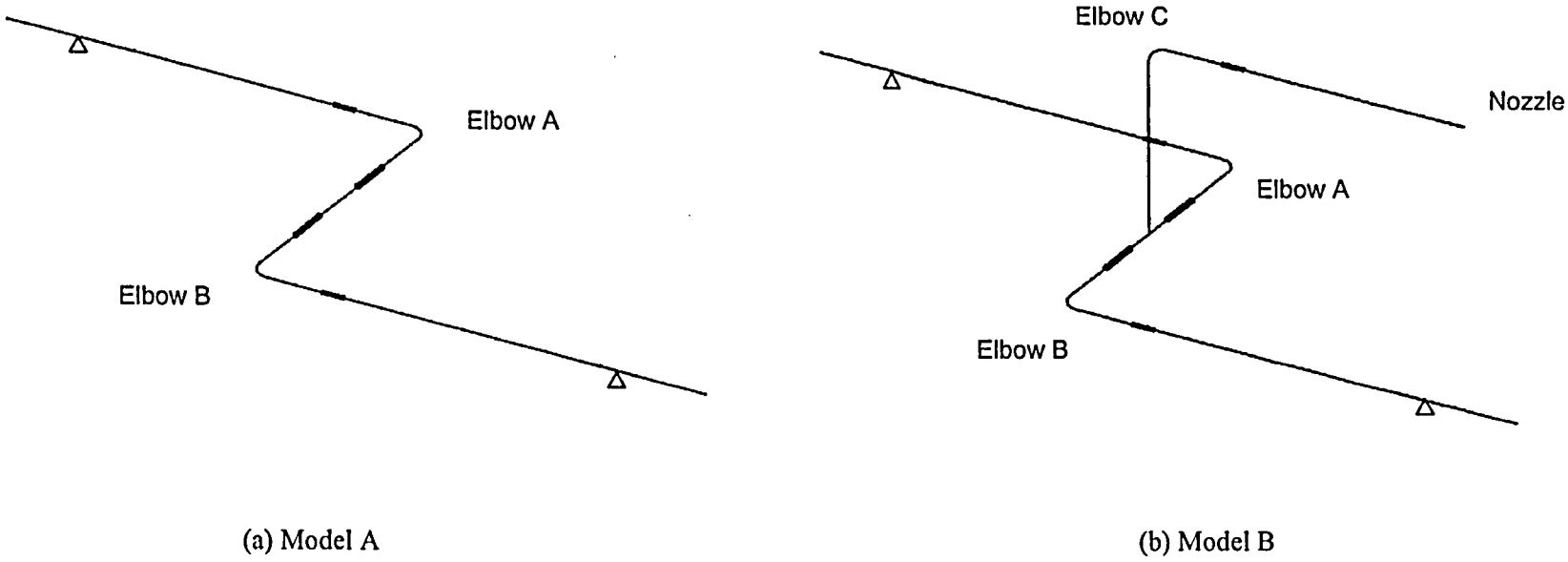

(a) Model A

(b) Model B

Figure 3-1 Simplified Piping System Test – Models A and B
Linear Elastic ANSYS Pipe Element Models

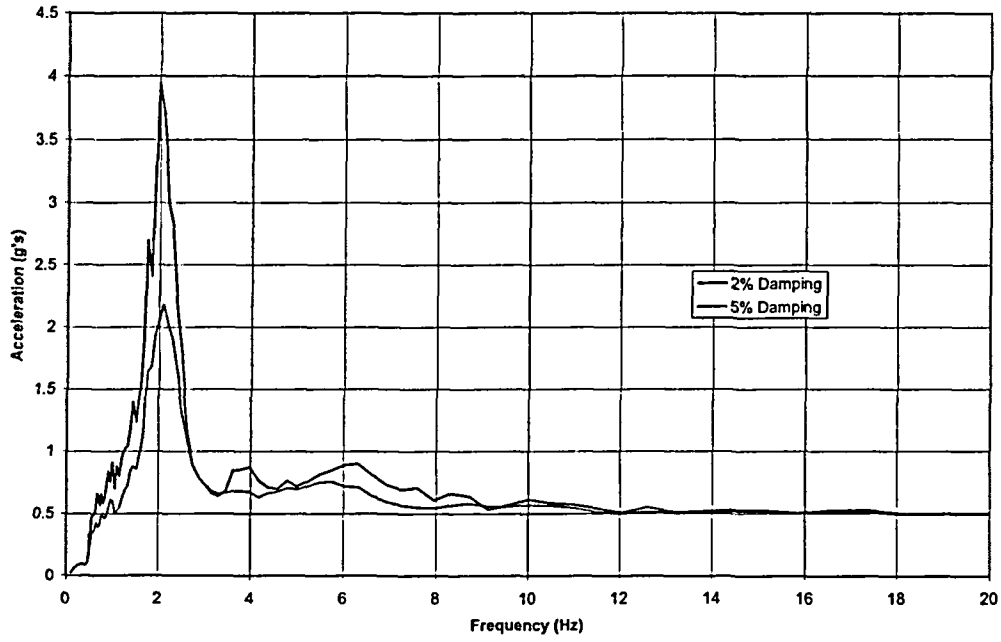

Figure 3-2 A-1 Test Horizontal Response Spectrum (2% and 5% Damping)

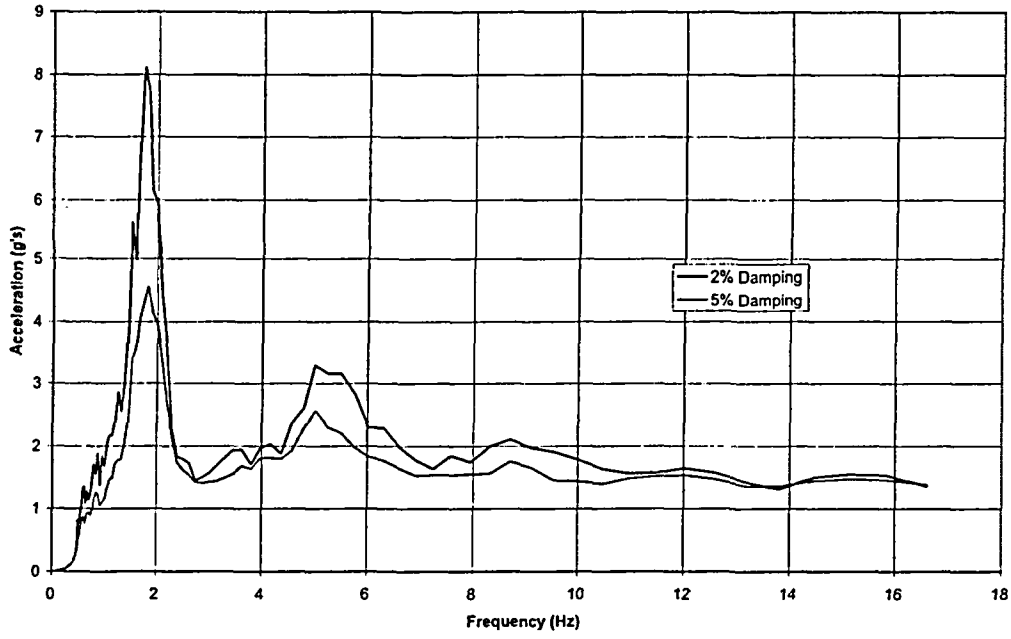

Figure 3-3 A-2 Test Horizontal Response Spectrum (2% and 5% Damping)

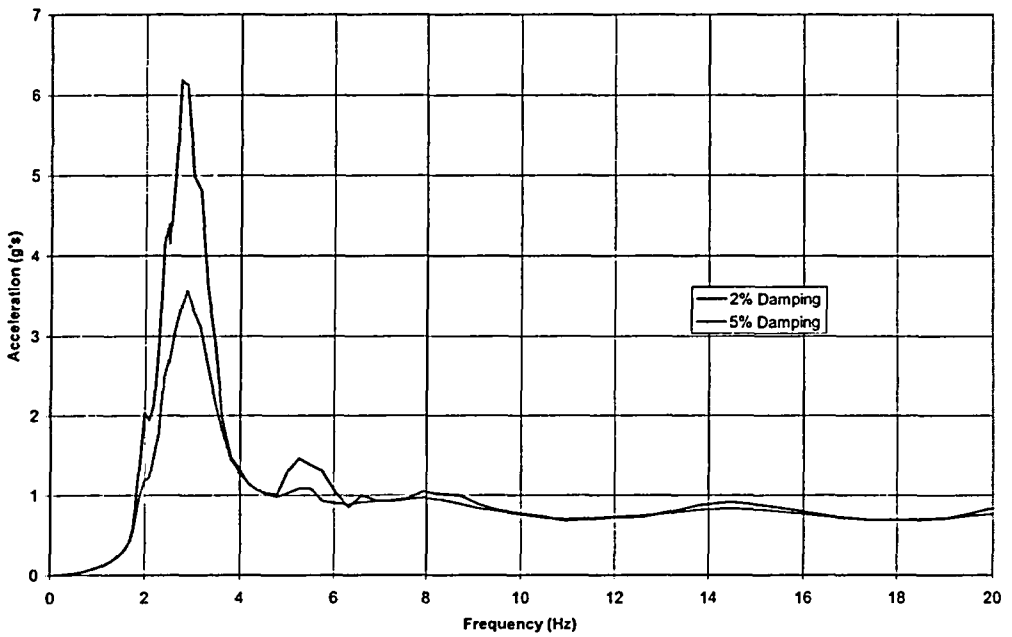

Figure 3-4 B-1 Test Horizontal Response Spectrum (2% and 5% Damping)

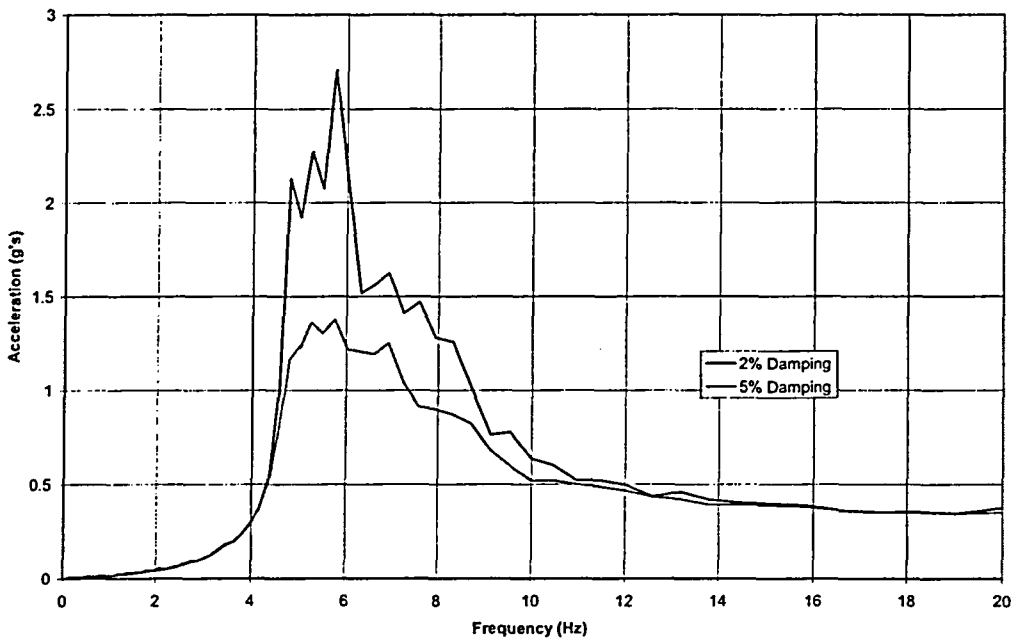

Figure 3-5 B-2 Test Vertical Response Spectrum (2% and 5% Damping)

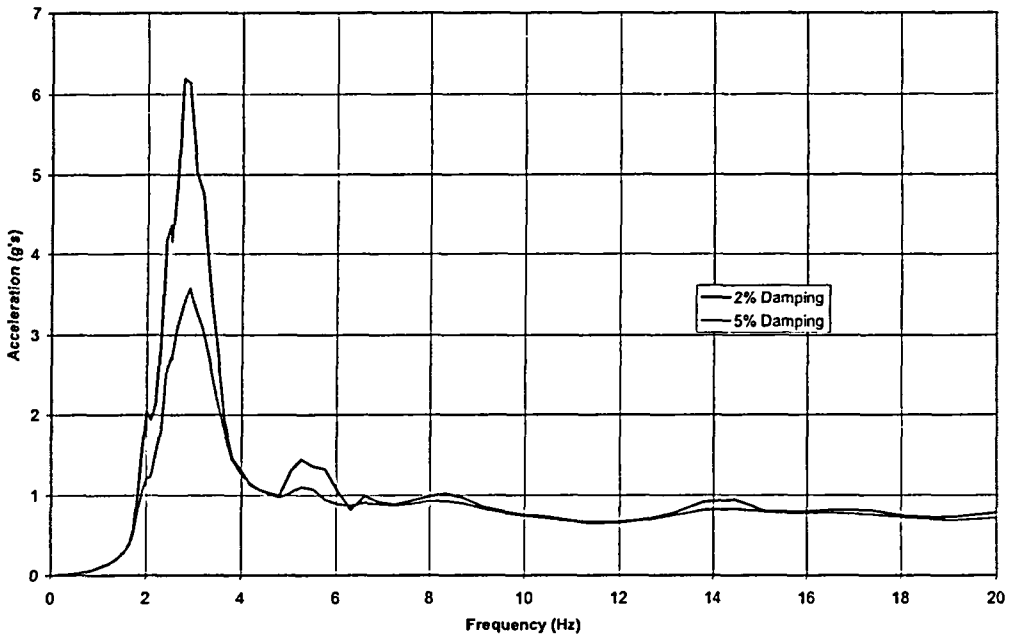

Figure 3-6 B-3 Test Horizontal Response Spectrum (2% and 5% Damping)

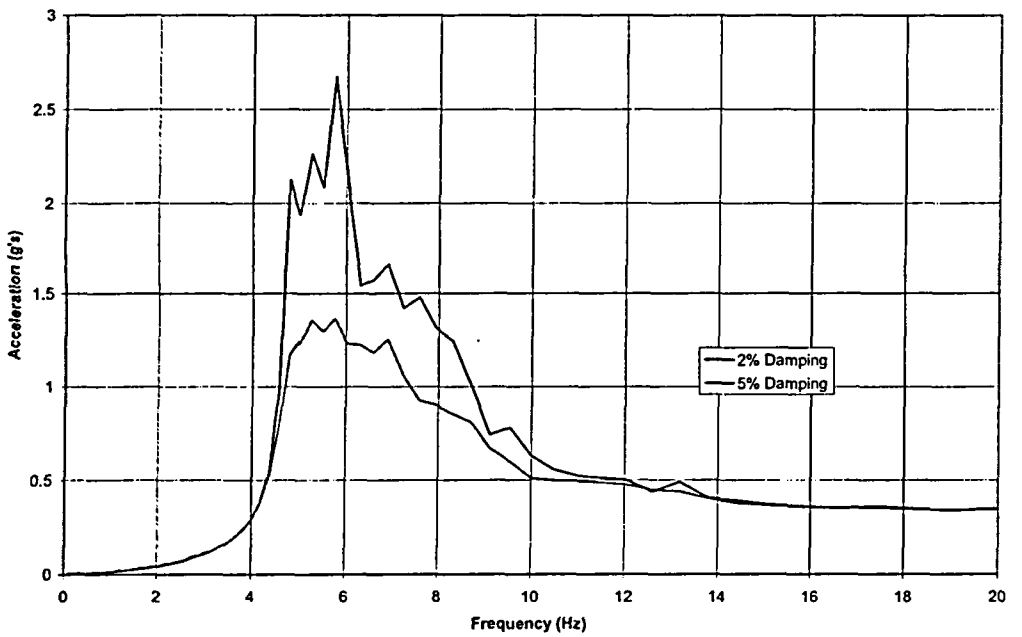

Figure 3-7 B-3 Test Vertical Response Spectrum (2% and 5% Damping)

4.0 BNL COMPONENT TEST NONLINEAR ANALYSES

4.1 Introduction

A major goal of the NRC/BNL collaboration effort was the performance of pre-test and post-test analyses for selected piping component and piping system tests. The objective of these analyses was to investigate and evaluate the adequacy of current commercially available methods and computer programs for predicting the elasto-plastic response of piping systems subjected to large earthquake loads. Upon initiation of the collaborative effort, NUPEC indicated that the ABAQUS computer program would be used by NUPEC to perform their analyses. In order to complement the NUPEC analytical effort, BNL selected the ANSYS computer program [3] for performing these analyses. ANSYS is a widely used, general-purpose finite element analysis program. In recent years, the program was enhanced to include a number of improvements in its nonlinear analysis capability. Among these improvements was the inclusion of the Chaboche nonlinear kinematic hardening model [5]. This plasticity model was expected to provide better simulation of the strain ratcheting behavior that a pressurized pipe is expected to exhibit under seismic loading than is possible with classical linear hardening models.

The major focus of the BNL simulation analyses was on the prediction of selected simplified piping system test responses. These included the two-dimensional Model A test load cases A-1 and A-2, and the three-dimensional Model B test load cases B-1, B-2, and B-3. However, in order to develop, calibrate and test elasto-plastic elbow components for the simplified piping system nonlinear models, analyses were performed to simulate the elbow component static cycling test SE-4. Results of the NUPEC material tests were used to develop the plastic material properties needed in the component and piping analyses. The following sections describe the modeling and analysis approach, and the analysis results for the elbow component test.

4.2 Development of Piping Elbow Model

The overall flexibility and dynamic properties of a piping system are typically dependent on the flexibility of the elbows in the system. Furthermore, under large seismic deformations, the largest plastic strains are expected to be concentrated in the elbows. Therefore, the development of accurate detailed finite element models of the piping system elbows was a critical step in the simulation analysis. A shell element model of the elbow used in static component test SE-4 was first developed and compared with the test data. The test specimen was a 65 mm (2 ½ inch) Schedule 40 carbon steel long radius elbow. At each end, the elbow was welded to a short section of straight pipe which terminated at a welded flange. Details of the specimen configuration are shown in Figure 4-1 and the test setup is shown in Figure 2-5. As-built measurements of the specimen outer diameter and wall thickness at various cross-sections were provided by NUPEC. The pipe was filled with water and pressurized to 19.8 MPa (2870 psi). The test was conducted at room temperature. Cyclic displacement of ±15.5 mm (±0.6 in) was applied at the ends of the specimen at a frequency of one cycle/min.

The ANSYS finite element model of the SE-4 test elbow is shown in Figure 4-2. The model utilized ANSYS SHELL181 large strain shell elements to represent the pipe wall. This element is appropriate for analyzing thin to moderately-thick shell structures. It is a four-noded element with six degrees of freedom at each node. This type of element is well suited for linear, large rotation, and large strain nonlinear applications. The element can be used with all ANSYS kinematic hardening plasticity models including Chaboche nonlinear kinematic hardening. The triangular option of this element was used to represent the flanges at the ends of the pipe. ANSYS elastic pipe elements (PIPE16) with rigid stiffness properties were used to represent the end links that connect the pipe to the test fixture. Since the test specimen was symmetric about two perpendicular planes, a quarter model with appropriate symmetry

boundary conditions was used. The pipe diameter and thickness of the shell element model was based on an average of the as-built values provided by NUPEC.

The elastic and plastic material properties for the elbow models were based on NUPEC material test data for carbon steel (STS410) specimens. The elastic modulus used for all models was 203,000 MPa (29.4 x 10^6 psi) which was based on a monotonic tension test (MTT-1-1). The stress-strain curve for this test is shown in Figure 2-2. The development of plasticity parameters was dependent on the plasticity model. Analyses were performed using three different plastic hardening models. The development of the plasticity parameters for the pipe is described in the next section.

4.3 Development of Plasticity Models

Plasticity theory provides a mathematical relationship that characterizes the elasto-plastic response of materials. The theory considers three basic components: the yield criterion, the flow rule, and the hardening rule. The yield criterion determines the stress level at which yielding is initiated. The flow rule determines the direction of plastic straining. The hardening rule describes the changes in the yield surface with progressive yielding, so that the stress states for subsequent yielding can be established. The ANSYS program provides several options for characterizing elasto-plastic material behavior. In performing the simulation analyses under this collaboration program, three different plasticity options were investigated: classical bilinear kinematic hardening, multilinear kinematic hardening, and nonlinear kinematic hardening. These options are based on the von Mises yield criterion, the associated flow rule, and different variations of kinematic hardening models as described below.

The kinematic hardening rule assumes that the difference between yield stresses under tension and compression loadings remains constant. Under plastic deformation, the elastic domain will retain a constant size but will move about in the stress space by translation. This translation can be characterized in terms of the location of the center of its elastic domain or yield surface, which is also referred to as a backstress. The ANSYS classical bilinear kinematic hardening option is based on the linear kinematic hardening rule introduced by Prager [6]. This theory assumes that the center of the yield surface moves linearly with plastic strain. For the simple case of uniaxial loading, this rule is expressed by the following incremental equation:

$$d\alpha = C_0 d\varepsilon_p \tag{4-1}$$

where α is the center of the yield surface (backstress), ε_p is the plastic axial strain, and C_0 is a material constant equal to the plastic modulus. The total stress during plastic flow is expressed as follows:

$$\sigma = \alpha \pm \sigma_0 \tag{4-2}$$

where σ is the total axial stress and σ_0 is the yield stress, and the sign is dependent on the direction of plastic flow. In applying the bilinear kinematic hardening (BKIN) option of ANSYS, the material stress-strain curve is represented as a bilinear curve in which the first slope represents the elastic modulus up to the yield stress, and the second slope represents a linear plastic modulus. When a material is loaded into the plastic range and subsequently unloaded, the reverse path follows the elastic slope back to a range of twice the yield stress and then follows the plastic slope.

The multilinear kinematic hardening (MKIN) option in ANSYS is based on the Besseling multilayer model [7]. When this rule is applied, the stress-strain curve is represented by several linear segments. This allows for a more accurate representation of a stress-strain curve. Under reversed loading, the load path again follows the elastic slope back to twice the yield stress and then follows the path of the multiple

plastic slopes. However, using either rule, the plastic modulus is always the same for loading and unloading and is unaffected by the presence of a mean stress. As a result, for a prescribed uniaxial stress cycle with a mean stress, the loading and reversed loading hysteresis curves will always produce a closed loop with no ratcheting.

The nonlinear kinematic hardening option (CHAB) in ANSYS is based on the work of Chaboche [5] who proposed the superposition of several "decomposed" Armstrong-Frederick hardening rules. Armstrong and Frederick [8] had introduced a nonlinear kinematic hardening rule with a "recall" term which introduced a fading memory effect of the strain path. For the case of uniaxial tension-compression loading, the translation of the yield surface is expressed by the following incremental equation:

$$d\alpha = Cd\varepsilon_p - \gamma\alpha\left|d\varepsilon_p\right| \tag{4-3}$$

where C and γ are material dependent constants. In applying this rule, the plastic modulus, H, is expressed by the following equation:

$$H = C \mp \gamma\alpha \tag{4-4}$$

In this equation, the negative sign is used for the forward loading curve and the positive sign is used for the reverse loading curve. This rule provides an exponential plastic modulus. For a uniaxial stress cycle with mean stress, this rule produces changes in shape between forward and reverse loading paths. Therefore the loop does not close and ratcheting occurs. A disadvantage of this model, however, is that an experimental stress-strain curve is not necessarily exponential in nature and an attempt to simulate it by a single exponential equation does not yield a good fit. In addition, for a high strain range, the model does not produce a constant plastic modulus as exhibited in experiments, but will instead always stabilize to a zero plastic modulus.

In order to improve the simulation of the hysteresis loop, Chaboche proposed the superposition of three hardening rules. The first rule (α_1) should simulate the initial high plastic modulus at the onset of yielding; the second rule (α_2) should simulate the transient nonlinear portion of the curve; and the third rule (α_3) should be a linear hardening rule ($\gamma_3 = 0$) to represent the subsequent linear part of the hysteresis curve at a high strain range. As is the case for the single Armstrong-Frederick rule, for a uniaxial stress cycle with mean stress, the rule will also produce a change in shape between the forward and reverse loading paths which results in ratcheting. However, because of the incorporation of the linear kinematic hardening rule (α_3), this model will eventually approach the complete shakedown of ratcheting which is not in agreement with experimental results. The ratcheting simulation can be improved by assigning a small value to γ_3, which introduces a slight nonlinearity which will improve the ratcheting simulation without producing a noticeable change in the hysteresis loop. The procedure for defining the parameters is described in the next section.

4.4 Determination of Material Parameters

The NUPEC material tests provided the basic material parameters needed for each of the three plasticity options investigated. The methodology used to define the parameters is described below.

4.4.1 Bilinear Kinematic Hardening Model

The stress-strain curve from a monotonic uniaxial tensile test of an STS410 carbon steel test specimen was used to define the parameters for the bilinear kinematic hardening (BKIN) model. The parameters included modulus of elasticity, yield stress, and plastic modulus. Consistent with the theory, the plastic

modulus was assumed to be constant and was approximated from the slope of the stress-strain curve from the yield strain to 3 percent strain as shown in Figure 4-3. The values used for this model were 203000 MPa (29.4 x 10^6 psi) for the elastic modulus, 1220 MPa (177000 psi) for the plastic modulus, and 270 MPa (39000 psi) for the yield stress.

4.4.2 Multilinear Kinematic Hardening Model

The cyclic stress-strain curve developed from a uniaxial strain cycling test of an STS410 carbon steel test specimen was used to define the parameters for the multilinear kinematic hardening (MKIN) model. The stress-strain curve was approximated by nine linear segments from zero to 2.5 percent strain as shown in Figure 4-3.

4.4.3 Chaboche Nonlinear Hardening Model

The Chaboche (CHAB) model required the definition of elastic modulus, yield stress, and the C_i and γ_i constants for each of the three Armstrong-Frederick hardening rules. A procedure for determination of the C and γ parameters was described by Bari and Hassan [9]. All parameters, except for γ_3, were determined from the stress-strain hysteresis curves generated from a strain-controlled uniaxial strain cycling test of an STS410 carbon steel test specimen shown in Figure 2-3. The procedure specifies that the decomposed backstress terms (α_1 or α_2) should start from $-C_i/\gamma_i$ at the starting plastic strain $-\varepsilon_{pl}$ and reach a value of C_i/γ_i at the final plastic strain ε_{pl}. The third linear backstress term should go through the origin. The equations used for the loading part of the hysteresis curve are as follows:

$$\sigma = \sigma_0 + \sum_{i=1}^{3} \alpha_i \tag{4-5}$$

$$\alpha_i = \frac{C_i}{\gamma_i}\left[1 - 2\exp\left\{-\gamma_i\left(\varepsilon_p - \left(-\varepsilon_{pl}\right)\right)\right\}\right], \text{ for } i = 1 \text{ and } 2 \tag{4-6}$$

$$\alpha_3 = C_3\varepsilon_p \tag{4-7}$$

where ε_{pl} is the strain limit of the stable hysteresis loop. The procedure first required the selection of a hysteresis loading curve with a reasonably large strain range. The yield stress and yield strain were then estimated from the curve and the curve was adjusted for elastic strain to produce a stress versus plastic strain plot. Using the above equations, the C_i and γ_i parameters were selected to match this test curve. A spreadsheet program was used to compare the loading part of the hysteresis test curve to the σ curve from Eq. (4-5). The C_3 parameter was first selected to match the slope of the linear segment of the hysteresis curve at a high strain range. The C_1 parameter was next selected as a large value such that the slope of α_1 nearly matched the plastic modulus at initial yielding, and the corresponding γ_1 value was also a large value to stabilize the hardening of α_1 immediately. The C_2 and γ_2 parameters were selected by trial and error to match the overall shape of the curve. Additional adjustments to C_1 and γ_1 were then made to match the initial slope of the test curve as well as the stress at both the start and end points. Figure 4-4 illustrates the contribution of each rule to the simulation of the stress-strain curve, and compares the final analytical stress-stress curve to the test curve. As suggested in [9], the final parameter, γ_3, may be determined from a uniaxial ratcheting test to provide a best fit. However, for this analysis effort, this parameter was determined from the results of an elbow component test strain cycling test as described below. The parameters determined for the simulation analyses using the Chaboche nonlinear hardening model were as follows: σ_0 = 270 MPa (39000 psi), E =203000 MPa (29.4 x 10^6 psi), C_1 = 70000 MPa (10.2 x 10^6 psi), C_2 = 30000 MPa (4.35 x 10^6 psi), C_3 = 1200 MPa (174000 psi), γ_1 = 3500, γ_2 = 210, γ_3 =1.

4.5 Elbow Static Cycling Test Nonlinear Analysis

As a preliminary test of the ANSYS shell element elbow model, a nonlinear static cycling analysis was performed to simulate the elbow component test SE-4. The quarter elbow model shown in Figure 4-2 was subjected to a constant internal pressure of 19.8 MPa (2870 psi) and equivalent cyclic end displacements of ±15.5 mm (±0.6 in) were imposed statically for 185 cycles. A separate analysis was performed for each of the three plastic hardening rules as described below. Additional analyses investigated the significance of geometric deformation effects by applying the large deflection analysis option in ANSYS and comparing results against those obtained using the small deflection analysis option. These studies demonstrated that the changes in geometric configuration due to elbow ovalization had a very small effect on elbow load deflection characteristics and on strain ratcheting. Therefore these effects were judged to be insignificant within the range of this application, and the final analyses presented below were based on small deflection theory.

For in-plane loading of elbows, the maximum strain is expected to occur at the elbow flank. The outer surface of the elbow flank was instrumented with strain gages which were monitored during the test. In the SE-4 test, the elbow was cycled until crack penetration occurred at the flank at 185 cycles. The hoop strain versus cycle history measured during the test is shown in Figure 4-5(a). As expected, significant strain ratcheting was observed during the test. As shown in the Figure 4-5(a), the rate of strain ratcheting was highest during initial cycling and then leveled off to a nearly constant rate until failure. Shakedown did not occur. At failure, the accumulated hoop strain was nearly 15 percent.

The corresponding strain histories predicted by the ANSYS nonlinear analyses using the three plastic hardening models are shown in Figures 4-5(b), 4-5(c), and 4-5(d). Using the bilinear kinematic hardening model (BKIN), initial strain ratcheting was overpredicted during the first ten cycles. The rate of strain then leveled off to zero (shakedown) with no additional strain accumulation. At 185 cycles, the accumulated strain was about 7 percent. The multilinear kinematic hardening model (MKIN) analysis predicted shakedown after only five cycles with a total strain accumulation of only 2 percent at 185 cycles.

As described in Section 4.4.3 above, the parameters needed for the Chaboche nonlinear kinematic hardening model (CHAB) were determined from a strain-controlled uniaxial strain cycling test of an STS410 carbon steel test specimen with the exception of the γ_3 parameter. This parameter was chosen by performing parametric studies which varied the γ_3 parameter and selecting the value that provided the best match to the strain ratcheting results. The first analysis used a value of γ_3 equal to zero. The hoop strain versus cycle history is shown in Figure 4-5(d). This curve provided a better simulation of the initial strain ratcheting behavior but also gradually leveled off and achieved shakedown with an accumulated strain of 8 percent. Results of analyses using γ_3 values of 1 and 2 are also shown in Figure 4-5(d). These strain histories more accurately simulated the test results by leveling off to a nearly constant rate of ratcheting. The analysis with a γ_3 value of 1 provided the best match to test results and was used in subsequent analytical models.

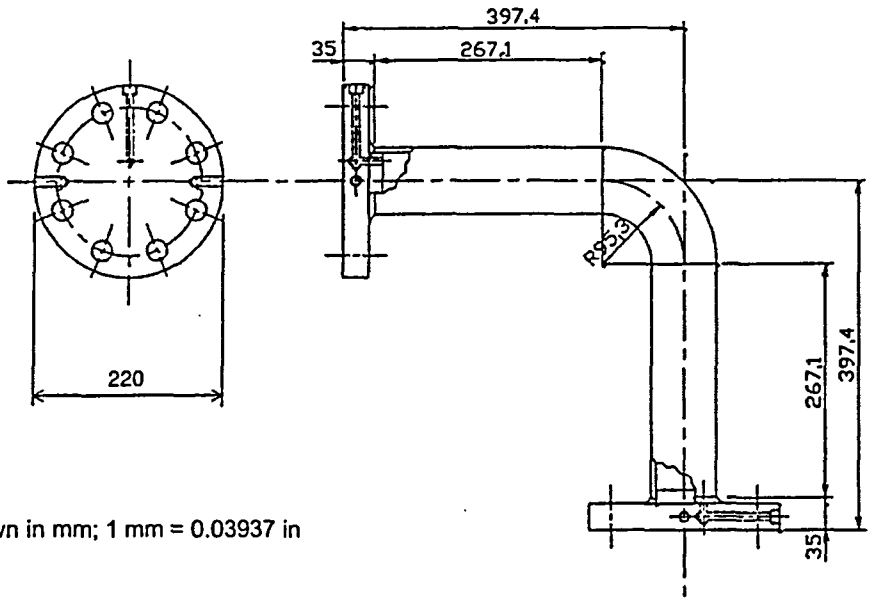

Dimensions shown in mm; 1 mm = 0.03937 in

Figure 4-1 SE-4 Component Test Elbow Specimen

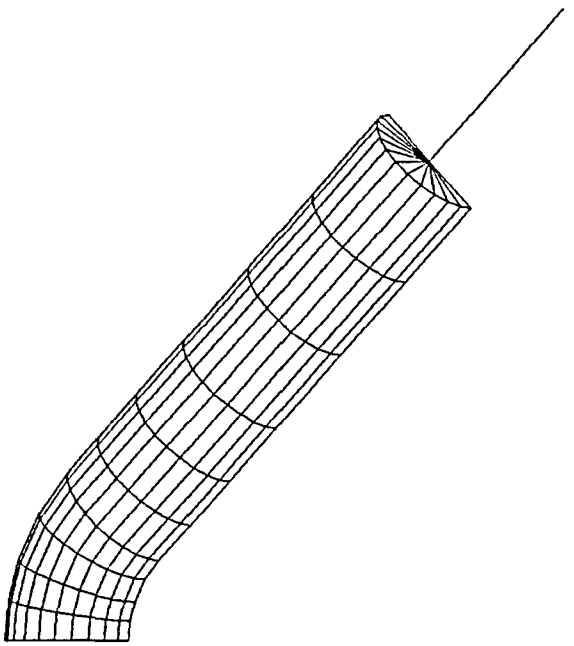

Figure 4-2 SE-4 Test ANSYS Shell Element Model

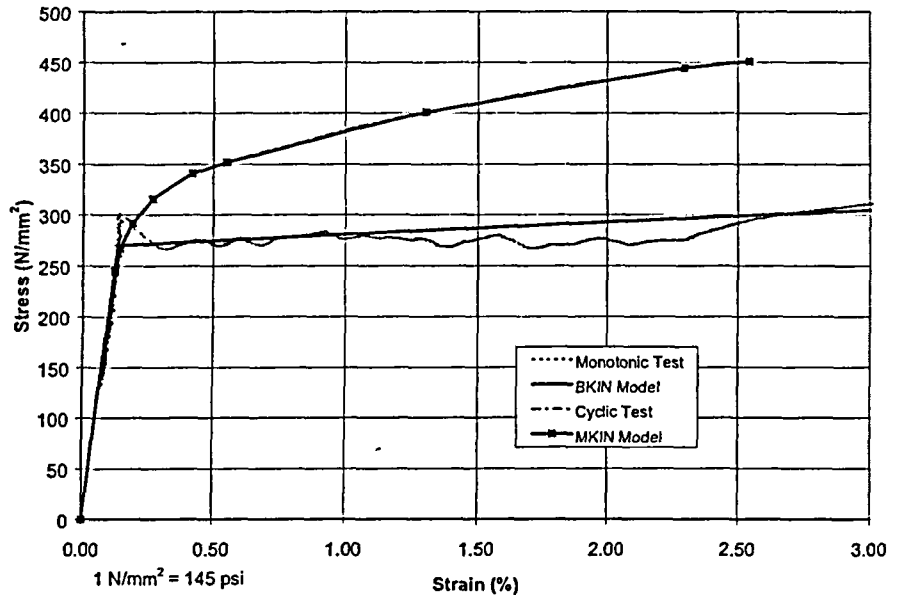

Figure 4-3 BKIN and MKIN Model Stress-Strain Curves

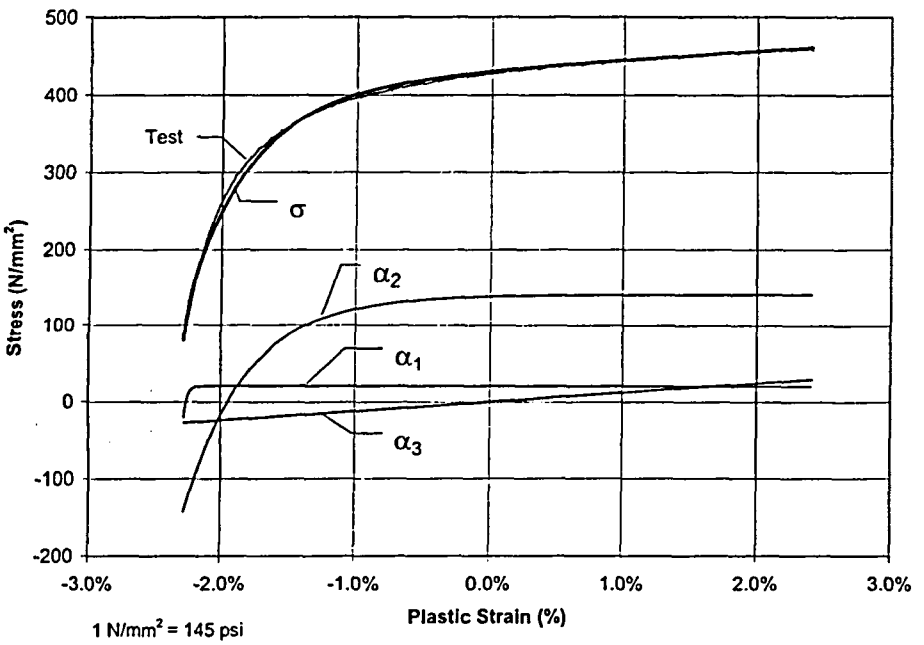

Figure 4-4 CHAB Model Stress-Strain Curve

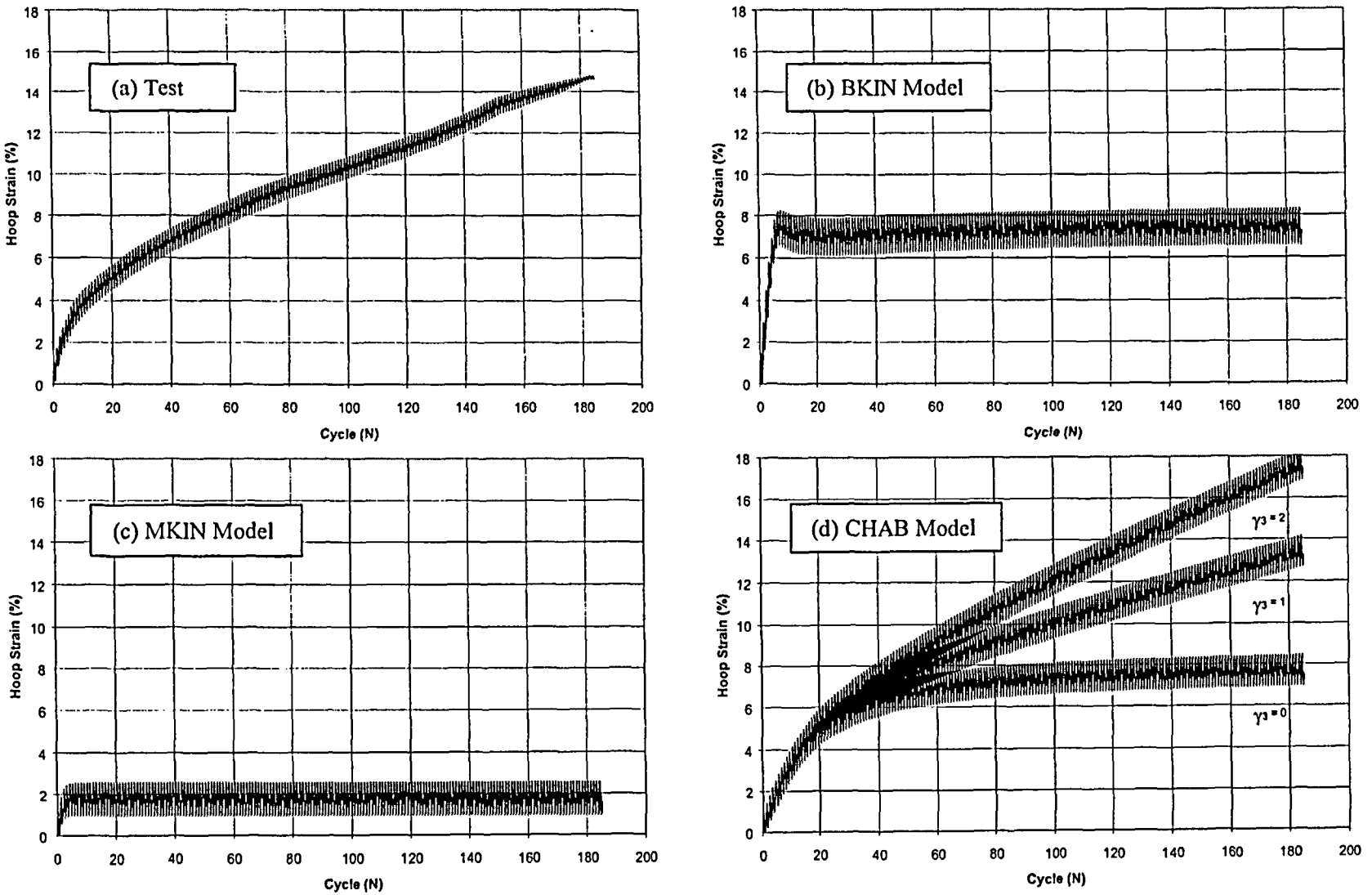

Figure 4-5 Elbow Static Cycling Test SE-4 – Hoop Strain vs. Number of Cycles at Elbow Flank

5.0 BNL SIMPLIFIED PIPING SYSTEM TEST NONLINEAR ANALYSES

5.1 Introduction

Initial analytical models of the piping systems and components utilized the ANSYS straight and curved plastic pipe line elements. Preliminary analyses, however, demonstrated that the curved plastic pipe elements were not adequate for simulating the elbow strain ratcheting behavior observed in the tests. As a result, the final models incorporated detailed shell element representations of elbows and other piping components expected to experience plastic deformation. The elbow models were based on the shell element elbow models developed for the SE-4 component test. The following sections describe the modeling and analysis approach, analysis results, and comparisons to test results.

5.2 Development and Pre-Test Analysis of Two-Dimensional Simplified Piping System Model

The ANSYS model of the two-dimensional Model A Simplified Piping System test specimen shown in Figure 2-9 consisted of a combination of elements. Because of symmetry about the horizontal plane, only the top half of the system was modeled and appropriate symmetry boundary conditions were defined at the horizontal mid-plane. The ANSYS model is shown in Figure 5-1. The elbows were modeled in the same manner as the SE-4 test elbow model described in Section 4.2 above using ANSYS SHELL181 large strain shell elements to represent the pipe wall. These elements were used to represent the elbows plus a 100 mm (4 in) length of straight pipe at each end of the elbows. Since it was anticipated that the plasticity would be localized to the elbows, the remaining straight pipes were represented by two-dimensional linear elastic beam elements (BEAM3) with dimensional properties equivalent to the cross-sectional properties of half the pipe. The transition from the straight pipe shell model to the straight pipe beam model was achieved through a series of rigid beam elements arranged in a wheel spoke configuration as shown in the elbow detail in Figure 5-1. The shell element representation of the additional length of straight pipe at the ends of the elbow was needed to ensure that the constraints at the transition from shell to beam elements did not inhibit elbow ovalization required for appropriate characterization of elbow flexibility. The selection of the 100 mm (4 in) length considered the guidance provided in the ASME Code, Section III, Subsection NB-3686.2 which states that the code elbow flexibility equations are applicable only if there are no flanges or stiffeners from the end of the elbow to within a distance equal to the mean radius of the pipe. For this case, a 100 mm (4 in) length is approximately three times the mean radius. Additional static load deflection analyses comparing a full shell element model to this combination shell element/beam element model verified the adequacy of the simplified shell/beam element model. ANSYS MASS21 elements with half the actual masses represented the added masses attached to the piping system. Symmetry boundary conditions were specified to constrain vertical translation and horizontal axis rotations for all nodes in the horizontal (x-y) plane. Horizontal translational restraints were defined at the two pinned support points.

During the pre-test analysis phase of the program, seismic analyses were performed to predict the responses for the A-1 and A-2 tests. A primary objective of these analyses was to investigate and compare responses using the three different plasticity models described in Section 4.3 and to select the best model for application in the post-test analysis. The analyses applied the ANSYS nonlinear full transient analysis option which utilizes the Newton-Raphson iteration procedure and the Newmark time integration method to solve the nonlinear equations of motion. An internal pressure of 19.8 MPa (2870 psi) was applied to the system. System damping was defined in terms of Rayleigh damping coefficients based on the expected modal damping value of 3 percent provided by NUPEC. The expected input motions were defined as x-direction digitized acceleration time histories of the shaking table divided into 4000 equal time increments. Duration times were 191.6 seconds for the A-1 test and 215.6 seconds for the A-2 test. Since the ANSYS program does not accept base acceleration input motion, the input was applied as an equivalent force time history to a fictitious large mass of 10^{11} kg (2.2×10^{11} lbm) connected

to the support points. The ANSYS automatic time stepping option was applied with an integration time step upper limit of one quarter of the input motion load step (.012 sec. for A-1 and .0135 sec. for A-2). Both the A-1 and A-2 analyses were performed for each of the three plastic hardening models. Key responses including displacements, rotations, stresses and strains at critical locations were saved at every load step for comparison with test results. Differences in both displacement and strain ratcheting results were observed between the different plasticity models.

During preliminary testing of the two-dimensional Model A simplified piping system, NUPEC determined that the system modal damping was lower than expected (1.8 percent versus 3 percent). As a result of this finding, NUPEC revised the final table acceleration input motions to achieve their target strain levels. Because of this change, a comparison between the BNL pre-test analysis results and test results was not meaningful. NUPEC made adjustments to both the time and acceleration level scales of the input motions and provided the new inputs, as well as the test results, to BNL for post-test analysis. Using the same methodology and the analytical model with Chaboche nonlinear kinematic hardening, BNL repeated the A-2 test analysis with the new seismic input motion and lower damping values. A comparison of these post-test analysis results to test results showed that the analysis significantly underpredicted displacements and strains. Peak displacement at the center of the pipe predicted by analysis was 50 mm (2 in) versus 178 mm (7 in) recorded in the test. The analysis predicted no strain ratcheting compared to 3.4 percent accumulated strain observed in the test. A series of additional analytical studies to investigate and identify the source of the underprediction and improve the accuracy of the simulation were initiated.

5.3 Additional A-2 Simplified Piping System Test Analytical Investigations

A series of additional A-2 test simulation analyses were carried out to examine the sensitivity of results to changes in various modeling and analysis parameters. The initial series of analyses investigated changes in analysis parameters. The following changes were considered:

- Reduction in integration time step from .015 sec. to .003 sec.
- Reduction in output time step from .09 sec. to .03 sec.

The analyses with the above reduced time steps showed no significant differences in results.

The load application method was investigated next. The original analysis had applied the base acceleration input time history as an equivalent force time history to a large fictitious base mass. Two alternate methods of load application were investigated:

- A displacement time history was calculated by performing a double integration of the acceleration input time history. This was applied directly to the model as a displacement input time history at the support points.
- The acceleration time history was converted to a set of equivalent inertia force time histories and applied directly to the concentrated masses in the piping system model.

Both the displacement time history and the equivalent inertia force time history analyses showed no significant differences in results. It was noted, however, that the inertia force time history analysis was more efficient and this method was applied in subsequent analyses.

Variations in material parameters were investigated next as follows:

- A 10% reduction in modulus of elasticity to better match the Model A test frequency

- A 20% and a 40% reduction in yield stress to induce more plasticity
- A modal damping ratio of 0% (vs. 1.8%) to induce greater amplified response
- Application of bilinear kinematic hardening model vs. Chaboche model

The results of these analyses showed small differences in results. The case with no damping provided slightly higher displacement but no strain ratcheting. The case with 40% reduction in yield stress demonstrated a small amount of strain ratcheting but no increase in displacement. The other cases provided nearly identical results to the original analysis.

All of the analyses were underpredicting the global seismic response of the system. Further investigations were conducted to establish additional reference information that may assist in understanding the cause for the underprediction. Additional analyses were performed with increased input motion. These analyses demonstrated that a close match to test results can be achieved by increasing the amplitude of the input acceleration time history by a factor of two to three times the A-2 input motion. A linear elastic time history analysis was also performed to establish an elastic baseline analysis. The elastic analysis considered no material (plasticity) or geometric (large deflection) nonlinearities. The analysis provided unexpected results. The maximum deflection was nearly twice the deflection predicted by the nonlinear analysis. Since the linear analysis had removed the geometric as well as the material nonlinearities, additional analyses were performed to identify the source of the difference. The elasto-plastic analysis was repeated with no geometric nonlinearity (small deflection theory) and the elastic analysis was repeated with geometric nonlinearity (large deflection theory). A comparison of deflection results demonstrated that the differences were due to the application of small deflection versus large deflection theory. Within the same geometric assumption cases, the differences in peak deflections between elastic and elasto-plastic analyses were relatively small. However, within the elastic and elasto-plastic cases, small deflection theory predicted almost twice the deflection than predicted by large deflection theory. Although these results demonstrated that application of small deflection theory would provide increased deflections closer to test, they were still below test results and additional investigations were needed.

Investigations on the sensitivity of results to dimensional variations were conducted next. The A-2 model used as-built dimensions for straight pipes and elbows based on average as-built diameter and wall thickness measurements provided by NUPEC. A comparison with nominal dimensions showed that the as-built thickness used in the model was 30% higher than nominal. This difference may be significant since it results in a stiffer, higher frequency system and lower strain in the elbow. To investigate the sensitivity of response to dimensional variations, the system was reanalyzed using nominal pipe dimensions. A frequency analysis demonstrated that by using nominal dimensions, the model provides a much closer match to the test frequency. The original as-built dimension model had a fundamental frequency of 2.34 Hz compared to the test frequency of 2.2 Hz. The nominal dimension model had a frequency of 2.18 Hz. The seismic analysis of the nominal dimension model with small deflection theory provided the closest match to both displacement and strain ratcheting test results than was observed in any previous analysis. Based on these results, further discussions were held with NUPEC to verify the parameters used in the BNL model.

BNL compared key modeling parameters between the ANSYS model and the NUPEC ABAQUS model. The as-built dimensions were found to be nearly identical, so there was no justification for using nominal dimensions. Other parameters and modeling assumptions were also compared. A difference in the modeling of added masses was identified. Both models included concentrated masses at the pipe nodes located at the centers of gravity of the added masses. The BNL model assumed that the added masses stiffened the pipe along their length and modified the cross-sectional properties of the pipe to correspond to the rigid stiffness of the added mass. The NUPEC model did not increase the stiffness of the pipe along the length of the added mass. Therefore, additional analyses were performed to investigate the effect of this difference. Frequency analysis of the A-2 model without the added mass stiffness showed a

reduction in piping system frequency which more closely matched the test specimen frequency. A nonlinear seismic analysis of this modified model using small deflection theory showed excellent comparisons to test displacements and strain ratcheting. Subsequent analyses for the simplified piping systems discussed in the following sections used this modeling assumption and were based on small deflection analysis.

Some additional analyses were performed to investigate why small deflection analysis was providing better results than large deflection analysis. Large deflection analysis was originally used to account for the effects of elbow ovalization on elbow stiffness. This change in cross-sectional geometry results in decreased elbow stiffness on closing and increased elbow stiffness on opening. In theory, a large deflection analysis should account for this change. A model of the SE-4 elbow was statically loaded by applying displacements in opening and closing directions using small deflection and large deflection analyses. A plot of force versus deflection showed that for small deflections, both analyses predicted the same elbow stiffness in both the opening and closing directions, as expected. At larger deflections, the large deflection analysis predicted higher elbow stiffness upon opening and lower stiffness upon closing. The same effect was observed with an elastic model and an elasto-plastic model. These analyses demonstrated that the ANSYS elbow model behaved as expected for large and small deflection analysis. A similar static analysis was performed for the A-2 piping system model. In these analyses, the center of the pipe was displaced in the positive and in the negative x-directions. In both directions, the large deflection analysis predicted about 40% higher stiffness at all values of displacement. This was observed for both elastic and elasto-plastic models. The higher initial stiffness seen in the large deflection analysis is believed to be an anomaly. At small deflections, the geometric effect is insignificant, and a large deflection analysis should provide the same results as a small deflection analysis. It appears that the large deflection analysis of the A-2 model introduces artificial stiffening which does not represent the actual behavior of the system and provides erroneous results. The higher stiffness would explain the reduced dynamic global response of the piping system seen in the original analysis. The cause of this anomaly is unknown. There may be incompatibilities between the different elements used in the model, but further investigations are needed to ascertain the root cause of this problem.

As noted above, subsequent simplified piping system analyses used small deflection analysis. Although this type of analysis does not account for the geometric effects of elbow ovalization, the effect was believed to have a small impact on the results. Some additional analyses were performed to support this assumption. Since large deflection analysis provided reasonable results for the SE-4 elbow, this model was further analyzed to compare large deflection analysis with small deflection analysis results. The load versus deflection curves from the monotonic loading analyses of the elbow describe above had already demonstrated that the difference in elbow stiffness between large and small deflection analysis was small. Additional static cycling analyses simulating the SE-4 test were carried out. A comparison of results demonstrated that the large deflection cycling analysis predicted only a slight increase in elbow equivalent stiffness along with a slight increase in strain ratcheting in the elbow. The differences in results were less than 10 percent. Since the strain levels in the elbow tests were comparable to the strain levels in the simplified piping system test, it was therefore concluded that within the range of interest, a small deflection analysis of the simplified piping system model would provide a reasonable level of accuracy in the results.

5.4 Final A-2 Simplified Piping System Test Analyses and Comparisons

Final nonlinear seismic analyses of the A-2 test were carried out based on the methodology described above using each of the three plastic hardening models. Comparisons of displacements and elbow strain time history results between the test and the different models are shown in Figures 5-2 and 5-3. As shown in Figure 5-2(a), test measurements indicated peak displacements of +170 mm (+6.7 in) and -178 mm (-7 in) at the pipe center with a permanent deformation of –12 mm (-0.47 in) at the end of the test.

The BKIN model (Figure 5-2(b)) predicted displacements of +146 mm (+5.75 in) and –166 mm (-6.54 in) with +2 mm (+0.08 in) permanent deformation. The MKIN model (Figure 5-2(c)) predicted +165/-161 mm (+6.5/-6.34 in) and –6 mm (-0.24 in) permanent deformation. The CHAB model (Figure 5-2(d)) predicted +162/-167 mm (+6.38/-6.57 in) and –6 mm (-0.24 in) permanent deformation. A close examination of the displacement time history plots shows that the Chaboche nonlinear kinematic hardening model predicts the closest match to the test displacement time history, although the multilinear kinematic hardening model also produces a reasonably good match.

A comparison of the Elbow A flank strain time history results shows more significant differences. As shown in Figure 5-3(a), the test results indicated hoop strain ratcheting in the elbow for the first 125 seconds of motion. By the end of the test, the accumulated strain was 3.35%. The BKIN model (Figure 5-3(b)) overpredicted the strain ratcheting with shakedown occurring at 75 seconds with a final permanent strain of 5.5%. The MKIN model (Figure 5-3(c)) also predicted strain ratcheting during the first 75 seconds but the final permanent strain only reached 1.3%. Finally, the CHAB model (Figure 5-3(d)) initially underpredicted the test strain ratcheting response during the first 50 seconds but continued ratcheting until 125 seconds with a final accumulated strain of 3.25% by the end of the test. An examination of the strain time history plots clearly shows that the Chaboche nonlinear kinematic hardening model provided the best simulation of the strain ratcheting observed in the test. These findings demonstrated the superior performance of the Chaboche plasticity model in predicting both global displacement and local strain ratcheting response. Therefore, the remaining post-test analyses were based on the Chaboche model.

5.5 Final Two-Dimensional and Three-Dimensional Simplified Piping System Test Analyses

The same analytical methodology, plastic hardening model, material properties, and modeling assumptions used in the final A-2 analysis were applied in the post-test simulation analyses for the two-dimensional A-1 test and for the three-dimensional B-1, B-2 and B-3 simplified piping system tests. The A-1 analysis used the same half-symmetry, combination shell and beam element model shown in Figure 5-1. Revised equivalent inertia force time histories at the concentrated masses corresponding to the lower level acceleration time history input for the A-1 test were calculated and applied to the model. The analysis results are discussed below.

For the three-dimensional Model B tests, a new ANSYS finite element model based on the test specimen configuration shown in Figure 2-12 was developed. The Model B specimen consisted of a similar run of pipe in the horizontal plane as Model A with an additional branch line in the vertical plane which terminated at a nozzle. It included an additional concentrated mass and relied on spring hangers rather than rollers for gravity support. The system was also pressurized to 19.8 MPa (2870 psi). Because of the three-dimensional configuration, a full model rather than a half-symmetry model was needed. The ANSYS model is shown in Figure 5-4. The three elbows were modeled using ANSYS SHELL181 large strain shell elements around the entire circumference of the pipe wall. A 100 mm (4 in) length of straight pipe was included at each end of the elbows. The same types of shell elements were used to model the nozzle plus 300 mm (12 in) of straight pipe. It was assumed that the plasticity would be localized to the elbow and nozzle, so the remainder of the piping system was modeled using three-dimensional elastic straight pipe elements (PIPE16). The straight pipe elements were connected to the elbow and nozzle shell element models by a series rigid beam elements arranged in a wheel spoke configuration as shown in Figure 5-4. ANSYS MASS21 elements were used to represent the added masses in the system. Boundary conditions included full constraint of all degrees of freedom at the end of the nozzle and restraint of translations and horizontal axes rotations at the pinned supports. Constant vertical forces were applied at the spring hanger attachment points to provide gravity support. Loads due to gravity and an internal pressure of 19.8 MPa (2870 psi) were applied to the system. System damping was defined in terms of Rayleigh damping coefficients corresponding to the measured modal damping of 0.7 percent

from the test. The analyses were performed in the same manner as the Model A analyses using the ANSYS nonlinear full transient analysis option. The actual horizontal and vertical acceleration time history input motions from the NUPEC tests were used to develop equivalent inertial force time histories at the concentrated masses. In the B-1 analysis, the forces were applied in the horizontal x-direction. In the B-2 analysis, they were applied in the vertical z-direction. In the B-3 analysis, the horizontal and vertical forces were applied simultaneously. The results of these analyses are discussed below.

NUPEC provided simplified piping system digitized test data at selected critical locations for comparison to BNL analysis results. This included displacement and strain time history response data. Table 5-1 summarizes the selected types of data and measurement locations. Plots of analysis and test time history results are shown in Figures 5-5 through 5-21 with analysis results shown on top for comparison to the test results shown on the bottom. A summary of the comparisons is presented below.

A-1 Test:

The comparison of test vs. analysis displacements at the pipe center shown in Figure 5-5 shows excellent agreement. The test indicated a slight negative permanent deformation which was not predicted by the analysis. Figure 5-6 compares hoop strains at the outside surface of the Elbow A flank. It shows that the analysis significantly underpredicts strain ratcheting in this case. Figure 5-7 shows the inside surface strain time history from analysis compared to the outside surface test strain time history (all test measurements were on the outside surfaces). This is not a one-to-one comparison, but demonstrates that the analytical model predicts a comparable amount of strain ratcheting at this elbow location.

A-2 Test:

A comparison of test vs. analysis displacements at the pipe center shown in Figure 5-8 shows excellent agreement in terms of overall shape of the plots, peak displacements and permanent deformation. The comparison of Elbow A opening displacements shown in Figure 5-9 also shows similar agreement. The comparison of Elbow A hoop strains shown in Figure 5-10 shows very good overall agreement. The comparison of axial strains at the same elbow location (Figure 5-11) shows that the analysis underpredicted the strain cyclic amplitudes and strain ratcheting. The magnitude of strain ratcheting in the axial direction, however, was much lower than in the hoop direction.

B-1 Test:

A comparison of test vs. analysis horizontal displacements at the pipe center shown in Figure 5-12 shows good agreement in terms of overall shape of the plots, peak displacements and permanent deformation. The comparison of hoop strains at the nozzle shown in Figure 5-13 shows that the analysis significantly overpredicted the ratcheting strain. The strain cyclic amplitudes, however, were observed to be small and appeared comparable between analysis and test. The comparison of axial strains at the nozzle location (Figure 5-14) shows comparable strain cyclic amplitudes and some overprediction of strain ratcheting.

B-2 Test:

Figure 5-15 shows that the peak vertical displacements at the pipe center were somewhat overpredicted by the analysis. The vertical displacements, however, were of smaller magnitude than the displacements in the horizontal motion tests. Both analysis and test showed no permanent deformation at the end of the test.

B-3 Test:

A comparison of test vs. analysis horizontal displacements at the pipe center presented in Figure 5-16 shows good agreement in terms of overall shape of the plots, peak displacements and permanent deformation. The comparison of vertical displacements presented in Figure 5-17 shows that the analysis overpredicts the test results. The vertical displacements, however, were of smaller magnitude than the horizontal displacements and the permanent deformation at the end of the test predicted by analysis was comparable to test. The comparison of hoop strains at the nozzle shown in Figure 5-18 was consistent with the B-1 test comparisons, which showed that the analysis significantly overpredicted ratcheting strain. As in the B-1 comparisons, the strain cyclic amplitudes were observed to be small and appeared comparable between analysis and test. The comparison of axial strains at the nozzle location presented in Figure 5-19 shows comparable strain cyclic amplitudes but overprediction of strain ratcheting. In this case, it was noted that in comparison with the B-1 test axial strains shown in Figure 5-14, the strain ratcheting observed in the B-3 test was less than half of the strain ratcheting observed in the B-1 test, despite the similar input excitation level in the horizontal direction. Furthermore, the analyses predicted nearly identical axial strain ratcheting for the B-1 and B-3 tests as expected. NUPEC, however, investigated and confirmed that the B-3 axial strain data was correct. The comparison of hoop strains at the Elbow A flank (Figure 5-20) shows comparable cyclic strain amplitudes, but the analysis underpredicted strain ratcheting. In Figure 5-21, hoop strain at the inside surface of the Elbow A flank is compared to the hoop strain at the outside surface of the Elbow A flank. Although this is not a one-to-one comparison, it demonstrates that the analytical model predicts a comparable amount of strain ratcheting at this elbow location.

In summary, the comparisons of simplified piping system post-test simulation analysis results demonstrated that displacement time history response was predicted with good accuracy. Accurate prediction of seismic strain and strain ratcheting was achieved in some cases, but in other cases, both overpredictions and underpredictions were observed.

Table 5-1 Summary of Post-Test Analysis Results and Test Comparisons

Test	Data	Location	Figure
A-1	Displacement at Center of Pipe	D1(X)	5-5
	Hoop Strain at Elbow A	SAD-3H	5-6
	Hoop Strain at Elbow A (Inside Surface)	SAD-3H	5-7
A-2	Displacement at Center of Pipe	D1(X)	5-8
	Opening Displacement of Elbow A	D2(L)	5-9
	Hoop Strain at Elbow A	SAD-3H	5-10
	Axial Strain at Elbow A	SAD-3A	5-11
B-1-1	Horizontal Displacement at Center of Pipe	D1(X)	5-12
	Hoop Strain at Nozzle Section A16 +90°	SA16-2H	5-13
	Axial Strain at Nozzle Section A17 +90°	SA17-2A	5-14
B-2-1	Vertical Displacement at Center of Pipe	D1(Z)	5-15
B-3	Horizontal Displacement at Center of Pipe	D1(X)	5-16
	Vertical Displacement at Center of Pipe	D1(Z)	5-17
	Hoop Strain at Nozzle Section A16 +90°	SA16-2H	5-18
	Axial Strain at Nozzle Section A17 +90°	SA17-2A	5-19
	Hoop Strain at Elbow A Section D –85°	SAD-7H	5-20
	Hoop Strain at Elbow A Section D –85° (Inside Surface)	SAD-7H	5-21

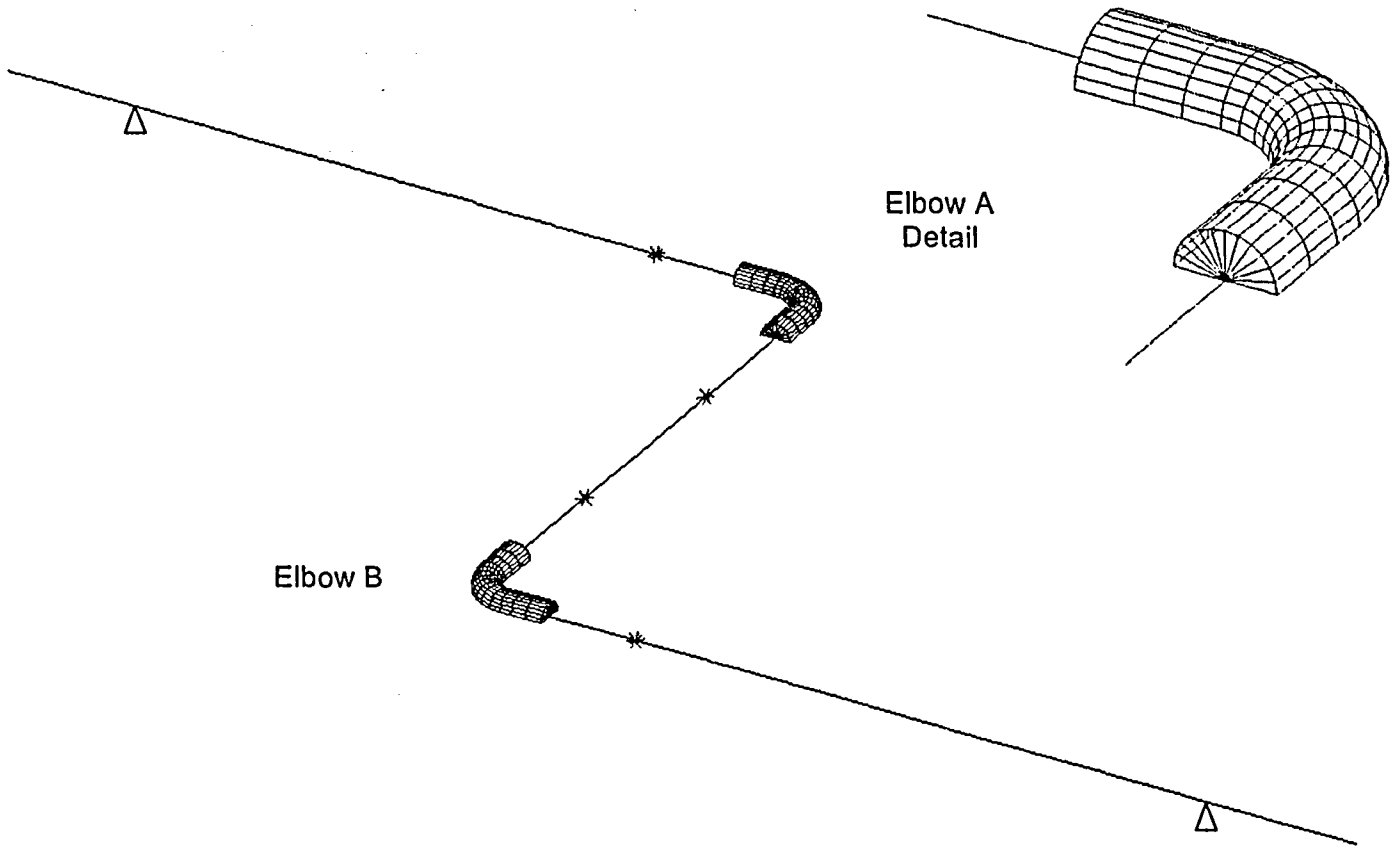

Figure 5-1 ANSYS Model A Elasto-Plastic Shell and Beam Element Model

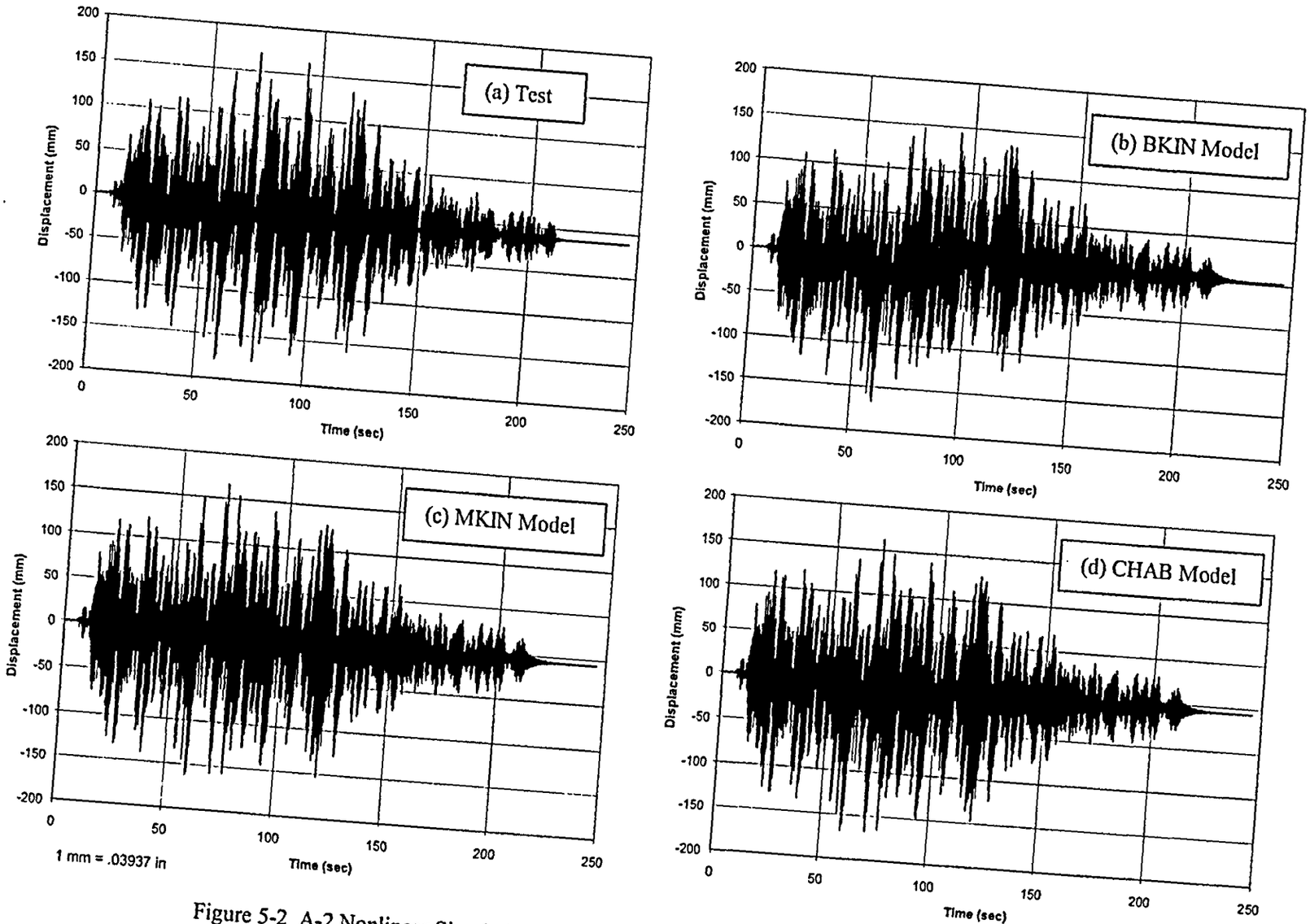

Figure 5-2 A-2 Nonlinear Simulation Analysis Results – Displacement at Pipe Center – D1(X)

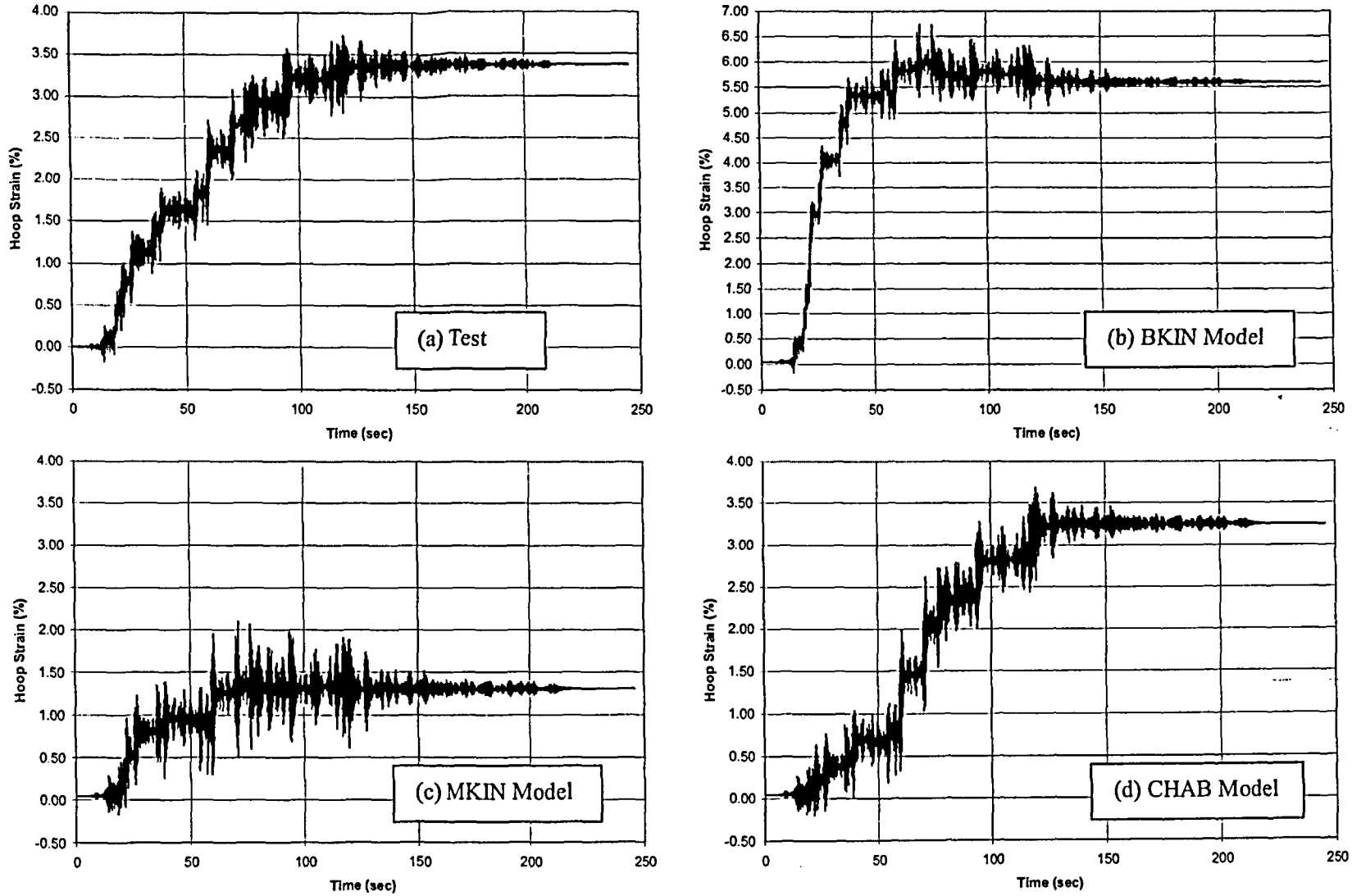

Figure 5-3 A-2 Nonlinear Simulation Analysis Results – Hoop Strain at Elbow Flank – SAD-3H

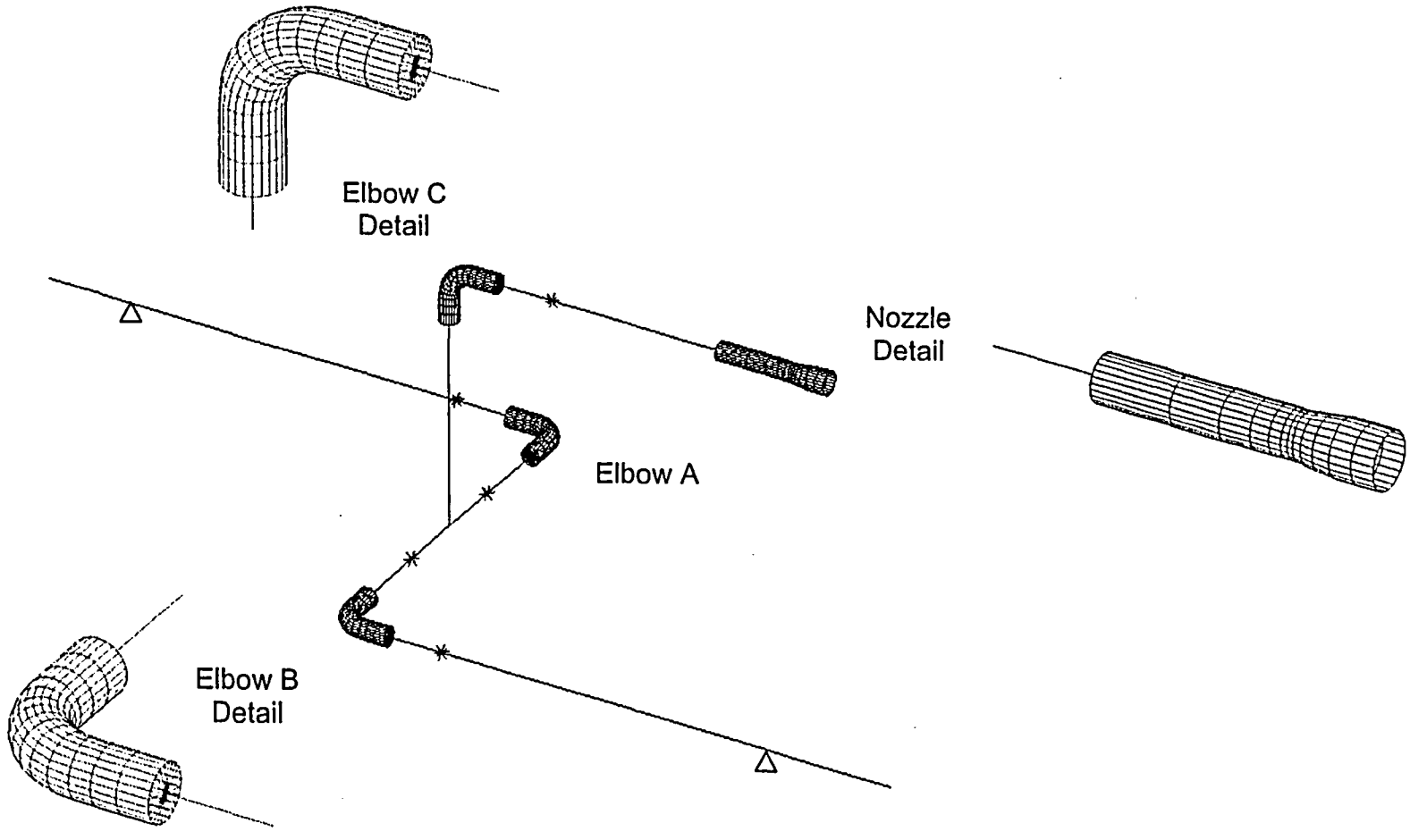

Figure 5-4 ANSYS Model B Elasto-Plastic Shell and Beam Element Model

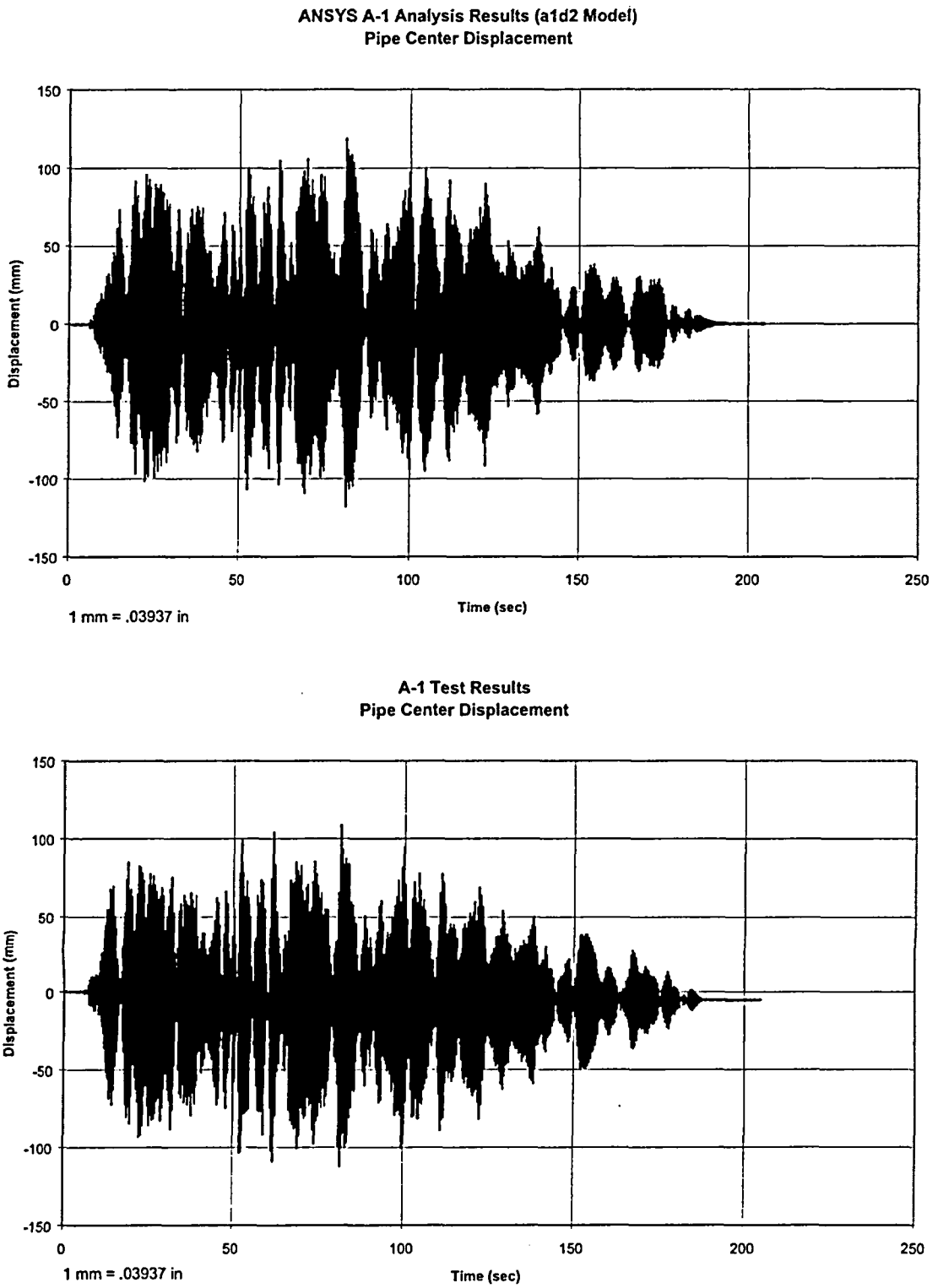

Figure 5-5 A-1 Test Pipe Center Displacement Comparison – D1(X)

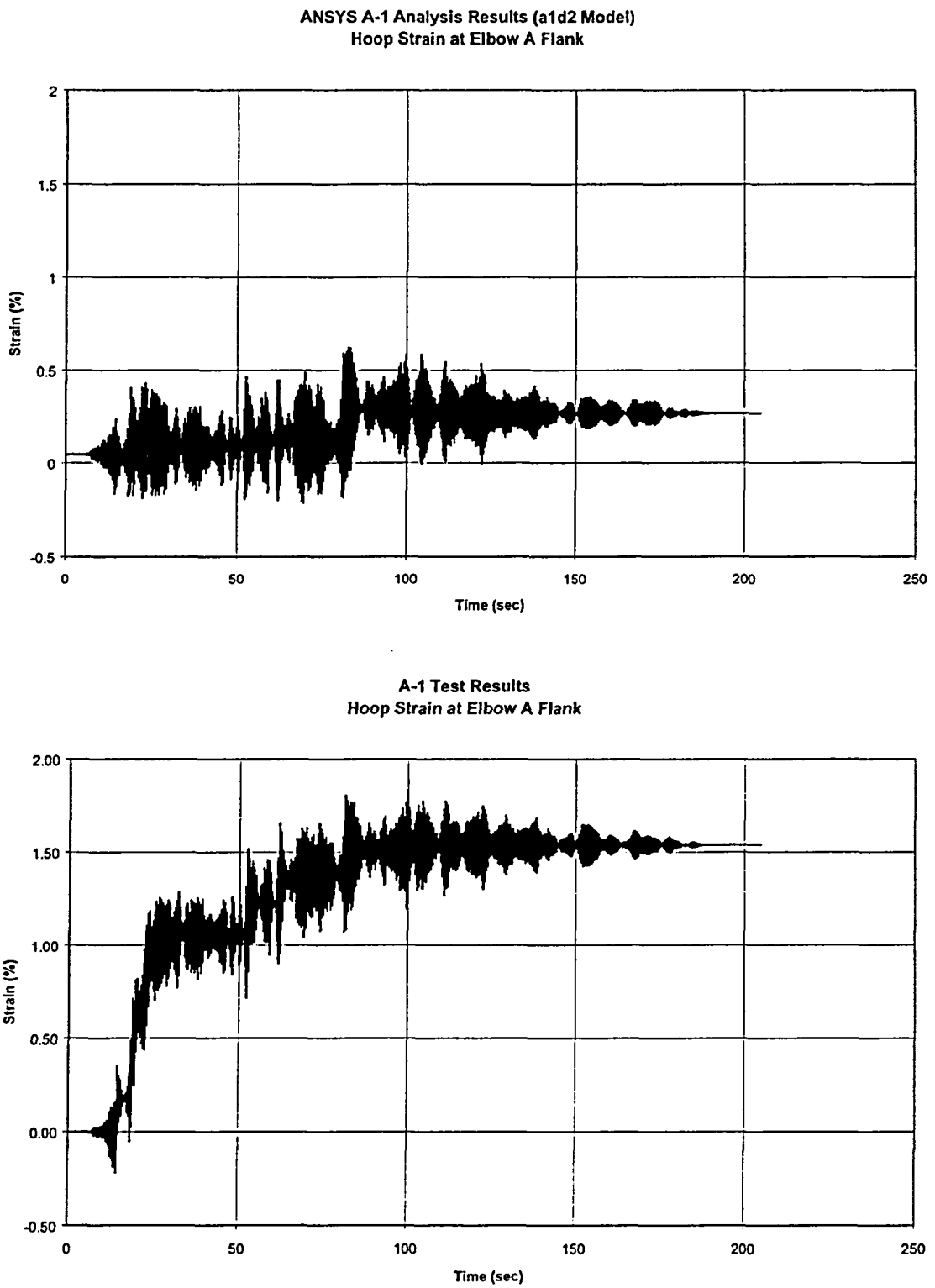

Figure 5-6 A-1 Test Hoop Strain at Elbow A Flank Comparison – SAD-3H

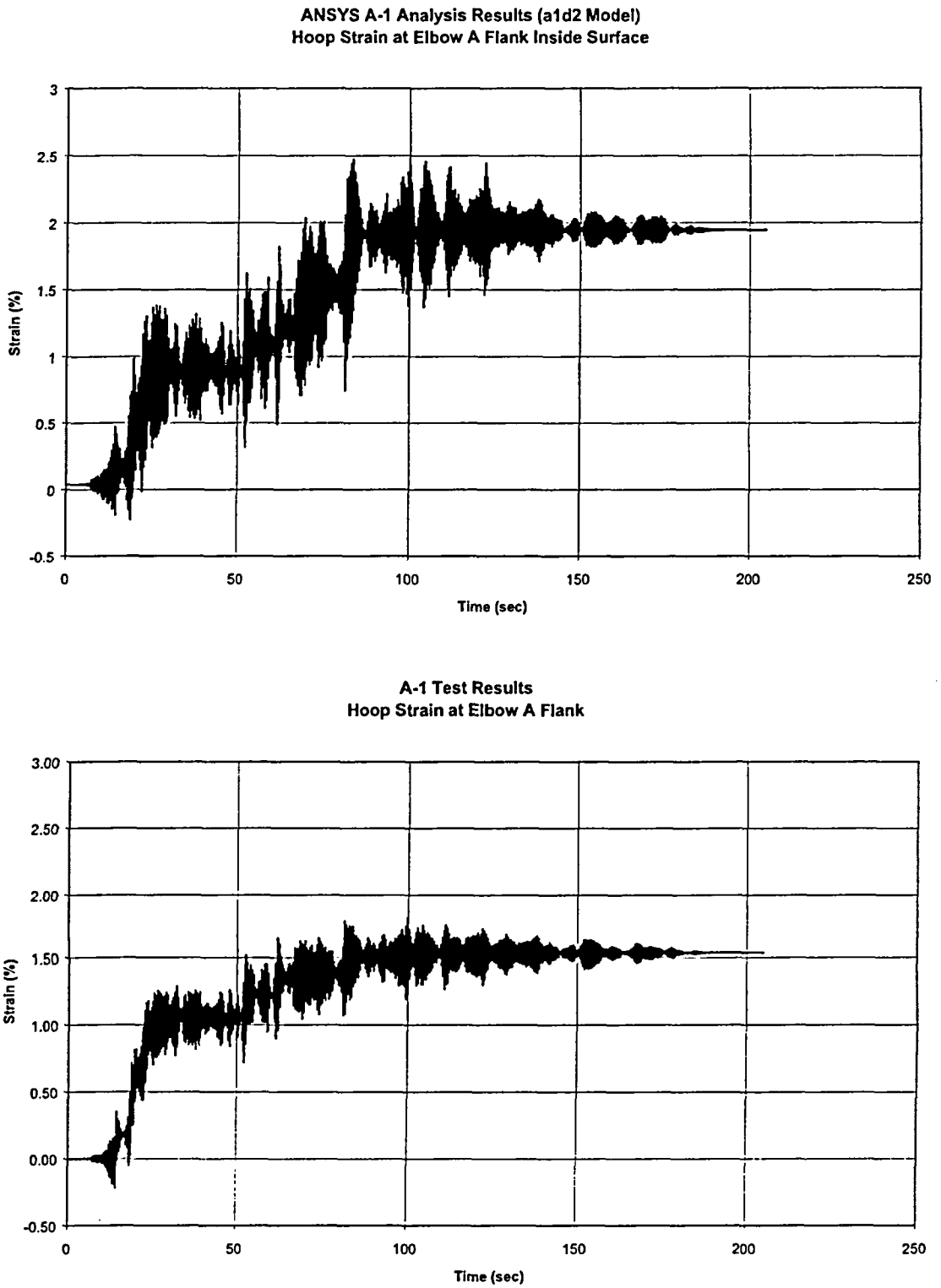

Figure 5-7 A-1 Test Hoop Strain at Elbow A Flank Inside Surface Compared to Test Hoop Strain at Outside Surface – SAD-3H

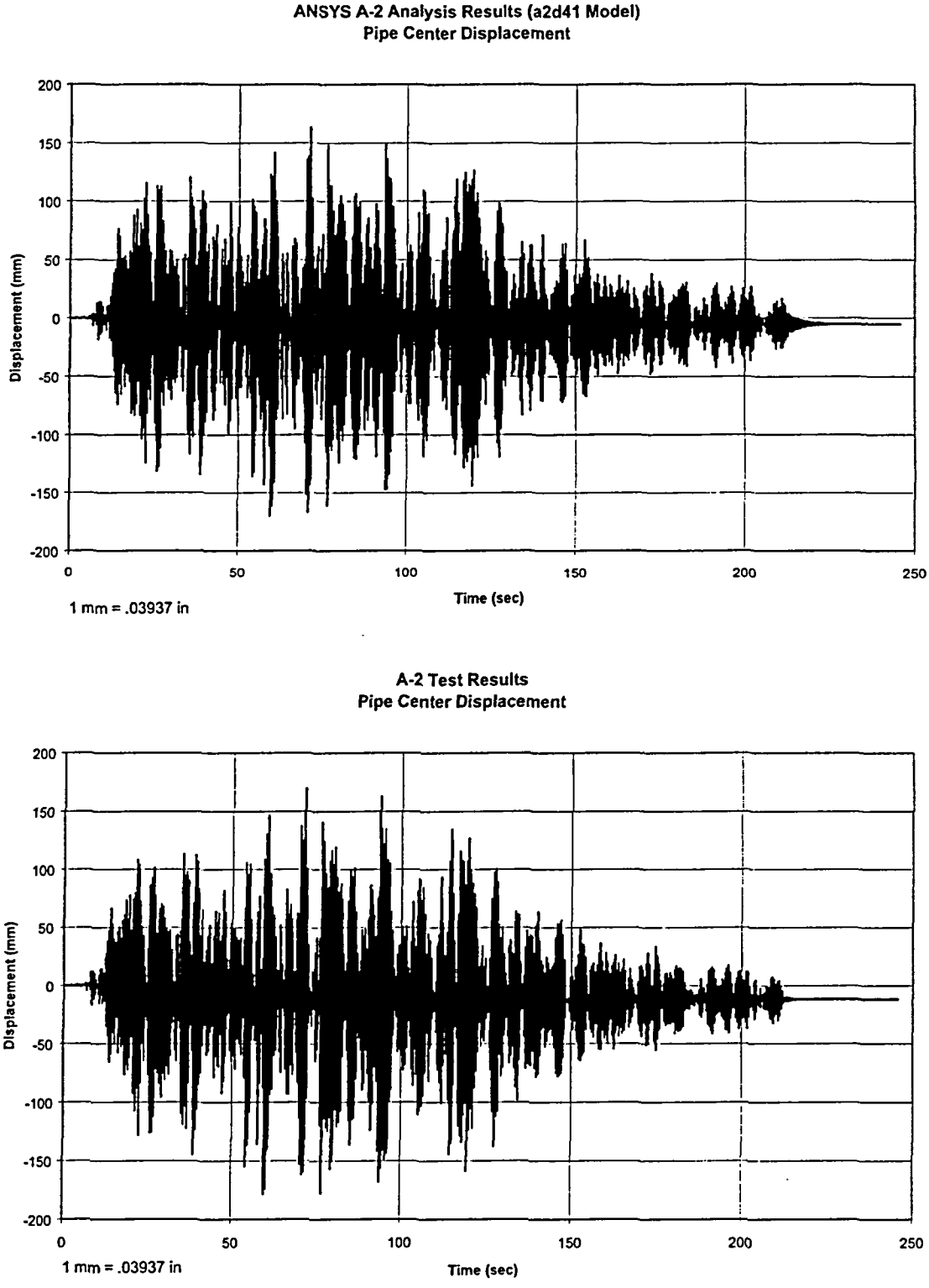

Figure 5-8 A-2 Test Pipe Center Displacement Comparison – D1(X)

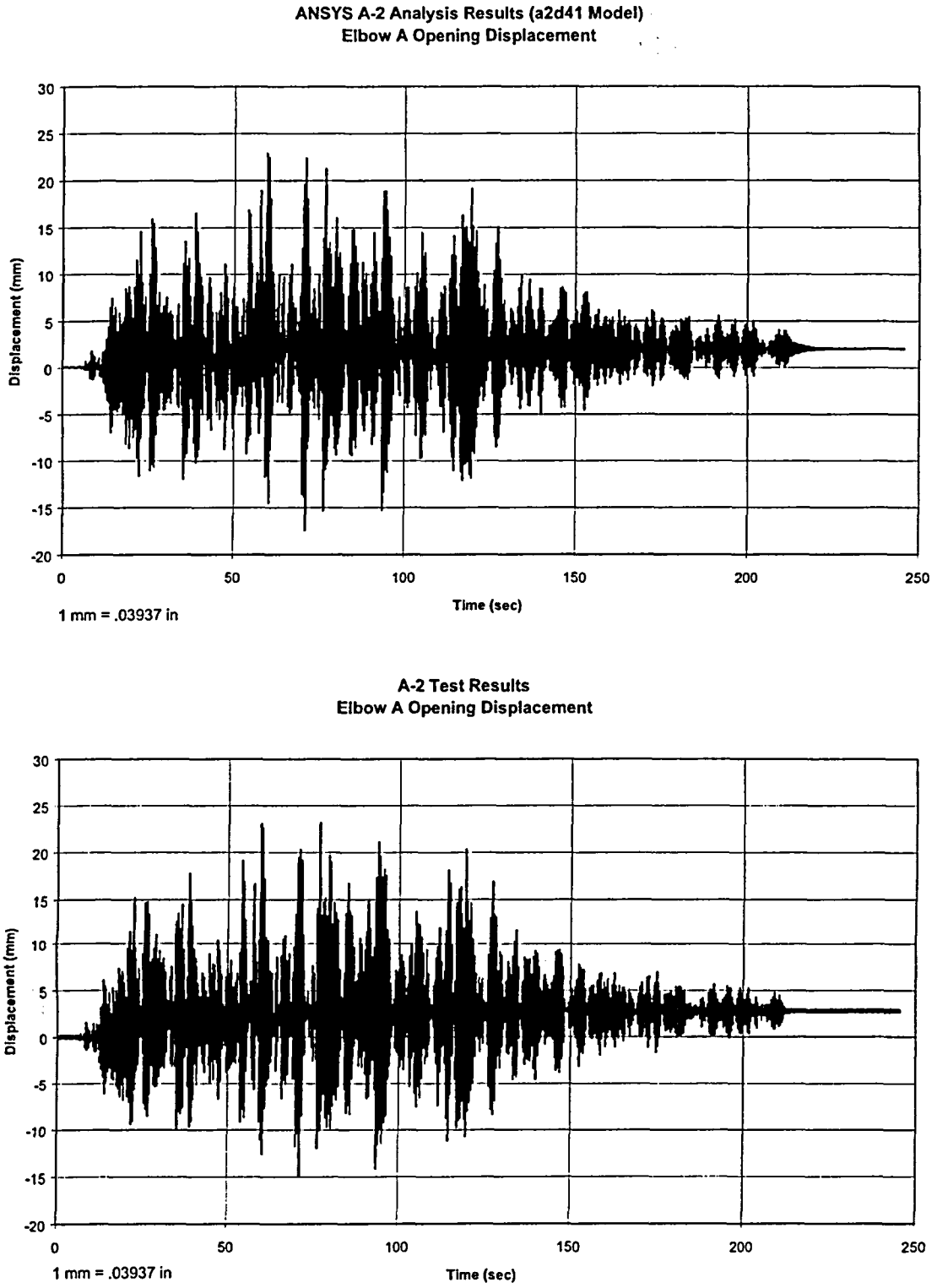

Figure 5-9 A-2 Test Elbow A Opening Displacement Comparison – D2(L)

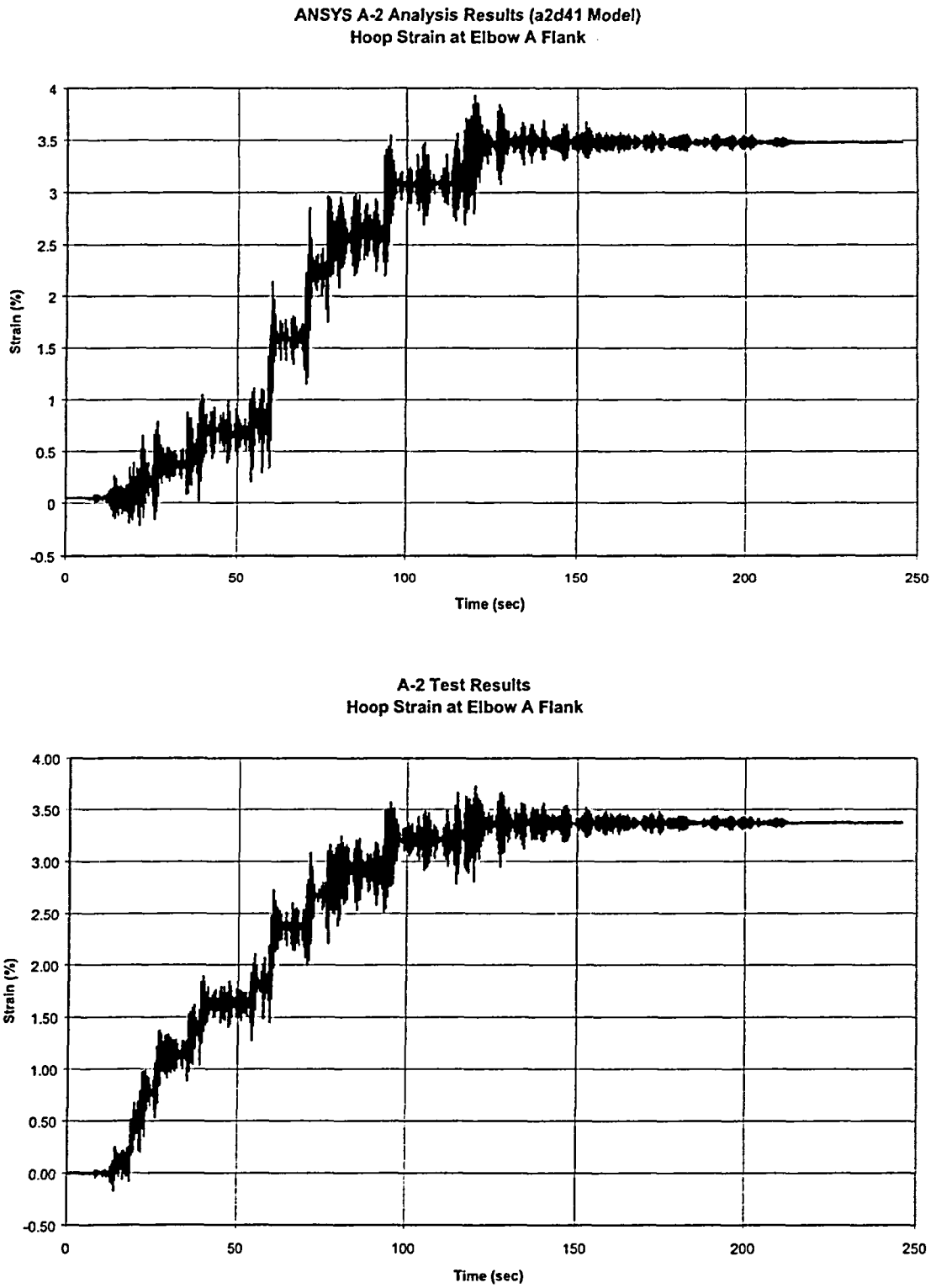

Figure 5-10 A-2 Test Hoop Strain at Elbow A Flank Comparison – SAD-3H

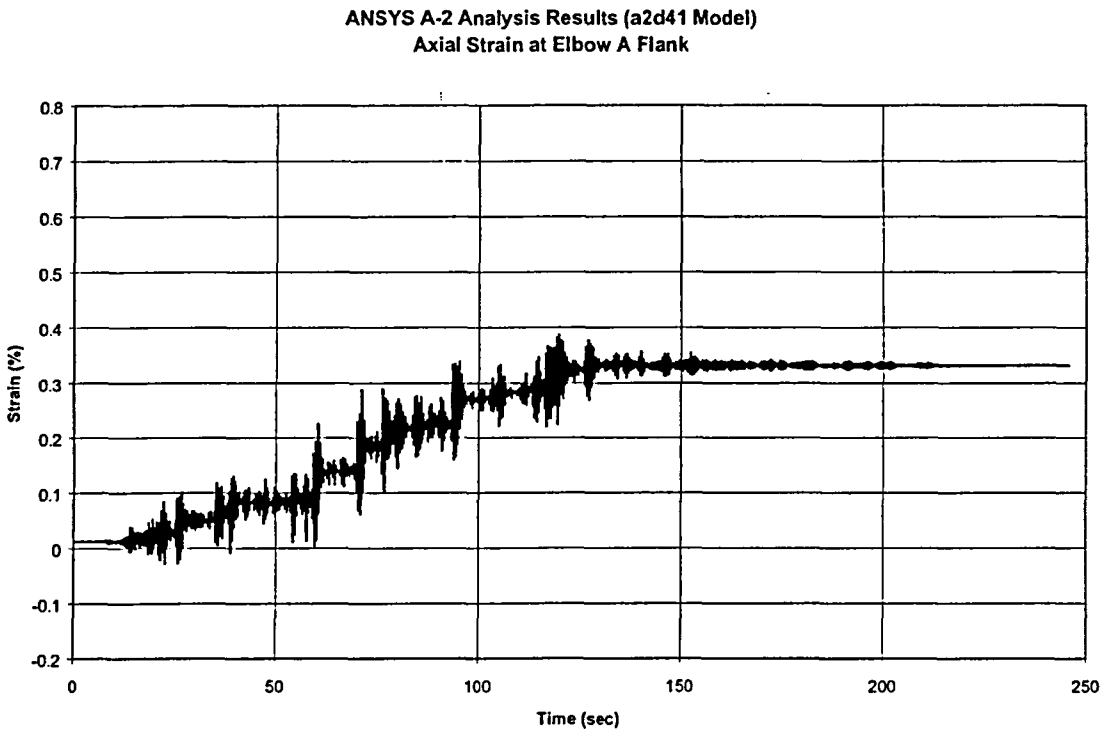

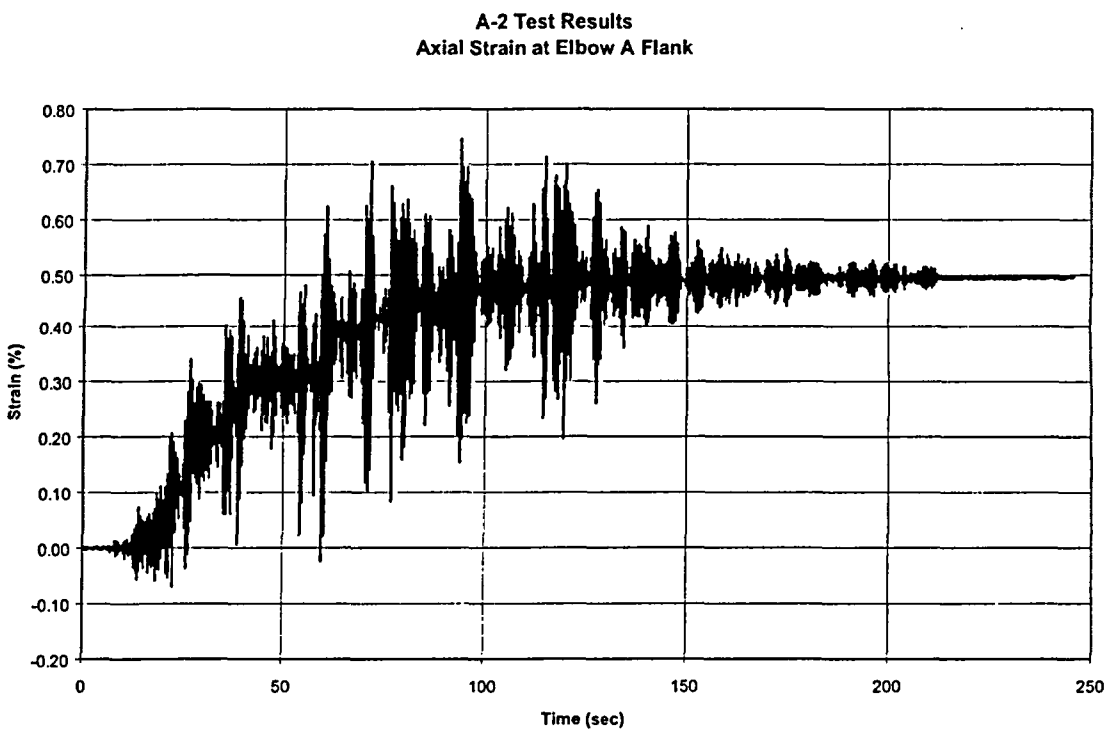

Figure 5-11 A-2 Test Axial Strain at Elbow A Flank Comparison – SAD-3A

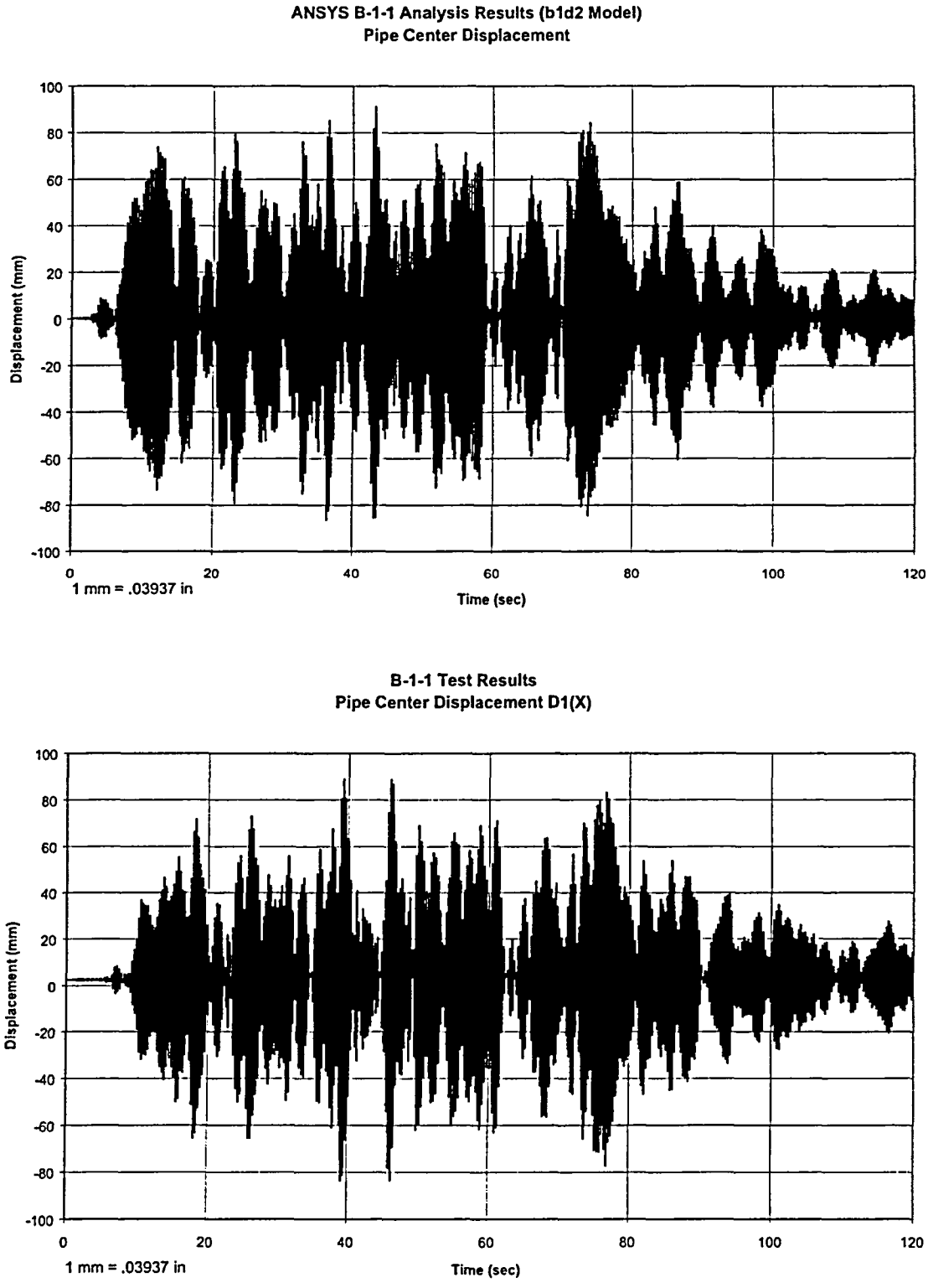

Figure 5-12 B-1 Test Pipe Center Horizontal Displacement Comparison – D1(X)

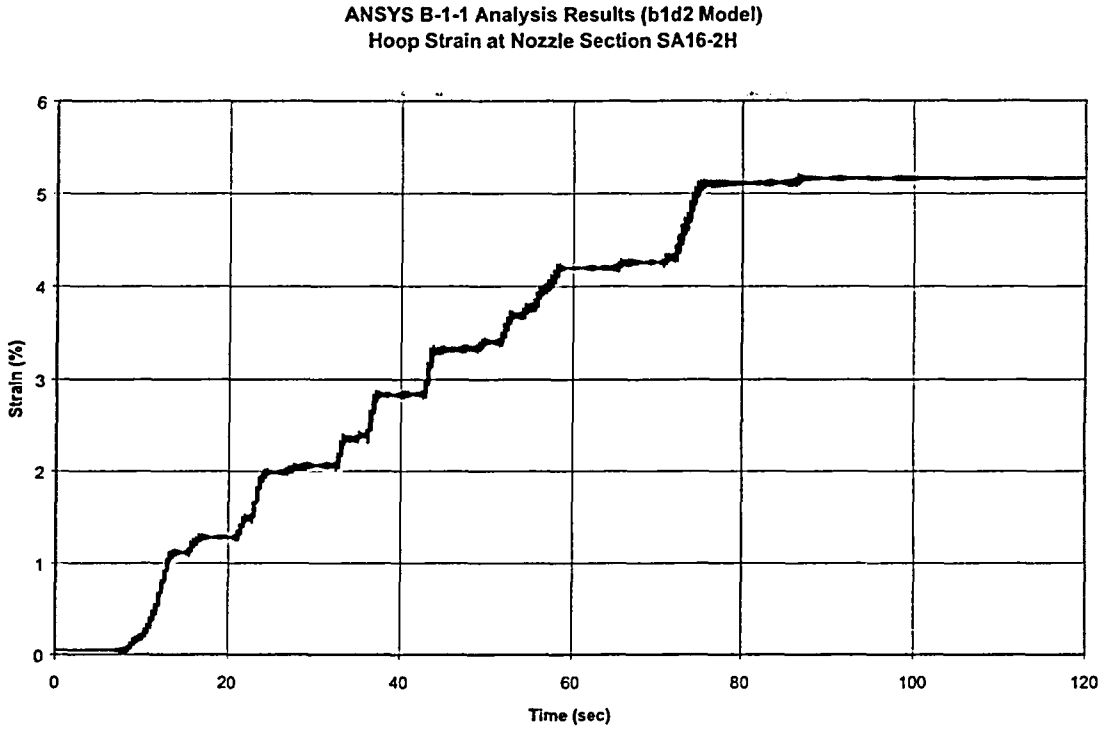

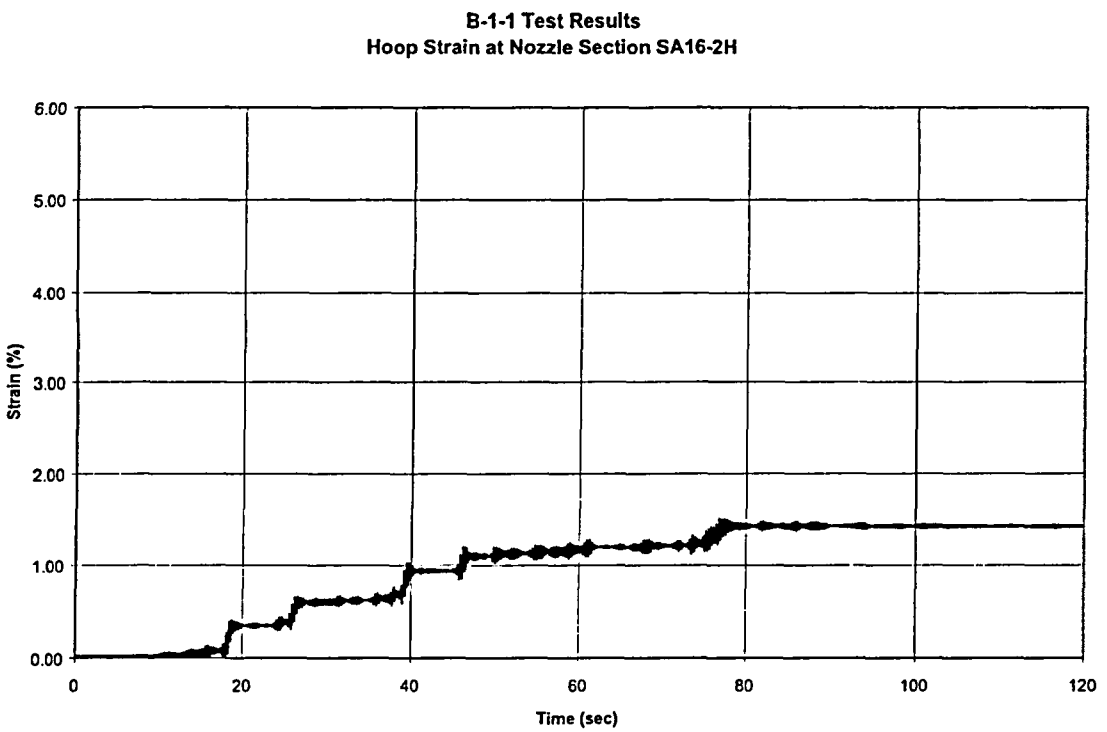

Figure 5-13 B-1 Test Hoop Strain at Nozzle Comparison – SA16-2H

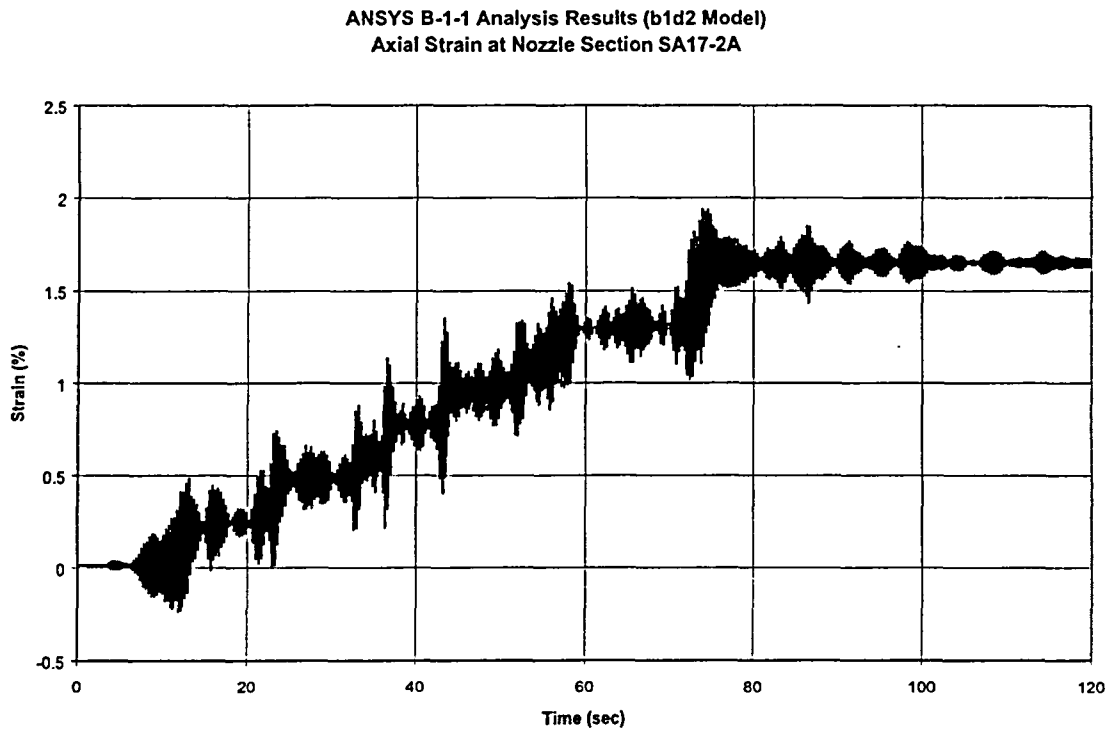

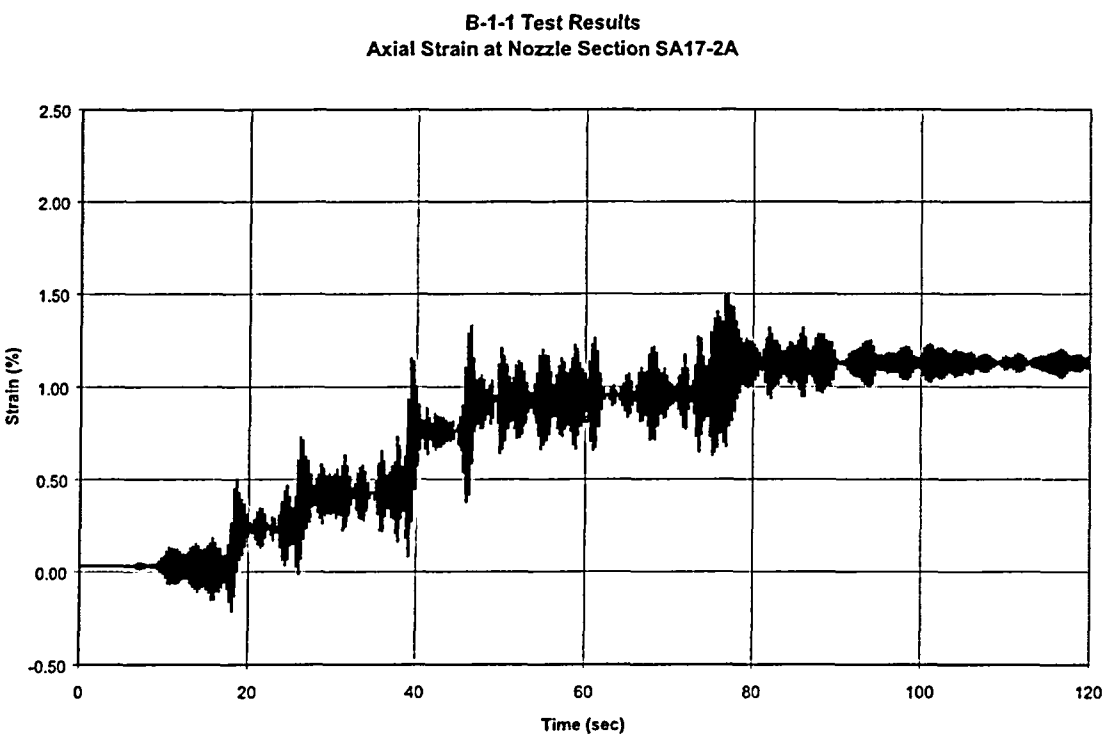

Figure 5-14 B-1 Test Axial Strain at Nozzle Comparison – SA17-2A

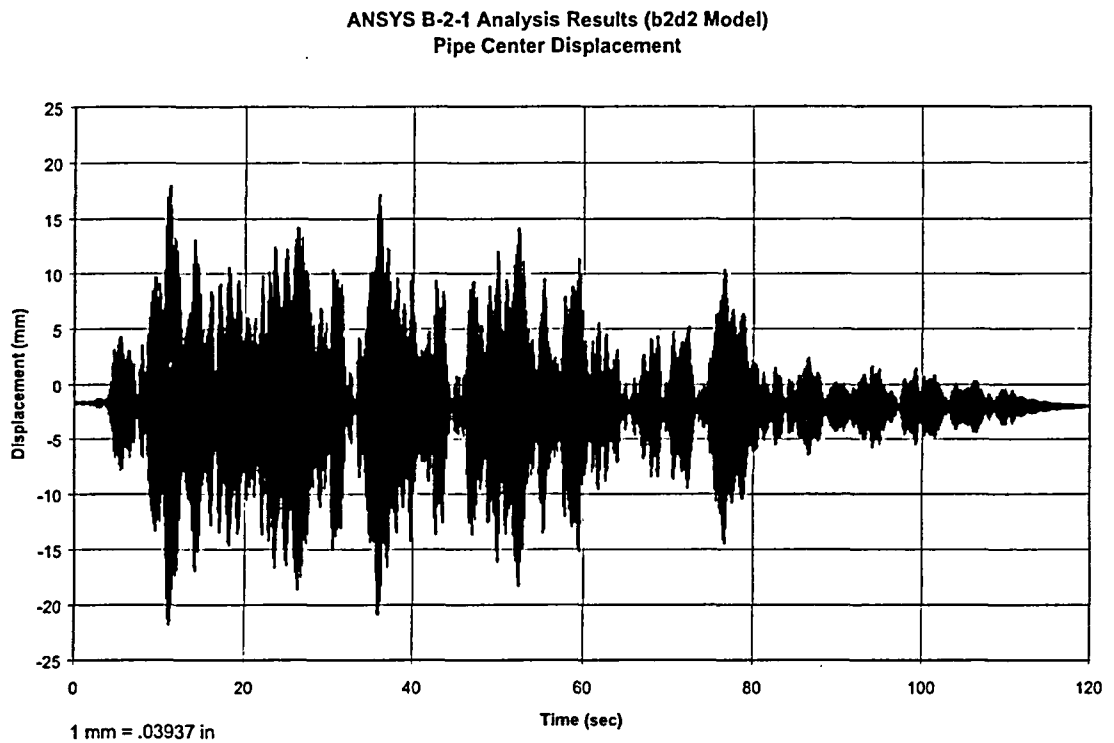

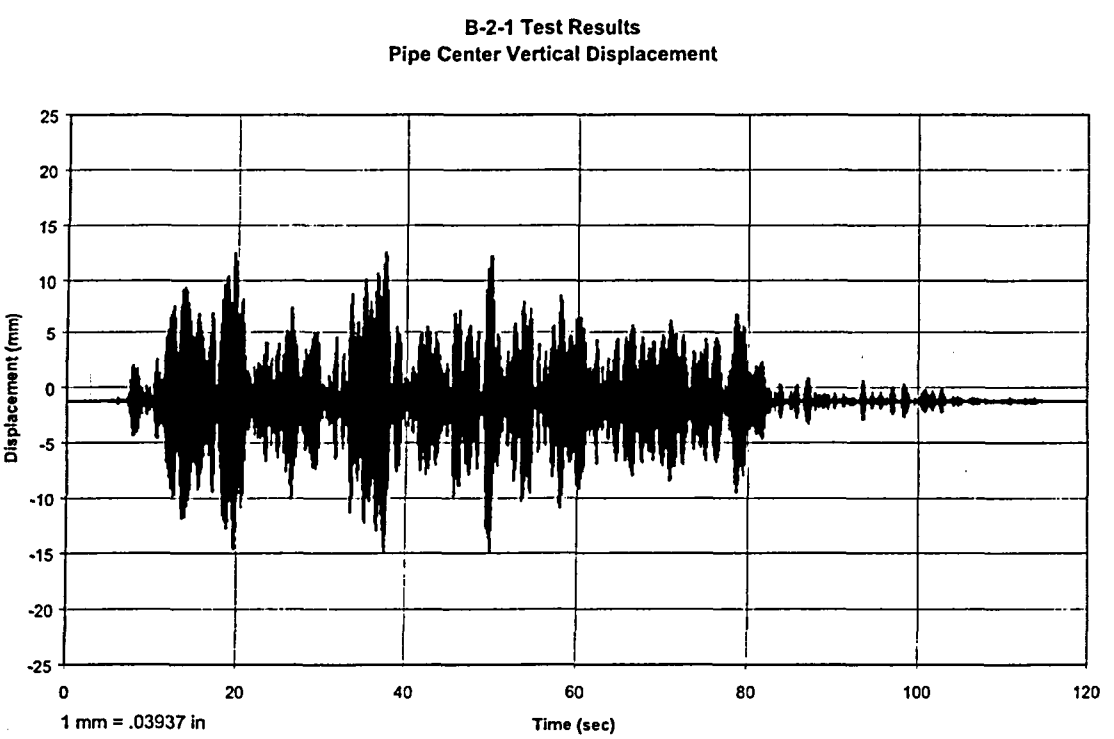

Figure 5-15 B-2 Test Pipe Center Vertical Displacement Comparison – D1(Z)

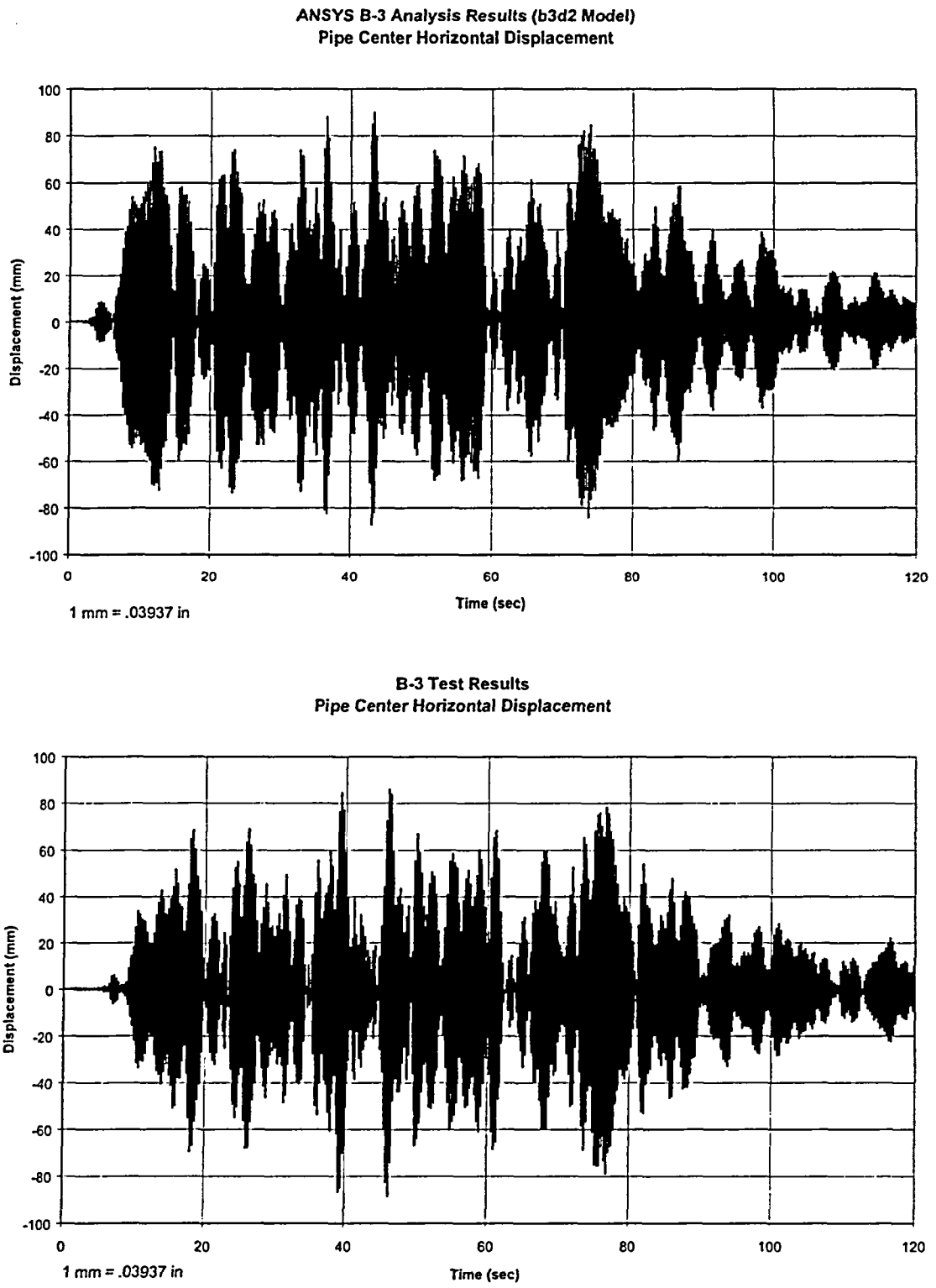

Figure 5-16 B-3 Test Pipe Center Horizontal Displacement Comparison – D1(X)

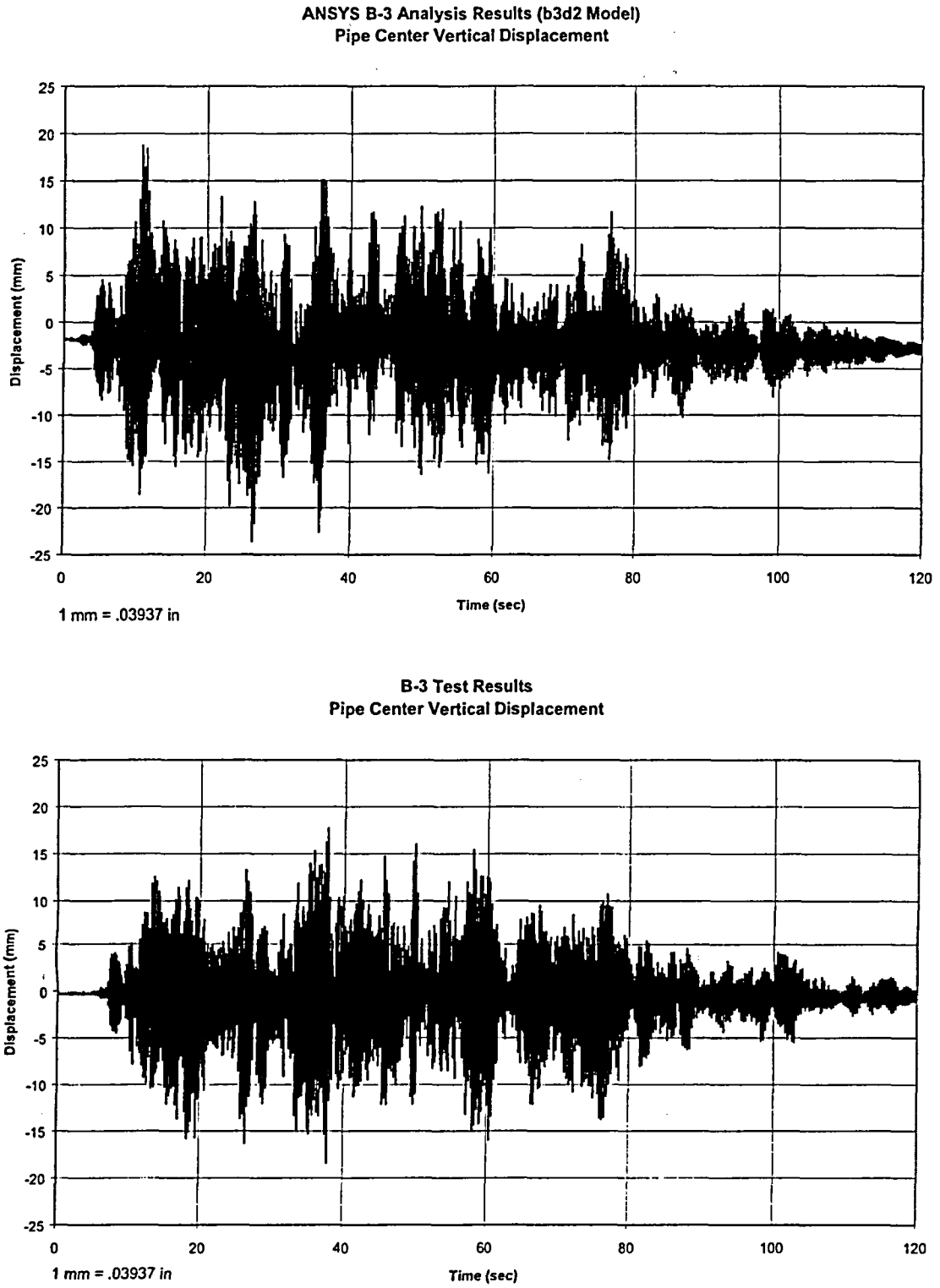

Figure 5-17 B-3 Test Pipe Center Vertical Displacement Comparison – D1(Z)

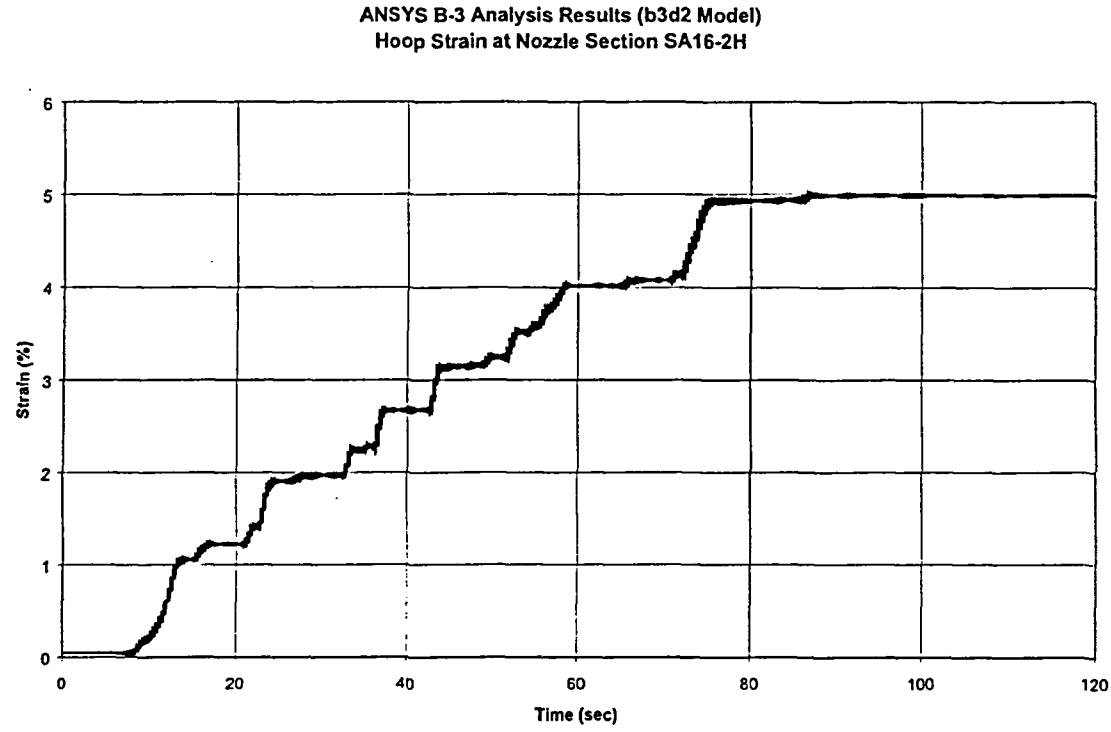

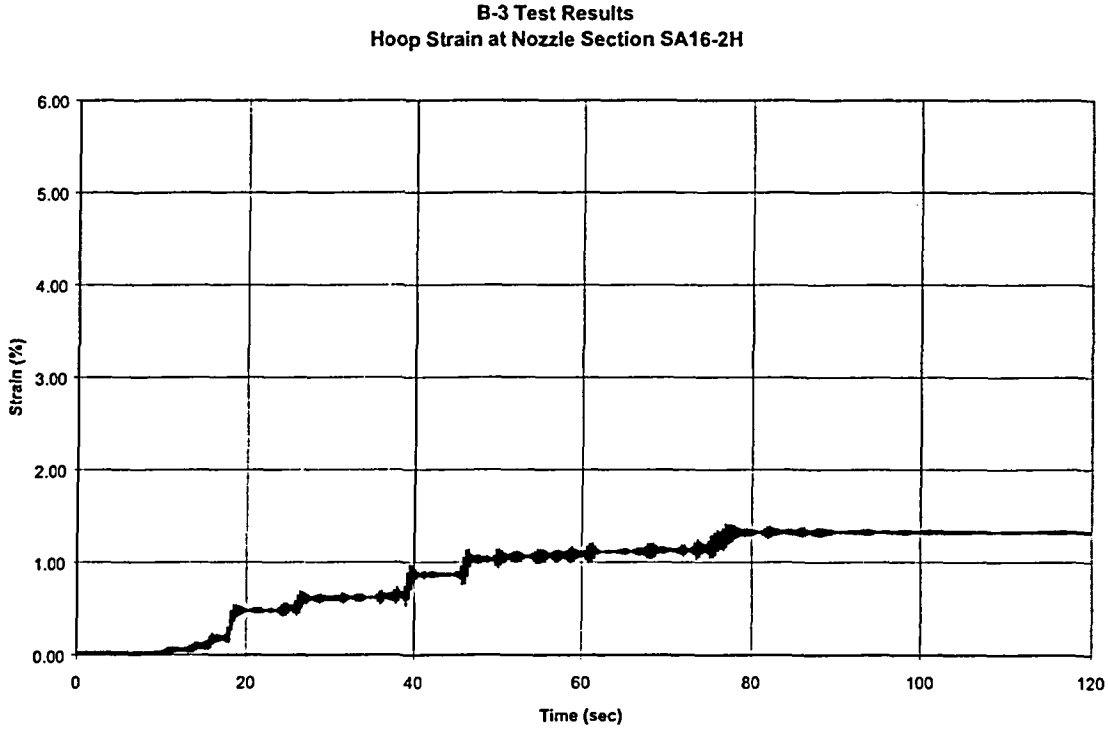

Figure 5-18 B-3 Test Hoop Strain at Nozzle Comparison – SA16-2H

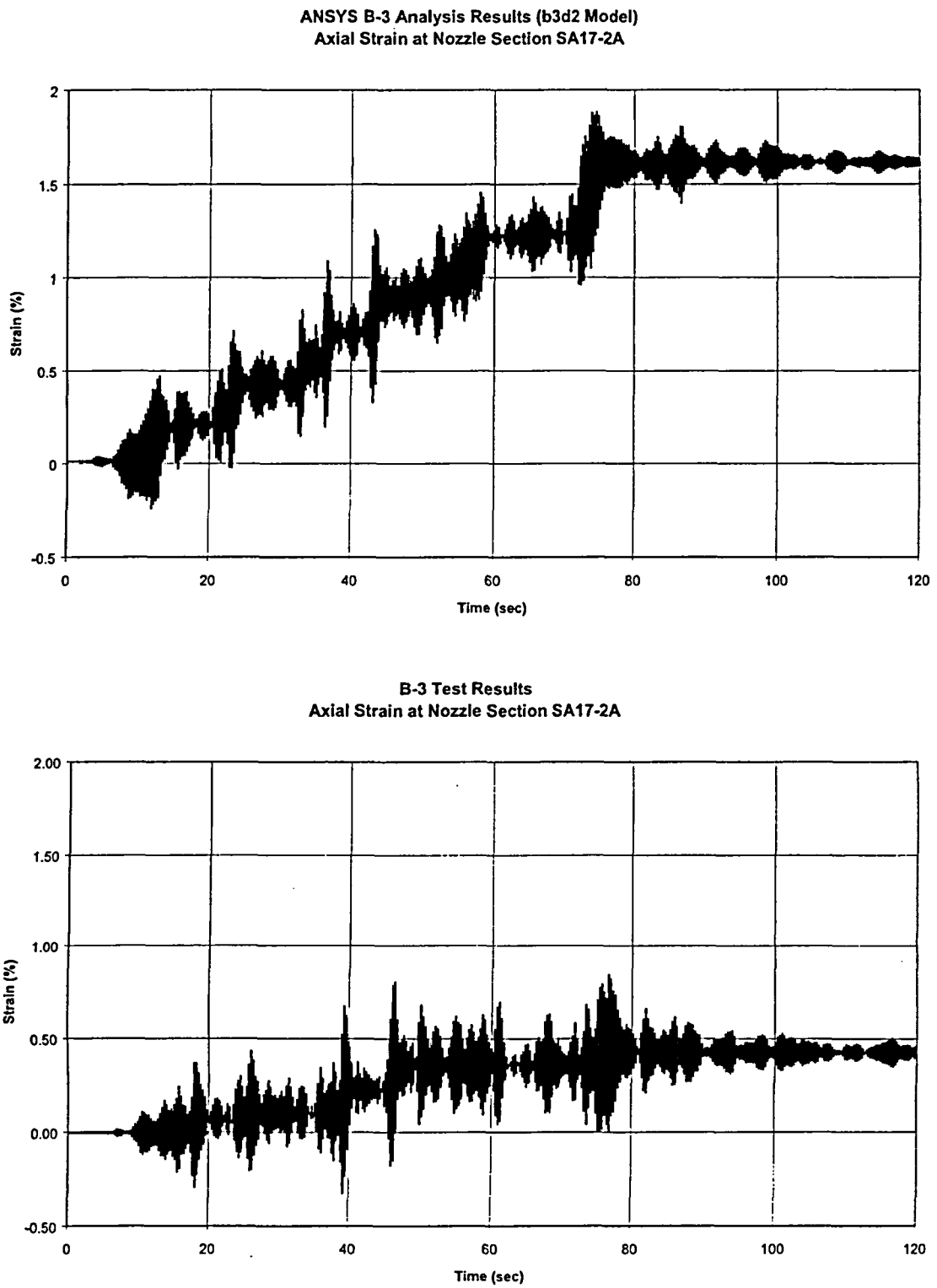

Figure 5-19 B-3 Test Axial Strain at Nozzle Comparison – SA17-2A

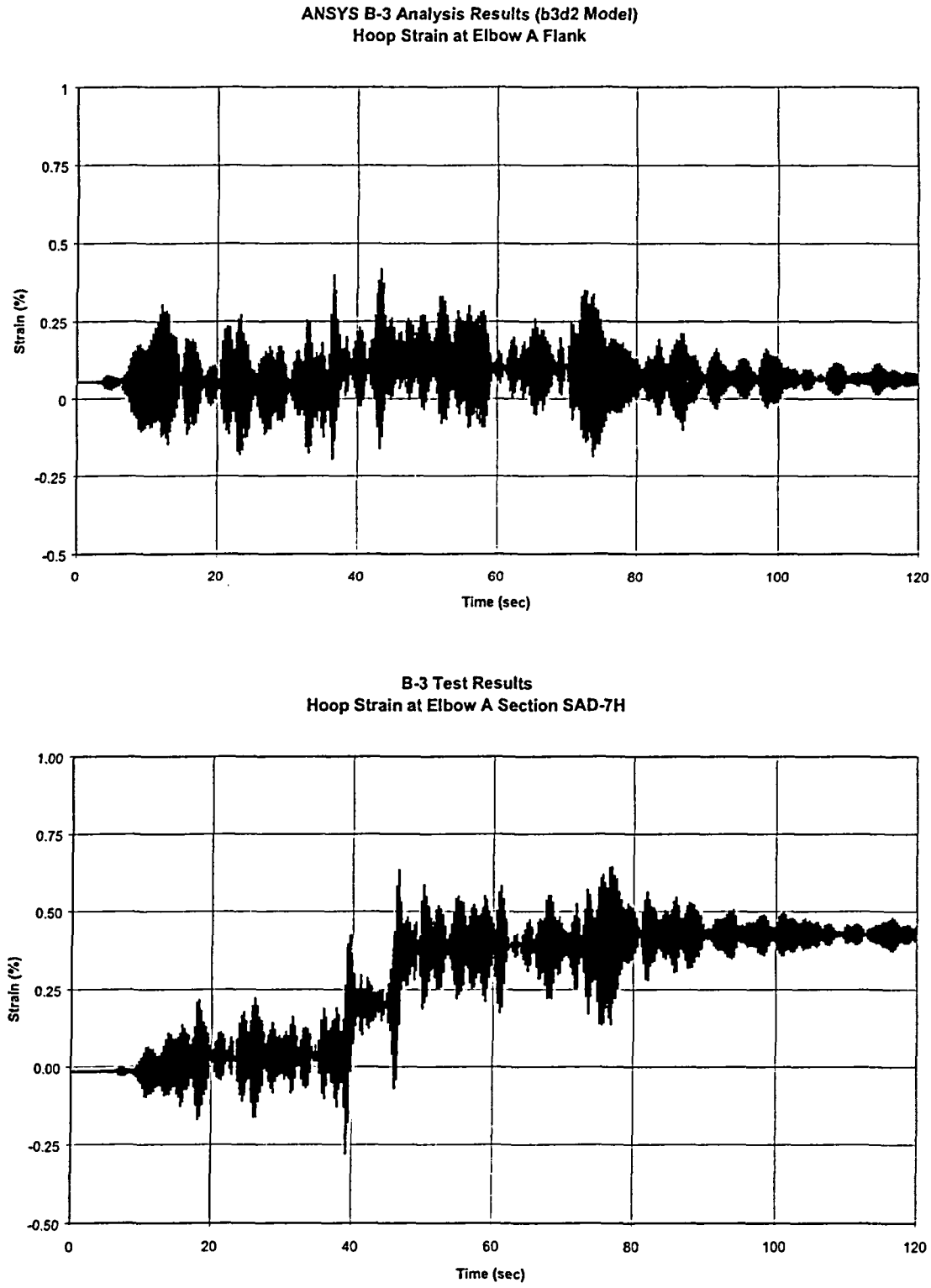

Figure 5-20 B-3 Test Hoop Strain at Elbow A Flank Comparison – SAD-7H

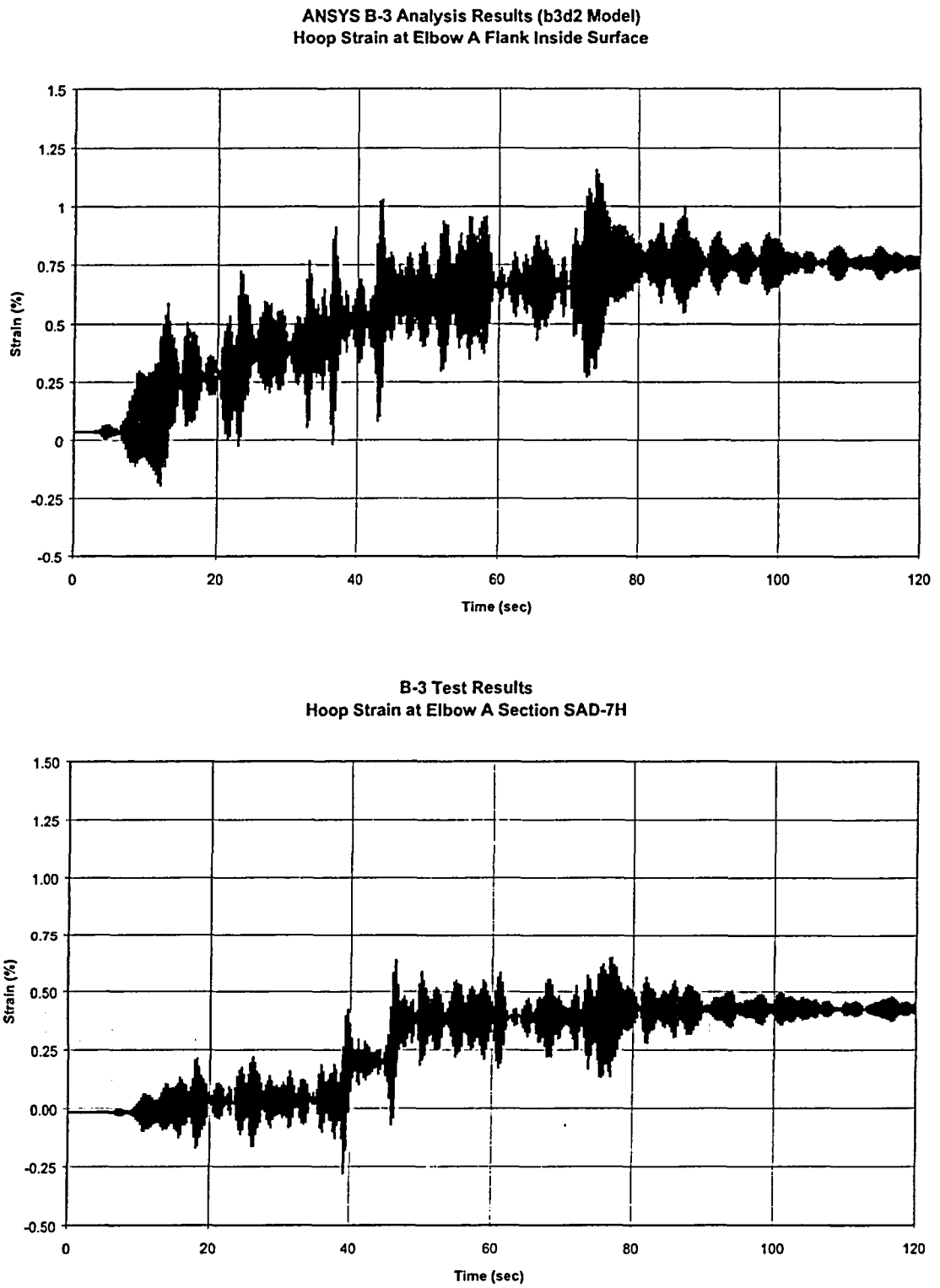

Figure 5-21 B-3 Test Hoop Strain at Elbow A Flank Inside Surface Compared to Test Hoop Strain at Outside Surface – SAD-7H

6.0 CONCLUSIONS AND RECOMMENDATIONS

The NUPEC Ultimate Strength Piping Test Program has provided valuable new test data on high level seismic elasto-plastic behavior and failure modes for typical nuclear power plant piping systems. The NUPEC program was a comprehensive program which included basic piping material tests, piping component static and dynamic tests, simplified piping system seismic tests, and shaking table seismic tests of a representative large-scale piping system to levels well above the typical design earthquake. A selected number of component and piping system tests including the large-scale piping test were carried out to failure. The test specimens were heavily instrumented to record displacements, accelerations and strains versus time at critical locations. The component and piping system tests demonstrated the strain ratcheting behavior that is expected to occur when a pressurized pipe is subjected to cyclic seismic loading. All pipe failures that were observed in this test program were characterized as through-wall cracks which occurred as a result of fatigue ratcheting. This report provides a summary of tests performed under this program and selected test results which were used by BNL for comparison to post-test analysis.

The test data generated under this program augments the database of existing information on full-scale piping system and component seismic tests performed in the U.S. Although the NUPEC program was geared toward demonstrating margins in Japanese piping design, there are a number of similarities in materials and design requirements that make the test results applicable to U.S. piping designs. Technical justification for recent changes in the ASME Code piping design rules relied primarily on data collected under the EPRI/NRC Piping and Fitting Dynamic Reliability Program. The NUPEC data may be evaluated in the same manner to provide additional technical justification from an independent test program. As reported in Section 3.0 of this report, BNL performed linear analyses and code evaluations for selected simplified piping system tests. Linear analysis methods were applied in accordance with current and earlier ASME Code requirements. The results demonstrated that the highest level NUPEC simplified piping seismic tests subjected the piping components to stress levels above Code allowables and illustrated the differences in minimum stress margins between recent revisions of the Code. Based on the latest NRC endorsed ASME Code rules (1993) and Code Case N-411 damping, the analyses showed minimum margins of 2.74 for elbows and 1.37 for nozzle welds. For the same test runs analyzed and evaluated according to the 2004 ASME Code rules, the analyses showed minimum margins of 1.84 for elbows and 1.76 for nozzle welds. Additional analyses and Code evaluations could be performed for other tests including the large-scale piping test to provide further substantiation of Code margins.

The NUPEC Ultimate Strength Piping Test Program also provided excellent test data for benchmarking inelastic analysis methods and computer codes. The BNL post-test nonlinear analyses described in Sections 4.0 and 5.0 of this report provided useful insights into the application of state-of-the-art elasto-plastic analysis methods for predicting the seismic response of a piping system.

The nonlinear analyses demonstrated that the use of classical linear kinematic hardening rules (which have been applied in NPP nonlinear analyses) may not be adequate for predicting the strain ratcheting behavior in piping systems. The application of either bilinear or multilinear kinematic hardening rules in the analysis of static elbow component cycling predicted high rates of initial strain ratcheting with shakedown occurring after only five to ten cycles. The tests demonstrated lower initial strain ratcheting eventually stabilizing to a constant rate of ratcheting without shakedown. The application of the Chaboche nonlinear kinematic hardening model provided an improved strain ratcheting simulation. The elbow cycling simulation analysis demonstrated that the Chaboche model more closely predicted the initial ratcheting followed by a constant rate of ratcheting in subsequent cycles as observed in the test. For the A-2 simplified piping system test, the Chaboche model also provided the most accurate overall simulation of strain ratcheting behavior. The accurate simulation of ratcheting is particularly important for Code evaluation of piping based on plastic or equivalent plastic analyses that rely on demonstration of

shakedown. For prediction of displacement response, the A-2 simplified piping system analyses showed that the Chaboche model also provided the best simulation although the multilinear kinematic hardening model also provided a reasonably good match. The application of the Chaboche nonlinear kinematic hardening model to the simulation analyses of the other four simplified piping system tests demonstrated that the displacement time history response was predicted with reasonably good accuracy. Accurate simulation of strain and strain ratcheting was achieved in some but not all cases which indicates that even the Chaboche nonlinear model has limitations which need to be better understood. From a regulatory standpoint, the reviewer must be aware of the limitations of commonly applied plasticity models. To gain further understanding of the model limitations, the NRC staff may consider additional studies to investigate the limitations of plasticity models on representative large-scale piping systems.

The difficulty in achieving precise test simulations during the preliminary A-2 simplified piping system analyses illustrated the importance of accurately modeling the piping system to predict correct system dynamic characteristics (frequencies and mode shapes) in an elasto-plastic analysis. In a linear response spectrum analysis of a piping system, modeling uncertainties such as dimensional variations in the system may be accounted for by peak broadening. This is important when the fundamental frequency of the system is on a steep slope of the response spectrum and a small shift in frequency can result in a large increase in response. In a nonlinear analysis, a small change in frequency of the model may have an even more significant impact on the response since it may lead to plastic strain ratcheting response versus elastic response. The application of 15% peak broadening may not provide sufficient safety margins when inelastic analysis is performed. Further studies to investigate the sensitivity of response due to modeling uncertainties for large scale piping systems may provide additional insights.

7.0 REFERENCES

1. K. Suzuki, et al., Seismic Proving Test of Ultimate Piping Strength, ICONE-9, Paper No. 155, 2001.
2. K. Suzuki, et al., Seismic Proving Test of Ultimate Piping Strength, ICONE-10, Paper No. 22225, 2002.
3. ANSYS, User's Manual, Release 5.6., ANSYS Inc., Canonsburg, PA 15317, U.S.A.
4. U.S. Nuclear Regulatory Commission, Standard Review Plan for the Review of Safety Analysis Reports, NUREG-0800, Sections 3.7.3 and 3.9.2, Revision 2, 1989.
5. Chaboche, J.L., Time Independent Constitutive Theories for Cyclic Plasticity, *International Journal of Plasticity*, Vol. 2, pp. 149-188, 1986.
6. Prager, W., A New Method of Analyzing Stresses and Strains in Work Hardening Plastic Solids, *Journal of Applied Mechanics*, Vol. 23, pp. 493-496, 1956.
7. Besseling, J.F., A Theory of Elastic, Plastic and Creep Deformations of an Initially Isotropic Material, *Journal of Applied Mechanics*, Vol. 25, pp. 529-536, 1958.
8. Armstrong, P.J. and Frederick, C.O., A Mathematical Representation of the Multiaxial Bauschinger Effect, CEGB Report No. RD/B/N 731, 1966.
9. Bari, S. and Hassan, T., Anatomy of Coupled Constitutive Models for Ratcheting Simulations, *International Journal of Plasticity*, Vol. 16, pp. 381-409, 2000.

NRC FORM 335
(9-2004)
NRCMD 3.7

U.S. NUCLEAR REGULATORY COMMISSION

BIBLIOGRAPHIC DATA SHEET

(See instructions on the reverse)

1. REPORT NUMBER
(Assigned by NRC, Add Vol., Supp., Rev., and Addendum Numbers, If any.)

NUREG/CR-6889
BNL-NUREG-74978-2005

2. TITLE AND SUBTITLE

Seismic Analysis of Simplified Piping Systems for the NUPEC Ultimate Strength Piping Test Program

3. DATE REPORT PUBLISHED

MONTH	YEAR
December	2005

4. FIN OR GRANT NUMBER

N-6076

5. AUTHOR(S)

DeGrassi, G., Hofmayer, C.

6. TYPE OF REPORT

Technical

7. PERIOD COVERED *(Inclusive Dates)*

8. PERFORMING ORGANIZATION - NAME AND ADDRESS *(If NRC, provide Division, Office or Region, U.S. Nuclear Regulatory Commission, and mailing address; if contractor, provide name and mailing address.)*

Brookhaven National Laboratory
Energy Sciences and Technology Department
Upton, NY 11973-5000

9. SPONSORING ORGANIZATION - NAME AND ADDRESS *(If NRC, type "Same as above"; if contractor, provide NRC Division, Office or Region, U.S. Nuclear Regulatory Commission, and mailing address.)*

Division of Engineering Technology
U. S. Nuclear Regulatory Commission
Washington, D.C. 20555-0001

10. SUPPLEMENTARY NOTES

Syed A. Ali, Program Manager

11. ABSTRACT *(200 words or less)*

The Nuclear Power Engineering Corporation (NUPEC) of Japan has conducted a multi-year test program for the Ministry of Economy, Trade and Industry (METI) of Japan to investigate the behavior of typical Nuclear Power Plant (NPP) piping systems under large seismic loads. The objectives of this program are to develop a better understanding of the elasto-plastic response and ultimate strength of nuclear piping systems, to ascertain the seismic safety margins in current piping design codes, and to assess new code allowable stress rules. The test program consisted of a series of static and dynamic material tests, piping component tests, simplified piping system tests, and large scale piping tests. As part of collaborative efforts between the United States and Japan on seismic issues, the U.S. Nuclear Regulatory Commission (NRC) and the Brookhaven National Laboratory (BNL) participated in this program by performing both pre-test and post-test analysis for selected tests, and by evaluation of program results. This report presents a summary of the NUPEC tests, describes the BNL post-test analyses of selected simplified piping system tests, and discusses the insights gained from this program.

12. KEY WORDS/DESCRIPTORS *(List words or phrases that will assist researchers in locating the report.)*

Seismic Analysis, seismic testing, piping design, ASME code evaluation, fatigue ratcheting, plasticity, kinematic hardening, fatigue failure.

13. AVAILABILITY STATEMENT

unlimited

14. SECURITY CLASSIFICATION

(This Page)
unclassified

(This Report)
unclassified

15. NUMBER OF PAGES

16. PRICE

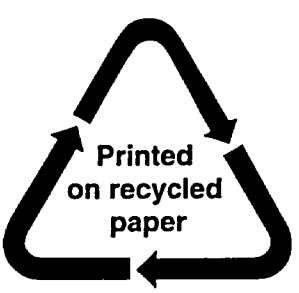

Federal Recycling Program

UNITED STATES
NUCLEAR REGULATORY COMMISSION
WASHINGTON, DC 20555-0001

OFFICIAL BUSINESS